universität wien

DISSERTATION

Titel der Dissertation

Molecular Pathology of Mitochondrial $tRNA^{Ile}$ Mutations

Verfasserin

Dipl.-Biol. Andrea Fettermann

angestrebter akademischer Grad

Doktorin der Naturwissenschaften (Dr. rer. nat.)

Wien, 2012

Studienkennzahl lt. Studienblatt:	A 091 441
Dissertationsgebiet lt. Studienblatt:	Genetik - Mikrobiologie
Betreuerin / Betreuer:	Univ.-Prof. Dr. Andrea Barta

CONTENTS

Contents…….... I
Abbreviations……..……..……..... V
Abstract…….……..……..... 1
Zusammenfassung……..……..……..…… 3
1. Introduction..... 5
1.1 Mitochondria 5
1.1.1 Organization of Mitochondria..... 5
1.1.2 Functions of Mitochondria 6
1.1.3 The Respiratory Chain..... 7
1.1.3.1 Complex I: NADH:Ubiquinone Oxidoreductase..... 8
1.1.3.2 Complex II: Succinate:Ubiquinone Oxidoreductase 8
1.1.3.3 Complex III: Ubiquinone-Cytochrome *c* Oxidoreductase 9
1.1.3.4 Complex IV: Cytochrome *c* Oxidase 9
1.1.3.5 Complex V: ATP Synthase 10
1.1.4 Reactive Oxygen Species (ROS) 10
1.1.5 The Mitochondrial Genome 11
1.1.6 Features of Mitochondrial Genetics 13
1.1.7 Transcription, Processing and Translation 14
1.2 Mitochondrial tRNAs 17
1.2.1 tRNA Function 17
1.2.2 tRNA Structure 18
1.2.2.1 Primary Structure 18
1.2.2.2 Secondary Structure 19
1.2.2.3 Tertiary Structure 20
1.2.3 Biogenesis of tRNA 21
1.2.3.1 5’ Processing 21
1.2.3.2 3’ Processing 22
1.2.3.3 Posttranscriptional Modifications.....23
1.2.3.4 CCA Adding 23

1.2.4 $tRNA^{Ile}$ 24
1.3 Mitochondriopathies 24
1.3.1 Nuclear DNA Mutations 25
1.3.2 Mitochondrial DNA Mutations 26
1.3.2.1 Homoplasmic Mutations 28
1.3.2.2 Heteroplasmic Mutations 29
1.3.3 tRNA Mutations 30
1.3.4 $tRNA^{Ile}$ Mutations 31
1.3.5 Model Systems 34
1.3.5.1 The Cybrid Model 35
2. Aim of the Project 37
3. Case Reports 38
3.1 m.4281A>G 38
3.2 m.4284G>A 39
3.3 m.4290T>C 40
3.4 m.4296G>A 40
3.5 m.4300A>G 41
4. Results 43
4.1 Cellular and Biochemical Phenotype of 143B Cybrid Cells 43
4.1.1 Cell Growth in Galactose Medium 44
4.1.2 Polarographic Analysis of Cell Respiration 46
4.1.3 Spectrophotometric Analysis of Respiratory Chain Enzyme Activity 49
4.1.4 mtDNA Copy Number 50
4.1.5 Sequencing of mtDNA 51
4.1.6 Structure of Mitochondria 53
4.2 Effects of the $tRNA^{Ile}$ Mutations at the Molecular Level 56
4.2.1 Steady-State Levels of $tRNA^{Ile}$ 56
4.2.2 Steady-State Levels of Precursor $tRNA^{Ile}$ 57
4.2.3 Processing of the $tRNA^{Ile}$ Precursor *in vitro* 60
4.2.4 $tRNA^{Ile}$ Stability and Resynthesis 61
4.2.5 $tRNA^{Ile}$ Aminoacylation in Cybrid Cells 64
4.2.6 $tRNA^{Ile}$ Aminoacylation "*in Organello*" 65
4.2.7 Mitochondrial Protein Synthesis 68

4.2.8 Steady-State Levels of Mitochondrial Proteins 68
4.2.9 Secondary Structure Prediction of $tRNA^{Ile}$ 71
5. Discussion 75
5.1 Aim of the Study 75
5.2 The Cybrid Model 75
5.3 Characterization of the Molecular and Cellular Phenotypes of Individual Mutations 77
5.3.1 m.4281A>G 77
5.3.2 m.4284G>A 82
5.3.3 m.4290T>C 85
5.3.4 m.4296G>A 90
5.3.5 m.4300A>G 94
5.3.6 m.4263A>G 97
5.4 Molecular Pathogenesis in Comparison 97
6. Materials & Methods 105
6.1 Cell Culture 105
6.1.1 Passaging, Freezing and Unfreezing of Cells 106
6.1.2 Cell Counting 106
6.1.3 Growth Assays 106
6.2 Miscellaneous Cell Treatment 107
6.2.1 Mitotracker Staining 107
6.2.2 Electron Microscopy 107
6.3 Biochemistry: Respiratory Chain Activity 107
6.3.1 Polarography: Cell Respiration 107
6.3.2 Spectrophotometry: Respiratory Chain Complex Activities 108
6.3.2.1 Preparation of Mitochondria 109
6.3.2.2 Analysis of Respiratory Chain Complex Activities 109
6.4 RNA and DNA Manipulations 112
6.4.1 Oligonucleotides 112
6.4.2 RNA Extraction and Northern Hybridization (tRNA Steady-State Levels and Aminoacylation) 118
6.4.3 DNA Extraction (mtDNA Content, Mycoplasma Test, mtDNA Sequencing) 119
6.4.4 cDNA Synthesis (tRNA Precursor Steady-State Levels) 119

6.4.5 Quantitative Real-Time PCR (tRNA Precursor Steady-State Levels) 120
6.4.6 Probe-Based Quantitative Real-Time PCR (mtDNA Content) 121
6.4.7 Quantitative Real-time PCR (Mycoplasma Test) 122
6.4.8 PCR (mtDNA Sequencing) 123
6.4.9 RNase Protection Assay (tRNA Steady-State Levels) 124
6.5 tRNA Maturation and Function 126
6.5.1 5' Processing 126
6.5.1.1 Precursor $tRNA^{Ile}$ Substrates 126
6.5.1.2 Mitochondrial RNase P 127
6.5.1.3 Enzyme Assays 127
6.5.2 tRNA Stability and Resynthesis 127
6.5.3 Aminoacylation Assay ("*in Organello*") 128
6.6 Mitochondrial Proteins 129
6.6.1 Metabolic Labeling of Mitochondrial Proteins 129
6.6.2 Western Blotting 130
7. Literature 132
Danksagung 145
Curriculum Vitae 146

Abbreviations

A	adenine
aaRS	aminoacyl-tRNA synthetases
abs	absorption
ADP	adenosine diphosphate
ATP	adenosine triphosphate
BrdU	bromodeoxyuridine
BSA	bovine serum albumine
C	cytosine
°C	Celsius
cDNA	complementary DNA
Ci	Curie
Cl	chloride
COX	cytochrome *c* oxidase
CPEO	chronic progressive external ophthalmoplegia
cpm	counts per minute
cyt*b*	cytochrome *b*
cyt*c*	cytochrome *c*
Da	Dalton
DCPIP	dichlorphenolindophenol
D-loop	displacement loop
DMEM	Dulbecco's modified Eagle's medium
DMSO	dimethyl sulfoxide
DNA	deoxyribonucleic acid
dNTP	deoxyribonucleoside triphosphate
DTNB	5,5'-dithiobis-(2-nitrobenzoic acid) or Ellman's reagent
DTT	dithiothreitol
e^-	electrons
EDTA	ethylenediaminetetraacetic acid
EF-Tu	elongation factor Tu
EGTA	ethylene glycol tetraacetic acid
EtBr	ethidium bromide
FAD	flavin adenine dinucleotide
FCCP	carbonyl cyanide 4-(trifluoromethoxy) phenylhydrazone

FCS	fetal calf serum
FeS	iron-sulphur protein
GAPDH	glycerinaldehyde-3-phosphate-dehydrogenase
G	guanine
HIV	human immunodeficiency virus
HSP	heavy strand promoter
H-strand	heavy strand
ileRS	isoleucyl-tRNA-synthetase
k	kilo
kb	kilobases
L-strand	light strand
LPA	linear polyacrylamide
LSP	light strand promoter
m	mili
M	molar
MELAS	mitochondrial myopathy, encephalopathy, lactic acidosis and stroke-like episodes
MERRF	myoclonic epilepsy and ragged red fibers
min	minute
mJ	miliJoule
mRNA	messenger ribonucleic acid
mt	mitochondrial
MT	mutant
mtDNA	mitochondrial deoxyribonucleic acid
NADH	nicotinamide adenine dinucleotide (reduced)
NaOAc	sodium acetate
nt	nucleotide
O_H	origin of the heavy strand
O_L	origin of the light strand
OxPhox	oxidative phosphorylation
ρ^0	rho zero
PA	polyacrylamide
PAGE	polyacrylamide gel electrophoresis
PBS	phosphate buffered saline
PCR	polymerase chain reaction
PEG	polyethylene glycol
RC	respiratory chain

RFLP	restriction fragment length polymorphism
RNA	ribonucleic acid
ROS	reactive oxygen species
rpm	rounds per minute
RRF	ragged red fibers
rRNA	ribosomal ribonucleic acid
rt	room temperature
RT-PCR	reverse transcriptase PCR
SDS	sodium dodecyl sulfate
sec	seconds
SNP	single nucleotide polymorphism
SSC	saline-sodium citrate
T	thymidine
TBE	Tris-borate EDTA buffer
TE	Tris-EDTA
TFAM	mitochondrial transcription factor A
TK	thymidine kinase
TMPD	N,N,N,N-tetramethyl-p-phenylenediamin
tRNA	transfer ribonucleic acid
U	unit
U	uridine
UCP	uncoupling protein
WT	wild type
µ	micro

Abstract

Pathogenic mutations in the mitochondrial genome can cause a variety of multisystemic as well as tissue-specific diseases, even if the mutations affect the same gene. Little is known about the genotype-to-phenotype relationship. 22 pathogenic base substitutions within mitochondrial $tRNA^{Ile}$, a hot spot gene for mutations in mitochondrial DNA, have been identified so far, of which some were associated with cardiomyopathy, while others caused ophthalmoplegia, encephalopathy or multisystemic pathologies. We studied five different pathogenic $tRNA^{Ile}$ mutations in the 143B osteosarcoma cybrid cell model. These cytoplasmic hybrids carry the nucleus of the 143B osteosarcoma cell line and homoplasmic (100% mutant or wild-type) mitochondrial DNA of the patients. Mutation 4281A>G was recently identified in a patient suffering from CPEO and exercise intolerance. 4284G>A was found in a family with a heterogeneous multisystem disorder. 4290T>C and 4296G>A were both found associated with degenerative encephalopathy, and 4300A>G was identified in two independent families with homoplasmic carriers specifically suffering from cardiomyopathy.

The aim of our study on the one hand was to describe and characterize the two unpublished mutations 4281A>G and 4296G>A on a molecular and cellular level, and on the other hand to better understand the molecular basis of the variable clinical outcomes caused by mutations located in the same mitochondrial gene.

The main function of mitochondrial tRNAs is the translation of the 13 mitochondrial encoded subunits of the respiratory chain, which consists of five enzyme complexes. Respiratory chain analysis of the mutant cybrid cell lines revealed isolated or combined complex deficiencies for mutations 4281A>G, 4284G>A, 4290T>C and 4296G>A. Cells containing mutation 4281A>G even showed a completely anaerobic metabolism. Cell growth in galactose medium, which forces the cells to rely on energy supply by their respiratory chain, was decelerated, when cells harbored mutations 4281A>G, 4290T>C or 4300A>G. For the latter, however, we did not detect respiratory chain alterations. Therefore, another mechanism must be responsible for the reduced growth in galactose medium. We found significant differences in the steady-state levels of mutated $tRNA^{Ile}$ molecules and their

precursors. We studied possible causative factors: the consequences of the mutations on 5' precursor processing by RNase P and the impact of the mutations on stability and resynthesis of the tRNA molecules in the cell lines. Mutation 4300A>G impaired 5' tRNA precursor processing, whereas mutation 4284G>A caused $tRNA^{Ile}$ instability. Aminoacylation of $tRNA^{Ile}$ by its cognate amino acid, necessary for the molecule's proper function, was decreased in case of mutations 4281A>G, 4284G>A and 4296G>A. Consequently, reduced mitochondrial translation and/ or reduced protein levels of respiratory chain subunits could be observed for mutations 4281A>G, 4290T>C and 4296G>A, but not for mutation 4284G>A. Not only steady-state levels of mitochondrial encoded subunits, but also of nuclear encoded subunits were reduced in case of mutations 4281A>G and 4290T>C. This may indicate a feedback mechanism between mitochondria and the nucleus. Copy number of mitochondrial DNA was only increased in cells harboring the 4290T>C mutation and may be a compensating effect to overcome the mutation's pathogenic effect. *In silico* structure predictions suggested an alternative conformation only for $tRNA^{Ile}$ 4281A>G, the mutation, which showed the most severe phenotype in the cybrid model. This point mutation also caused an altered morphology of the cells' mitochondria and a severe reduction and distortion of their Cristae.

The results of our study showed that the five mutations at different positions in $tRNA^{Ile}$ had different molecular effects on the cells. They serve as a basis for a better understanding of the pathogenesis of mitochondrial diseases, which are caused by mitochondrial mutations; like a piece of a complicated puzzle. Further studies will hopefully reveal the whole picture in the near future, and would thereby make implementations of efficient treatment strategies possible.

Zusammenfassung

Pathogene Mutationen des mitochondrialen Genoms können verschiedenste multisystemische als auch gewebsspezifische Krankheiten auslösen, selbst wenn es sich um Mutationen im gleichen Gen handelt. Über den Zusammenhang zwischen Genotyp und Phänotyp ist noch wenig bekannt. Im mitochondrialen $tRNA^{Ile}$ Gen, welches besonders häufig von Mutationen betroffen ist, sind bisher 22 pathogene Basensubstitutionen beschrieben worden, welche beispielsweise Kardiomyopathie, Ophthalmoplegie, Enzephalopathie oder multisystemische Symptome verursacht haben. In der vorliegenden Studie untersuchten wir fünf verschiedene pathogene $tRNA^{Ile}$ Mutationen im 143B Osteosarcom-Zybridmodell. Diese zytoplasmatischen Hybride tragen den Zellkern der 143B Osteosarkomzelllinie und homoplasmische (zu 100% mutierte oder gesunde) mitochondriale DNA der Patienten. Die Mutation 4281A>G wurde kürzlich in einem Patienten diagnostiziert, welcher an CPEO und mangelnder körperlicher Belastbarkeit litt. In einer Familie mit heterogenen multisystemischen Symptomen wurde die Mutation 4284G>A diagnostiziert. Zwei weitere Mutationen, 4290T>C und 4296G>A, waren mit einer degenerativen Enzephalopathie assoziiert, während die Mutation 4300A>G in zwei voneinander unabhängigen Familien entdeckt wurde, welche spezifisch an Kardiomyopathie litten.

Das Ziel unserer Studie war zum einen die molekulare und zelluläre Charakterisierung der beiden bisher unpublizierten Mutationen 4281A>G und 4296G>A, und zum anderen wollten wir zu einem besseren Verständnis der molekularen Grundlagen beitragen, auf Basis derer Mutationen im selben mitochondrialen Gen so verschiedenartige Symptome auslösen können.

Die Hauptfunktion der mitochondrialen tRNAs ist die Translation der 13 mitochondrial kodierten Untereinheiten der aus fünf Enzymkomplexen bestehenden Atmungskette. Eine Untersuchung der Amungskette in den mutierten Zybridzellen zeigte separate oder kombinierte Komplexbeeinträchtigungen für die Mutationen 4281A>G, 4284G>A, 4290T>C und 4296G>A. Die 4281A>G mutierten Zellen wiesen sogar einen vollständig anaeroben Stoffwechsel auf. In Galaktose brachten wir die Zellen in eine Abhängigkeit von einer funktionsfähigen Atmungskette zur Energieversorgung. Das Zellwachstum war für jene Zellen verlangsamt, welche die Mutationen 4281A>G,

4290T>C oder 4300A>G trugen. Letztere hatte keine Fehlfunktion der Atmungskette gezeigt, daher dürfte ein anderer Mechanismus, möglicherweise eine erhöhte Radikalentstehung, für das verlangsamte Zellwachstum in Galaktose verantwortlich sein. Des Weiteren detektierten wir signifikante Unterschiede in der vorliegenden Menge der reifen $tRNA^{Ile}$ und ihres unreifen Vorläuferproduktes. Wir untersuchten mögliche Ursachen, wie Einflüsse der fünf Mutationen auf die 5‘ Reifung des Vorläuferproduktes durch das Enzym RNase P oder auf Stabilität und Neusynthese der tRNA. Die Mutation 4300A>G führte zu einer gestörten 5‘ Reifung, während Mutation 4284G>A eine $tRNA^{Ile}$-Instabilität verursachte. Die Aminoacylierung der tRNA mit der Aminosäure Isoleucin, ein für die Funktion der tRNA notwendiger Schritt, war durch die Mutationen 4281A>G, 4284G>A und 4296G>A beeinträchtigt. Folglich konnten für die Mutationen 4281A>G und 4296G>A, sowie auch für 4290T>C, eine reduzierte mitochondriale Translation und/ oder eine verminderte Proteinexpression von Untereinheiten der Atmungskette festgestellt werden, jedoch nicht für die Mutation 4284G>A. Nicht nur die Expression der mitochondrial kodierten Untereinheiten, sondern auch jene von nukleär kodierten Untereinheiten war durch die Mutationen 4281A>G und 4290T>C vermindert. Dies lässt auf einen Rückkopplungsmechanismus zwischen Mitochondrien und Nukleus schließen. Die Menge der mitochondrialen DNA-Moleküle war lediglich durch die Mutation 4290T>C erhöht, was auf einen Versuch der Zellen hinweisen dürfte, den patholgischen Effekt der Mutation auszugleichen. *In silico*-Berechnungen der Sekundärstruktur zeigten nur für $tRNA^{Ile}$ 4281A>G wesentliche Veränderungen. Diese Mutation zeigte im Zybridmodell den auffälligsten Phänotyp. Weiterhin war in jenen Zellen die Mitochondrienstruktur verändert und deren Cristae reduziert und deformiert.

Die Ergebnisse unserer Studie zeigten, dass die fünf Mutationen an verschiedenen $tRNA^{Ile}$ Nukleotidpositionen unterschiedliche molekulare Auswirkungen auf die Zellen hatten. Sie dienen als Grundlagenwissen auf dem Weg zu einem besseren Verständnis der Pathogenese von Mitochondriopathien, die von mitochondrialen Mutationen verursacht werden; wie Teile eines komplizierten Puzzles. Weiterführende Studien werden wünschenswerterweise in naher Zukunft das Gesamtbild darstellen können, und dadurch die Realisierung von effizienten Behandlungsmöglichkeiten möglich machen. Diese sind bisher nicht verfügbar.

1. Introduction

1.1 Mitochondria

1.1.1 Organization of Mitochondria

Mitochondria are cytoplasmic cell organelles, which supply the cell with chemical energy in form of ATP, the universal energy currency of the cell. Depending on the energy demand of a specific tissue or cell type, one up to several thousand mitochondria coexist in one cell, and each contains several copies of the mitochondrial genome, a condition called polyplasmy. Muscle and nerve cells are highly active; this is why they contain an above average number of mitochondria. Mitochondria are not single entities, but form highly dynamic tubular networks, and their interaction is maintained by permanently ongoing and balanced fusion and fission events. These vital events are crucial for the cell, e.g., in apoptosis, which is associated with a main-player of mitochondrial fusion (OPA1) (Lee et al., 2004), or to perpetuate mitochondrial function in case of a mutation within mtDNA (Nakada et al., 2001; Ono et al., 2001).

Mitochondria are remnants of aerobic proteobacteria, which colonized their anaerobic host cell more than 1.5 billion years ago (Gray et al., 1999; van der Giezen and Tovar, 2005). The symbiosis developed and became permanent. This happening enabled the eukaryotic cell to metabolite aerobically, a much more efficient way than driving solely glycolysis to generate energy. Intriguing similarities between bacteria and mitochondria substantiate this theory: a similar size, a double membrane, an own circular genome with a similar size and a separated protein synthesis apparatus with a similar size of ribosomes (70S) and N-formylmethionine as initiating amino acid.

Mitochondria generate chemical energy as ATP by use of an electrochemical gradient (Mitchell, 1961), which necessities a specialized compartmentalization of the

organelles. It is provided by a double membrane system: the outer membrane encloses the mitochondrion, whereas the inner membrane envelops the matrix and thereby separates it from the intermembrane space, which is located between the two membranes. The inner membrane is folded into several Cristae, whereby the surface is increased extensively. This allows a higher number of membrane proteins to locate there, which are, e.g., the ADP/ATP carrier or the five polypeptide complexes of the respiratory chain. They create a proton gradient and utilize the energy to generate ATP. A precondition for this process is the non-permeability of the inner membrane to ions. The outer membrane is porous and allows a passive diffusion of molecules up to 5000 Da in size between the cytosol and the intermembrane space.

1.1.2 Functions of Mitochondria

Mitochondria hold several functions, but the one noted most is the supply of ATP. The chemically energetic molecule is most efficiently generated aerobically by the respiratory chain and, with much lower efficiency, anaerobically by the glycolytic substrate level phosphorylation in the cytoplasm. One glucose molecule yields 36 ATP molecules by oxidative phosphorylation, compared to 2 ATP by the cytosolic glycolysis. ATP is then either used for biochemical reactions within the mitochondrion or transported into the cytosol, where the energy rich molecule is available for cell maintenance and function.

Furthermore, mitochondria are players in calcium based cell signaling, play a key role in apoptosis regulation by, e.g., release of cytochrome *c* or apoptosis inducing factor (Mei et al., 2010b), are involved in fatty acid (β-oxidation) and amino acid metabolism, porphyrin synthesis, cell differentiation or can produce heat by decoupling of the respiratory chain. The heat production is a well-known mechanism of the brown fat tissue, mainly abundant in newborns and hibernating mammals. The role of mitochondria in ageing (Larsson, 2010; Trifunovic et al., 2004), cancer (Chandra and Singh, 2011; Wallace, 2005) and neurodegenerative diseases like Alzheimer disease (Mao and Reddy, 2011; Yang et al., 2011) or Parkinson disease (Morais and De Strooper, 2010) is heavily discussed.

1.1.3 The Respiratory Chain

The respiratory chain is located in the inner mitochondrial membrane and is composed of five enzyme complexes (*figure 1.1*): NADH:ubiquinone oxidoreductase (I), succinate:ubiquinone oxidoreductase (II), ubiquinone-cytochrome *c* oxidoreductase (III), cytochrome *c* oxidase (IV) and ATP synthase (V) (Fernandez-Vizarra et al., 2009; Rustin et al., 1994; Smeitink et al., 2001). With the exception of complex II, which is only nuclear DNA-encoded, all the other enzyme complexes are genetic mosaics, with subunits derived from cytoplasmic and mitochondrial translation.

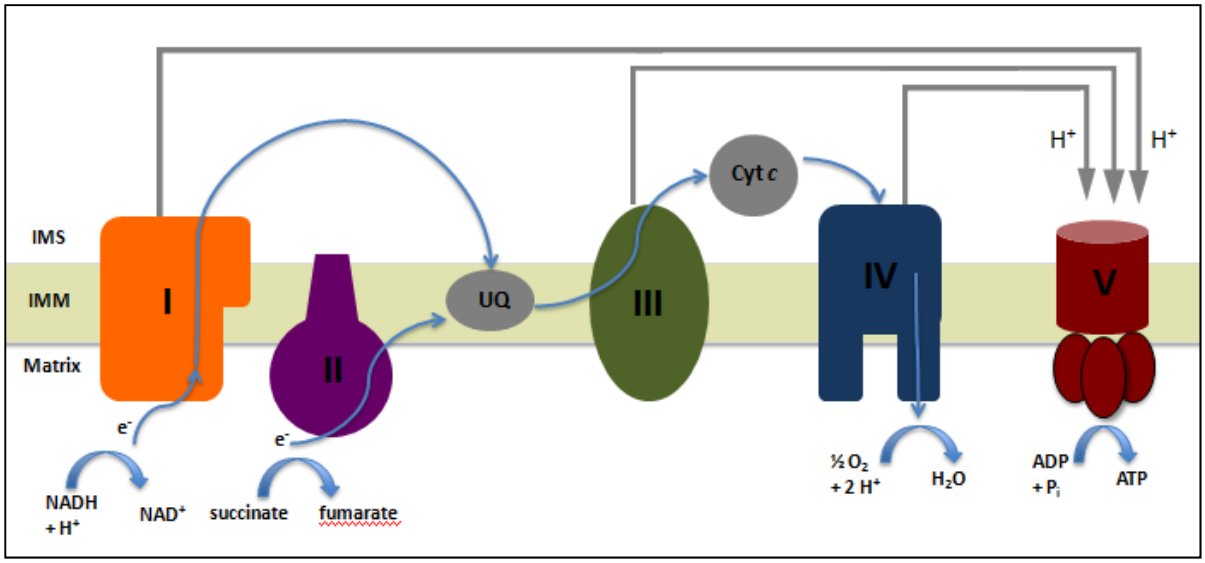

Figure 1.1. *Respiratory chain, located in the inner mitochondrial membrane. Complex I and complex II oxidize substrates in the matrix, transfer electrons to ubiquinone, which reduces complex III. Cyt c oxidizes complex III and reduces complex IV. Complex IV reduces oxygen to water. Complexes I, III and IV utilize the energy of the redox reactions to pump hydrogen from the matrix into the intermembrane space, generating a proton gradient, which is used by complex V to generate ATP from ADP and inorganic P. IMS=intermembrane space; IMM=inner mitochondrial membrane; cytc=ctochrome c; UQ=ubiqinone.*

Complexes I, II, III and IV form an electron transport chain, transferring electrons from the electron donors NADH (derived by the oxidation of pyruvate, amino acids and fatty acids) or succinate (derived from fatty acids and the citrate cycle) to the electron acceptor O_2. The two small electron carriers ubiquinone and cytochrome *c*

are required for the electron transport. The transfer is accomplished by redox reactions, where the electron acceptor of each step is more electronegative than the electron donator. During this process, complex I, III and IV pump protons from the matrix into the intermembrane space, building up an electrochemical proton gradient and a membrane potential of about 180 mV across the inner mitochondrial membrane. Complex V employs the gradient energy to generate chemical energy as ATP. The adenine nucleotide translocator (ANT) exchanges the ATP of the matrix with ADP of the cytosol. In case of a respiratory chain defect or anaerobic conditions, ATP is generated by glycolysis only, resulting in 2 ATP and 2 pyruvate molecules and 2 reduction equivalents $NADH/H^+$. As glycolysis depends on NAD^+, its recycling is catalyzed by lactate dehydrogenase by reducing pyruvate to lactate and concomitantly oxidizing NADH to NAD^+.

1.1.3.1 Complex I: NADH:Ubiquinone Oxidoreductase

Complex I is the most intricate complex of the respiratory chain with a molecular mass of close to 1 MDa in eukaryotes (Clason et al., 2010). The L-shaped enzyme with a membrane domain and a peripherical arm is composed of 45 polypeptides, of which seven of the membrane domain are encoded by the mitochondrial genome and the residual 38 by the nuclear genome. The enzyme is subdivided into three functional modules: the N-, Q- and P-modules. The N-module oxidizes the electron donator NADH to NAD+, whereby two electrons are accepted by the noncovalently-bound FMN (flavin mononucleotide) prosthetic group of complex I. The electrons are transferred upon a chain of eight iron-sulfur clusters and finally reduce ubiquinone by the Q-module. The reduced form ubiquinol diffuses freely in the membrane. During the electron transfer the P-module of complex I pumps 4 H^+/ 2 e^- across the inner membrane. The mechanism is still unknown, but it is suggested that conformational changes of the complex drive the proton pumping process (Brandt, 2006).
Efficient inhibitors of complex I activity are the pesticide rotenone, which binds to the ubiquinone binding site, and piericidin A.

1.1.3.2 Complex II: Succinate:Ubiquinone Oxidoreductase

Complex II is anchored in the inner membrane and protrudes into the matrix. It consists of four protein subunits, which are exclusively nuclear encoded: the two hydrophilic subunits flavoprotein SdhA (containing a succinate-binding site and the

covalently bound FAD cofactor) and SdhB (containing three iron-sulfur clusters) and the hydrophobic membrane anchor subunits SdhC and SdhD, which contain a heme *b* and the ubiquinone binding-site. Complex II takes part both in the citrate cycle and the respiratory chain activity. In the matrix it oxidizes succinate to fumarate in step 8 of the citrate cycle and transfers the electrons via the iron-sulfur clusters to ubiquinone in the membrane, which is thereby reduced to ubiquinol (Yankovskaya et al., 2003). A potent inhibitor of complex II is oxalacetate.

1.1.3.3 Complex III: Ubiquinone-Cytochrome c Oxidoreductase

The ~240 kDa protein complex consists of 11 subunits of which one, Cyt*b*, is mitochondrially encoded. It transfers electrons from the hydrophobic ubiquinol to the hydrophilic cytochrome *c* in the intermembrane space and at the same time pumps protons into the intermembrane space. The active redox centers are cytochrome *b* with two heme groups, cytochrome c_1 with one heme group and the “Rieske” iron-sulfur protein (Iwata et al., 1998). A potent inhibitor of complex III is antimycin A.

1.1.3.4 Complex IV: Cytochrome c Oxidase

As the terminal enzyme in the respiration cascade, complex IV oxidizes cytochrome *c* and reduces the final electron acceptor, molecular oxygen, to water. During this oxygen consuming process, four protons are pumped out of the matrix and thereby contribute to the electrochemical gradient (Tsukihara et al., 1995). Complex IV is the rate limiting enzyme for respiration and ATP synthesis, as it can allosterically be inhibited by ATP. Carbon monoxide and cyanide are examples for competitive inhibitors of complex IV activity.

Of the 13 subunits of complex IV, three are encoded by the mitochondrial genome. They contain a heme and a copper prosthetic group and form the catalytical core. Not only the 10 other structural subunits have to be imported from the cytosol, but also assembly chaperons and factors required for the disposal of unassembled subunits. The import and assembly is highly regulated by a crosstalk network between the mitochondrium and the nucleus (Fontanesi et al., 2006). This is also the case for the other complexes of the respiratory chain, but until now it is not known how the coordinated expression of genes in both, the nuclear and mitochondrial genome, is regulated.

1.1.3.5 Complex V: ATP Synthase

The ATP synthase is the world's tiniest rotary machine, which utilizes the electrochemical potential energy of protons to convert ADP into ATP (Elston et al., 1998). Noteworthy, Paul D. Boyer and John E. Walker were awarded the Nobel Prize in Chemistry 1997 for their elucidation of the enzymatic mechanism. It is a lollipop-shaped complex, which is composed of the two motors F_0 and F_1, connected with a motor shaft. The mechanical rotor of the membrane spanning F_0 subunit uses the chemical energy of the H^+ gradient to drive the rotation of the F_1 subunit in the matrix. By rotation, the F_1 subunit can assume three different conformations to allow for ADP + Pi binding, reaction and ATP release. (Noji and Yoshida, 2001). Depending on the relation of substrates and products, the proton-driven ATP synthase can also act the other way around as an ATP consuming proton pump.

Coupling of proton gradient generation and ATP synthesis can be disconnected by uncouplers like FCCP, dinitrophenol, the natural uncoupling proteins UCP1, UCP2, UCP3, UCP4 and UCP5 (Yu et al., 2000) or by transport processes for nucleotides or ions.

Of the 16 polypeptide subunits, two are encoded by the mitochondrial genome, namely ATP6 and ATP8.

1.1.4 Reactive Oxygen Species (ROS)

During the process of electron transfer by redox reactions in the respiratory chain, 1-2% of the electrons leak and reduce oxygen, the final electron acceptor, incompletely. This results in radical generation, i.e., the superoxide anion $O_2^{\cdot -}$, which is reduced to the protonated form hydrogen peroxide (H_2O_2) (Rhee, 1999). This oxygen containing molecules possess highly reactive unpaired valence shell electrons. In a healthy tissue the generation is well regulated and adequate. The molecules function in cell signaling and help maintaining homeostasis, but they are also able, especially in an elevated presence, to destroy biomolecules, that is DNA, RNA or proteins (Devasagayam et al., 2004; Druzhyna et al., 2008). Antioxidants can neutralize free radicals. In the case of a strongly elevated ROS production, cells undergo apoptosis, the programmed cell death, as precaution.

1.1.5 The Mitochondrial Genome

Based on their bacterial origin, mitochondria contain an own circular genome with a size of 16.569 bases and up to several thousand copies per cell. The complete sequence of the mitochondrial DNA molecule was first determined by Anderson et al. (1981).

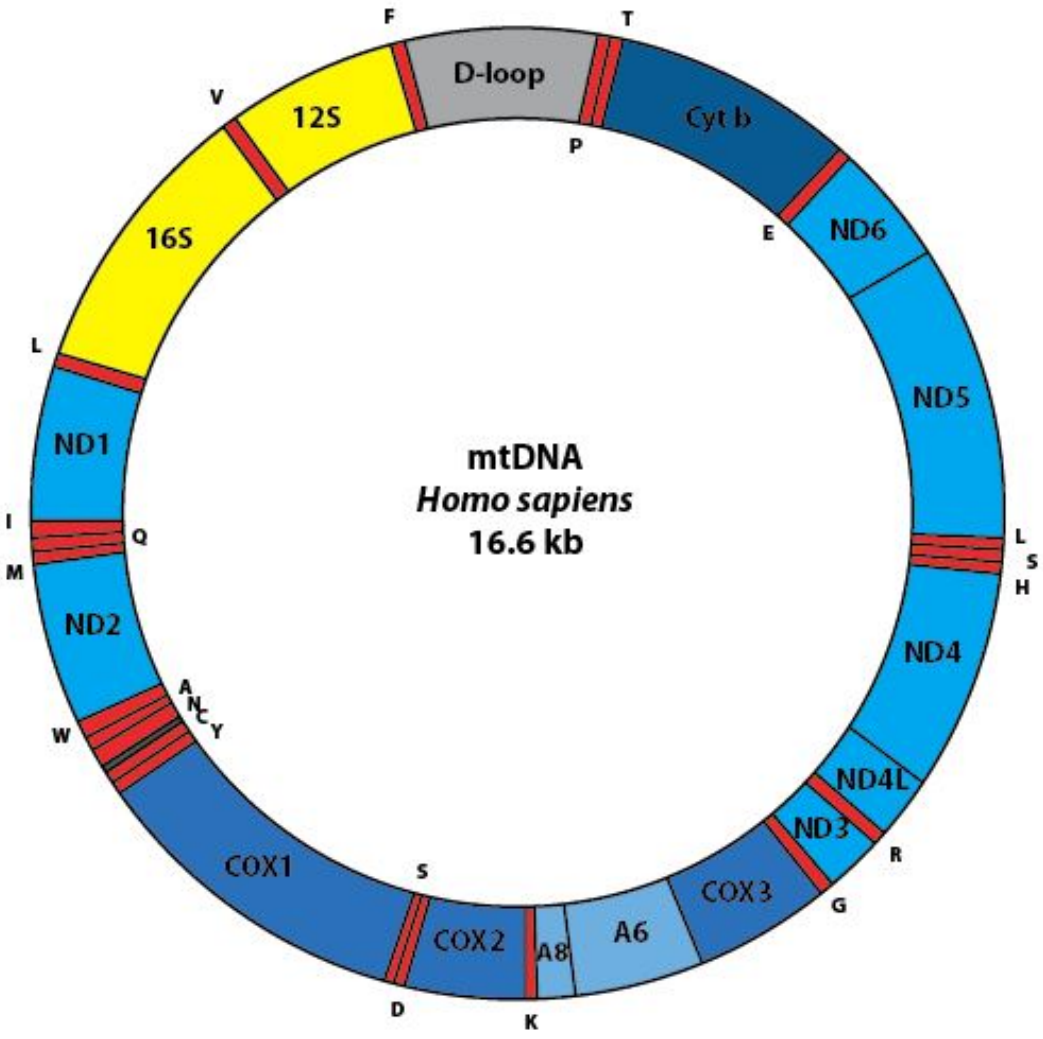

Figure 1.2. *Human mitochondrial genome. mtDNA encodes 22 tRNAs (in red), 2 rRNAs (in yellow) and 13 polypeptides (in blue). tRNAs are illustrated in the standard single letter code. Heavy-strand encoded tRNAs are labeled outside the genome and light-strand encoded tRNAs inside. rRNAs and proteins are encoded by the heavy strand, except for ND6, which is encoded by the light strand. A=ATP synthase; COX=cytochrome c oxidase; Cytb=cytochrome b; D-loop=displacement loop; ND=NADH dehydrogenase.*

The DNA is arranged in DNA-protein packages called nucleoids, frequently containing only a single copy of mtDNA (Kukat et al., 2011). Besides mtDNA, the mitochondrial transcription factor A (TFAM) is the main constituent of nucleoids. TFAM is able to wind, compact and bend DNA, with an abundance of about one TFAM molecule per 15 – 20 bp mtDNA (Ekstrand et al., 2004).

In total, 37 genes are encoded by the mitochondrial genome (f*igure 1.2*), which are 13 mRNAs and 22 transfer RNAs plus 2 ribosomal RNAs, required for the intramitochondrial translation of the 13 mRNAs. The translation products are subunits of the respiratory chain. Mitochondrial rRNA is encoded by RNR1 (12S rRNA) and RNR2 (16S rRNA). The complete set of tRNAs for mitochondrial translation is encoded by the circular genome, one specific for each amino acid but two isoacceptors exist for $tRNA^{Leu}$ ($tRNA^{Leu(UUR)}$ and $tRNA^{Leu(CUN)}$) and $tRNA^{Ser}$ ($tRNA^{Ser(AGY)}$ and $tRNA^{Ser(UCN)}$). All the other components for the translation of only the 13 polypeptides, like initiation, elongation or transcription factors, the polymerase or ribosomal proteins, have to be imported from the cytosol (Spinazzola and Zeviani, 2009). Unlike tRNA import into mitochondria in other organisms, as extensively studied in *Saccharomyces cerevisiae* or *Trypanosmona brucei* (Schneider, 2011), human mitochondria code the full set of tRNAs on their genome, and there seems no need to import this RNA species, although their inert ability to import tRNA was reported (Rubio et al., 2008).

The 13 proteins comprise seven subunits of complex I (ND1, ND2, ND3, ND4, ND4L, ND5 and ND6), the complex III subunit CytB, three complex IV subunits (COX1, COX2 and COX3) and two ATP synthase subunits (ATP6 and ATP8) (DiMauro and Schon, 2003). The residual 74 subunits of the respiratory chain as well as approximately 1500 other proteins, which function in mitochondria, are encoded by the nuclear genome (Calvo et al., 2006). Thus, the vast majority of the mitochondrial proteome has to be translated in the cytosol and imported into the mitochondria (Spinazzola and Zeviani, 2009). About half of the imported proteins are required for the organelle's functions and the other half for the maintenance of the mitochondrium (Schon and DiMauro, 2007). The mitochondrial encoded polypeptides are all strongly hydrophobic. This could explain the disposition of the genes in the organelle's genome, whereas others of the primordial endosymbiont were swapped to the nuclear genome during evolution (von Heijne, 1986). Another hypothesis asserts that the genes are kept in the organelle's genome, and therefore closely located to the

final protein products in the respiratory chain, for regulatory reasons (Allen, 2003). However, mtDNA sequences are still transferred to the nucleus and may remain there as nonfunctional pseudogenes, the nuclear mitochondrial DNA sequences (NUMTs) (Mishmar et al., 2004).

The double-stranded mtDNA is differentiated in a guanine-rich heavy strand and a cytosine-rich light strand. The heavy strand contains most of the genes, whereas only the ND6 mRNA and 8 tRNAs are located on the light strand. Two overlapping reading frames exist on the heavy strand, which is one for ND4 and ND4L mRNA and one for A6 and A8 mRNA (Montoya et al., 1982). mtDNA is compactly arranged, without introns and with only one major non-coding region, containing the ~0.65 kb long triple-stranded displacement- or D-loop. Apart from containing an origin of replication for the heavy strand and a heavy- and light strand promter, no function could be assigned to this region over decades, but recent studies hint that it could have a function in nucleoid formation by binding the protein ATAD3 (He et al., 2007).

1.1.6 Features of Mitochondrial Genetics

Human mitochondrial genomes show many sequence variations between different individuals, and phylogenetic analyses of these polymorphisms define clusters of haplogroups with characteristic sequence similarities (Cann et al., 1987; van Oven and Kayser, 2009). Based on them, a phylogenetic tree of human evolution was established. It is assumed that all the types of mtDNA can be traced back to a common matrilineal ancestor, the so called Mitochondrial Eve or MRCA (most recent common ancestor), who had lived approximately 200.000 years ago (Ienco et al., 2011). She allegorizes the root of the haplotypes A-Z, which are named in the order of their discovery (Wallace, 2005). These studies base on the fact, that cytoplasm-located mitochondria are passed to the offspring solely by the mother's oocytes, without recombination (Giles et al., 1980). The mitochondrial genome has a small size compared to nuclear DNA, and mtDNA shows a high mutation rate. This is due to a weak DNA repair system, which basically consists of base excision repair, and a close location to the respiratory chain (Druzhyna et al., 2008), where reactive oxygen species are produced permanently. The nucleotide substitution rate of the mitochondrial genome is appromximately 10 – 20 times higher than in the nucleus,

and in case of mitochondrial tRNA it is even 100 times faster than in the nuclear counterparts (Pesole et al., 1999).

Mitochondrial DNA molecules replicate independently of the cell-cycle. The balance of replication and degradation, the so-called turn-over, as well as the distribution of mtDNA molecules during cell division occur randomly, the characteristic random segregation of the mitochondrial genome (Clayton, 1982).

Apparently, two different modes of replication coexist in mitochondria. According to the orthodox strand-asynchronous (strand-displacement) model, replication starts from the origin of the H-strand (O_H), located in the D-loop. The replication proceeds with formation of a replication bubble two-thirds around the genome, where the L-strand origin (O_L) is located (Shadel and Clayton, 1997). L-strand synthesis starts from the then accessible O_L in the opposite direction (Clayton, 1982).

Holt et al. (Holt et al., 2000) proposed a coexisting synchronous leading- and lagging-strand synthesis, deriving from multiple replication origins downstream the O_H in the D-loop. Changes in the mtDNA copy number may be the reason for an alteration of the replication mode.

The mitochondrial enzyme DNA polymerase gamma (POLG) catalyzes mtDNA replication, but additional team-players are required for its function. The minimal replisome is composed of the polymerase plus the helicase Twinkle and mitochondrial single-strand binding protein (mtSSB). DNA ligase and topoisomerases are involved in addition (Falkenberg and Larsson, 2009; Fernandez-Silva et al., 2003).

1.1.7 Transcription, Processing and Translation

The mitochondrial genome possesses two promoters, called heavy strand promoter (HSP) and light strand promoter (LSP), depending on the strand which serves as template for transcription. Both are located in the non-coding region upstream of the D-loop. Transcription leads to three different polycistronic transcripts: two large ones covering the total sequence of both strands and a shorter one of the heavy strand, containing only three tRNAs ($tRNA^{Phe}$, $tRNA^{Val}$ and $tRNA^{Leu(UUR)}$) and the two ribosomal genes (Montoya et al., 1982). This explains the high abundancy of rRNA molecules relative to mRNA molecules. The expression of a higher rRNA copy number may be regulated by the mt transcription termination factor mTERF, with a

binding site within the $tRNA^{Leu(UUR)}$ sequence (Kruse et al., 1989). A putative second heavy strand promoter (HSP2) downstream of HSP1 is doubted by a recent study (Litonin et al., 2010), as the authors could not reconstitute transcription from HSP2 *in vitro* with the defined components of the basal transcription machinery. They demonstrated *in vitro* that the basal transcription machinery exclusively requires a single subunit RNA polymerase POLRMT, LSP and HSP as initiation sites and TFAM and TFB2M as synergistically active transcription factors. The putative transcription factor TFB1M was recently unmasked as rRNA methyltransferase, essential for the integrity of the small ribosomal subunit (Metodiev et al., 2009).

All components for transcription have to be imported from the cytoplasm. This also counts for the players in primary transcript processing. According to the punctuation model (Ojala et al., 1981), the 22 tRNA sequences are scattered across the mtDNA, and therefore also across the polycistronic transcripts, and lie in between the 13 mRNA and 2 rRNA sequences. Processing and thereby maturation of the 22 tRNAs by endonucleases RNase P at the 5' end and RNase Z at the 3' end of the tRNAs simultaneously deliberate the flanking mRNA and rRNA sequences (Holzmann et al., 2008; Rossmanith, 2011b). Subsequently, mRNAs are polyadenlylated, a process that is not fully understood, but seems to regulate mRNA stability and generates stop codons in some transcripts (Ruzzenente et al., 2012).

For intraorganellar translation of the 13 mRNAs in the matrix, mitochondria possess the full set of tRNAs and two ribosomal RNAs, but 77 ribosomal proteins, ribosomal assembly proteins and all other proteinaceous components of the translation machinery, like aminoacyl-tRNA-synthetases, tRNA modification enzymes, translation initiation and elongation factors, the termination factor mTERF or release factors, have to be imported from the cytoplasm of the cell (Gaspari et al., 2004). An estimated total number of 150 cytosolic proteins is required to translate the 13 mitochondrial encoded proteins (Rotig, 2011). Until now, the complete translation apparatus is not entirely identified, and no complete functional *in vitro* translation system is established, comprising the four phases: initiation, elongation, termination and release of final polypeptide and recycled ribosomes. Mitochondrial translation is different from the cytosolic counterpart, not only in translating alternative codons, e.g., the stop codon UGA codes for tryptophan and AUA codes for methionine instead of isoleucine. In contrast to cytosolic ribosomes, which consist of 50-60% RNA, the mitochondrial ones comprise only 25-30% RNA (Christian and Spremulli,

2011). Together with the ribosomal proteins, they build up two ribosomal subunits, 28S and 39S, with a total size of 55 S.

Two mitochondrial initiation factors, $IF2_{mt}$ and $IF3_{mt}$, have been identified. According to the current knowledge of translation initiation, IF3 binding dissociates the 55S complex, resulting in a 28S:IF3 complex. GTP-bound IF2 joins the complex, followed by mRNA and fMet-tRNA, although the order of binding is yet not clear. The 5' end of the mRNA localizes at the P-site of the ribosome, where it is scanned for its start codon. The large 39 S subunit assembles in case of presence of the correct codon. Accompanied by hydrolysis of GTP to GDP, the IFs split and leave the 55S:fMet-tRNA:mRNA complex for subsequent elongation (Christian and Spremulli, 2011). GTP-bound elongation factor Tu (EF-Tu) binds then to aa-tRNA and enters the A-site of the ribosome. By cognate codon-anticodon interactions it is accepted and thereby provokes hydrolysis of GTP to GDP and release of EF-Tu:GDP. This complex is re-activated by elongation factor Ts, which forms an intermediate EF-Tu:EF:Ts complex and enforces a GDP exchange to GTP. At the ribosome, a peptide bond formation is catalyzed, resulting in a deacylated tRNA at the P-site and a peptidyl-tRNA at the A-site, with one additional amino acid. Another elongation factor (EF-G1) catalyzes the removal of the deacylated tRNA and translocation of the peptidyl-tRNA from the A-site to the P-site. Cryo-EM data suggest a lacking E-site in the mitochondrial translation machinery (Christian and Spremulli, 2011). The two codons UAA and UAG were assumed to serve as stop codons, while the third cytoplasmic standard stop codon UGA codes for tryptophan in human mitochondria. A recent study revealed that the stop codons UAA and UAG promote a -1 frameshifting, which moves them to the A-site, where they can be recognized by the release factor mtRF1a (Temperley et al., 2010). In presence of GTP, this factor promotes the hydrolysis of the peptidyl-tRNA bond and the release of the final polypeptide. The ribosome recycling factor $RRF1_{mt}$ binds in combination with $RRF2_{mt}$ to the ribosome and triggers ribosome dissociation into the subunits, accompanied by liberation of mRNA and deacylated tRNA, followed by RRF1 and RRF2 release (Christian and Spremulli, 2011).

1.2 Mitochondrial tRNAs

1.2.1 tRNA Function

Transfer RNAs hold a fundamental role in the translation of mRNA in proteins, by transferring the appropriate amino acid to the translation machinery, based on a specific mRNA codon. The attachment of the specific amino acid to the acceptor stem of the tRNA is catalyzed by specific enzymes, the aminioacyl-tRNA-synthetases (aaRS). Different tRNAs, which can be recognized by the same aaRS, are called isoacceptors. Whereas in humans all 22 tRNAs are encoded by the mitochondrial genome, 19 aaRS are encoded by the nucleus and have to be imported from the cytoplasm (Sissler et al., 2008). So far, no corresponding aaRS for $tRNA^{Gln}$ has been identified in the nuclear genome, and Gln-$tRNA^{Gln}$ synthesis by an indirect mitochondrial pathway was suggested (Nagao et al., 2009). While most mitochondrial aaRS genes are mitochondria-specific, the two genes for LysRS and GlyRS are shared for cytosolic and mitochondrial tRNA aminoacylation, and are dedicated to their target by alternative splicing or alternative translation initiation (Tolkunova et al., 2000). According to their structures, aaRS are subdivided into two different classes: class I enzymes possess the typical Rossmann fold, an ATP-binding site, and class II enzymes include three structural motifs (motifs 1, 2 and 3) (Yadavalli and Ibba, 2012).

Besides the key function in protein synthesis (Weisblum, 1999), tRNAs as well as aaRS are involved in other processes, e.g., aaRS were found to cause inflammation-responsive gene-specific translational silencing (Sampath et al., 2004). tRNAs are able to regulate aaRS expression (Ryckelynck et al., 2005) and can act as primer for reverse transcription of RNA genomes, e.g., the HIV genome (Barat et al., 1989). In case of amino acid deficiency, the uncharged tRNA can up-regulate the amino acid synthesis (Wek et al., 1989). $tRNA^{Met}$ was identified as splicing regulator of pre-mRNA in the nucleus. Recently, cytosolic and mitochondrial tRNAs were shown to bind to cytochrome *c* and thereby regulate the sensitivity of the cell to cyt*c* induced apoptosis (Mei et al., 2010b). Mutations in aaRS and tRNA can cause mitochondrial disease (see *chapter 1.3*).

1.2.2 tRNA Structure

A principle in molecular biology is that form follows function, and inversely, knowledge of a molecule's structure leads to better understanding of its function. Classical cytosolic tRNAs show a highly conserved primary structure among mammals (within a tRNA species), a typical secondary cloverleaf structure with defined sizes of loops and stems and a L-shaped tertiary structure with intricate tertiary interactions between conserved nucleotides. They possess many characteristic base modifications, which are added posttranscriptionally by specific tRNA modification enzymes and are essential for structure and function (Motorin and Helm, 2010). Mitochondrial tRNAs hold this typical characteristics, with the exception of human mt tRNAs or rare other cases, in which they form bizarre structures, as shown for *Caenorhabditis elegans* (Wolstenholme et al., 1987) or *Ascaris suum* $tRNA^{Ser}$ (Ohtsuki et al., 2002). Human mitochondrial tRNAs retain several characteristics, but also exhibit some bizarre features, as detailed below. Further clarification of mitochondrial tRNA structures is a necessary basis for gaining a deeper and more detailed insight in molecular processes mt tRNAs are involved in, in which way they interact with maturation enzymes, modification enzymes, elongation factors or ribosomal proteins.

1.2.2.1 Primary Structure

Consisting of about 70 nucleotides, mitochondrial tRNAs are in general shorter than their nuclear counterparts with 70–95 nucleotides. Depending on their gene location on the heavy or light DNA strand, mt tRNAs contain less C or G nucleotides. Hence, the 8 tRNAs transcribed from the light strand are poor in cytosine residues and designated heavy tRNAs, the 14 tRNAs encoded by the heavy strand are poor in guanines and called light tRNAs (Florentz et al., 2003). Therefore, CpA and UpA sites are more frequently present in light tRNAs, and these sites are very sensitive to degradation (Florentz et al., 2003). In heavy tRNAs, a higher non-common G·U pairing is found. The 3' CCA sequence is not encoded by the mt genome and has to be added enzymatically by tRNA nucleotidyltransferase.

Compared to cytosolic tRNAs, much less nucleotide positions are conserved in mt tRNAs. Most of this few strongly conserved positions play a role in folding of the tertiary structure (Helm et al., 2000). By vertical tRNA sequence alignments within 31

mammalian mt tRNA sequences, Helm et al. revealed a differing extent of conservation among the different tRNA species. Whereas $tRNA^{Asn}$ primary sequences share the lowest sequence identity, the strongest conservation was found for $tRNA^{Met}$, $tRNA^{Ile}$ and both $tRNA^{Leu}$ species (all are light tRNAs). Most strictly conserved nucleotides or whole regions concern the D-stem, the anticodon-loop and -stem or the T-stem.

1.2.2.2 Secondary Structure

The classical tRNA secondary structure shapes a cloverleaf with the typical four branches: the acceptor arm is terminated by the sequence CCA, to which the amino acid is attached, the D- and T-arms (named for the presence of specific modifications) and the anticodon arm, containing the anticodon triplet (*figure 1.3*).

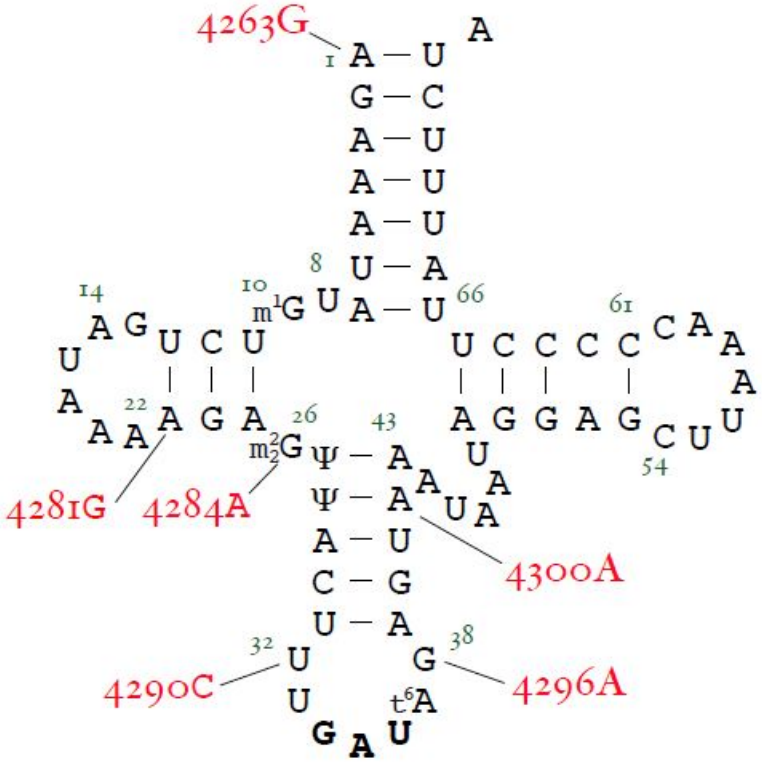

Figure 1.3. *Human mitochondrial $tRNA^{Ile}$ sequence including modifications in the typical secondary cloverleaf structure. Highlighted positions (in red) show the mutations analyzed in this study and the numbers refer to their position in mtDNA (*http://www.mitomap.org/MITOMAP*). Nucleotide numbering indicated (in dark green) is referred to the international standard tRNA numbering.*

20 of the 22 mt tRNAs fold into a cloverleaf-like structure, but the two isoacceptors for serine do not. The canonical tRNAs show a 7-bp acceptor stem, followed by a 2-nt connector, a 4-bp D-stem and D-loop differing in size, a single nucleotide connector, a 5-bp anticodon stem with a 7-nt anticodon loop, a variable loop and a 5-bp T-stem and T-loop differing in length. In contrast to the cytoplasmic and prokaryotic tRNAs with a variable loop of up to 23 nucleotides in size, the variable loop of mt tRNAs are much smaller, consisting of 4-5 nucleotides only (Putz et al., 2007). $tRNA^{Ser(AGY)}$ exhibits a bizarre structure without any D-arm. $tRNA^{Ser(UCN)}$ shows a four-branched structure with an extended anticodon stem by an additional base pair added to the five canonical ones, and the connector between acceptor stem and D-stem consists of one nucleotide only (Helm et al., 2000; Yokogawa et al., 1991).

In the secondary structure of mt tRNAs, G-U base pairs and mismatches are frequently tolerated. Whereupon light tRNAs are poor in G-U and rich in mismatches, heavy tRNAs are poor in mismatches, but rich in G-U base pairs. No mismatch was found for the base pairs at positions 12-23 and 11-24 in the D-stem of any mammalian mt tRNA, suggesting them as the most strictly conserved secondary interactions. In contrary, the bases next to the D- and T-loop, which are positions 53-61 and 13-22 of the D- and T-stem respectively, are most often engaged by noncanonical interactions. The weak pairing opens the possibility to enlarge the D- and T-loop. The mismatches seem to happen randomly but occupy positions, which are not exposed to selective pressure, as they seem not to be essential for structure and therefore function of the tRNA (Helm et al., 2000). The weak pairing also reflects the low melting temperature of the secondary structure found for human mitochondrial tRNAs (Yokogawa et al., 1989), which is counterbalanced by extensive nucleotide modifications (see *chapter 1.2.3.3*).

1.2.2.3 Tertiary Structure

In classical tRNAs, nine long range tertiary interactions between distinct positions lead to a L-shaped tertiary structure. Specified, this interactions are the triple interactions U8-A14-A21, 9-23-12, 25-10-45, 13-22-46 and the pair interactions R15-Y48, G18-Y55, G19-C56, 26-44 and T54-A58 and the conservation of the anticodon nucleotides Y32, U33 and R37 plus base-pair G53-C61.

Most mitochondrial tRNAs hold only some of these classical interactions, specifically the pairing of the core unit with the base interactions 25-10-45, 9-23-12, 26-44 and frequently U8-A14-A21 and 13-22-46. With the exception of $tRNA^{Leu(UUR)}$, $tRNA^{Leu(CUN)}$, $tRNA^{Asn}$ and $tRNA^{Gln}$, the three classical interactions between the D- and T-loop are not present in mitochondrial tRNAs (Helm et al., 2000). It is not yet clear how they anyway accomplish the L-shape folding, whether they just interact in a weaker manner or feature alternative interactions. Beside a few studies of tertiary interactions of mt tRNAs by sequence alignments (Helm et al., 2000) or structural probing (Messmer et al., 2009), many questions remain unanswered.

1.2.3 Biogenesis of tRNA

tRNA genes are scattered around the mitochondrial genome between the mRNA and rRNA genes (Ojala et al., 1981). They must be released from the primary polycistronic transcripts (see *chapter 1.1.7*) by processing enzymes: RNase P at the 5' end and RNase Z at the 3' end of the tRNA sequence, whereby also the mRNA and mRNA species are released. Subsequently, tRNAs are modified at certain nucleotides, CCA trinucleotide is added at the 3' end and the mature tRNA can then be aminoacylated by aaRS.

1.2.3.1 5' Processing

The universal 5' processing enzyme RNase P exists in many variants and latest findings are very fascinating from the evolutionary point of view. A long time it was believed that they are ribozymes only, consisting of a catalytical RNA subunit and a varying number of additional proteins, as found, e.g., in bacteria and the eukaryotic *Saccharomyces cerevisiae* or in the human nuclear system (Stark et al., 1978).

Recently identified, human mitochondrial RNase P was the first member of an apparently large group of proteinacious RNase P enzymes. Human mt RNase P consists of three protein subunits: the metallonuclease MRPP3, later referred to as PRORP (proteinaceous RNase P), with the complementing subunits MRPP1 (TRMT10C) and MRPP2 (SDR5C1), and the trilogy is active without any RNA component (Holzmann et al., 2008). MRPP1 is a methyltransferase homolog to the yeast TRM10 and is involved in tRNA methylation at nucleotide position 9 (Vilardo et

al., 2012). Its role in processing activity remains elusive, but a role in substrate recognition is speculated and may base on the bizarre structures of mitochondrial tRNAs (Rossmanith, 2011b). The third component of human mitochondrial RNase P, MRPP2, is a hydroxysteroid (17-β) dehydrogenase 10 (HSD17B10), which is best known for branched-chain amino and fatty acid degradation. The link of this protein's function to tRNA processing is still unclear. The enzyme activity of mitochondrial RNase P is similar to its nuclear counterpart: it binds to a tRNA precursor, requires the cation Mg^{2+} and generates 5' phosphate and 3' hydroxyl ends (Holzmann et al., 2008).

Further studies revealed that this proteinaceous enzyme is not the exception, but the first example of PRORP enzymes: plants, algae and several protists carry homologs of the nuclease MRPP3/ PRORP in their genome, which are apparently active in mitochondrial processing without any additional subunit (Rossmanith, 2011b), as explicitly shown for chloroplast and mitochondrial RNase P of *Arabidopsis thaliana* (Gobert et al., 2010). The complex three-component protein assembly of human mitochondrial RNase P appears to be the exception and the single protein enzyme the rule.

1.2.3.2 3' Processing

RNase Z is responsible for 3' processing of tRNA precursors and can present in a long (RNase Z(L)) and a short form (RNase Z(S)) in eukarya. In human cells, RNase Z(S) is only found in the cytosol, whereas RNase Z(L) locates to the nucleus and to mitochondria, where it acts endonucleolytically (Rossmanith, 2011a). Silencing of the RNase Z coding gene ELAC2 leads to impaired 3' processing of different mitochondrial tRNAs (Brzezniak et al., 2011). Recent research showed that the two different forms are generated by alternative translation initiation of ELAC2 (Rossmanith, 2011a). Evolutionary, RNase Z seems to be more conserved than RNase P; all hitherto identified tRNA 3' end processing endonucleases belong to the same family, which is a subgroup of the β–lactamase superfamily.

In independent analyses, the succession of RNase P and RNase Z tRNA processing activity was not described homogeneously and may depend on the organism, the cell type, or the substrate (Rossmanith, 2011b). Nevertheless, RNase Z activity follows RNase P activity in most cases. Also in mammalian mitochondria, RNase P activity

apparently precedes RNase Z activity. RNase Z does not cleave substrates carrying an additional 5' leader but only 5' processed substrates (Manam and Van Tuyle, 1987).

1.2.3.3 Posttranscriptional Modifications

Mitochondrial tRNAs are less modified than their cytoplasmic counterparts, but still they carry a variety of different modifications. Emanating from a low melting temperature of the tRNAs' secondary structure, they have to be modified at particular nucleotide positions for structural and functional reasons, catalyzed by specific modification enzymes (Helm, 2006; Motorin and Helm, 2010). Whereas modifications on the D- or T-arm are considered to be relevant for correct folding of the tRNA, the anticodon loop modifications ensure accurate codon-anticodon interactions (Suzuki et al., 2011). The modifications occur sequentially, with the nucleotides of the acceptor domain being modified first, thereby stabilizing the T-loop and enhancing D- and T-loop interactions. These structural interactions facilitate modifications at the anticodon (Helm, 2006). Until now, in 11 mitochondrial tRNAs 16 different modifications at 18 positions are described, of which three are mitochondria-specific (5-formylcytidine, 5-taurinomethyluridine and 5-taurinomethyl-2-thiouridine) (Suzuki et al., 2011). Of the characterized modification enzymes, many are of bacterial origin, and therefore function mitochondria-specific, whereas some are shared with the cytosolic tRNAs.

Hypomodifications can cause mitochondrial disease, as shown for a lacking Wobble base modification in case of the MELAS causing 3243A>G mutation in $tRNA^{Leu(UUR)}$ or the MERRF causing $tRNA^{Lys}$ mutation 8344A>G. They showed a pathological effect in different cell types (Yasukawa et al., 2005). Also other MELAS causing mutations in $tRNA^{Leu(UUR)}$ were shown to be accompanied by the missing modification at the anticodon, leading to speculations that this might be the underlying reason for the clinical presentation (Kirino et al., 2005).

1.2.3.4 CCA Adding

The CCA trinucleotide sequence, which is found at the 3' end of mitochondrial tRNAs, is not encoded by the mitochondrial genome, but must be added by the CCA adding enzyme or ATP(CTP):tRNA nucleotidyltransferase. The enzyme acts dually,

extending also the cytosolic tRNAs. The CCA addition is a necessary process for tRNA aminoacylation (Nagaike et al., 2001; Reichert et al., 2001) .

1.2.4 tRNA^{Ile}

Human mitochondrial tRNA^{Ile} is 72 nucleotides in length (including the CCA 3' end, which is not encoded by mtDNA) and can read the codons AUU and AUC with its anticodon GAU (*figure 1.3*). The heavy strand-encoded light tRNA possesses a high A-U content (72%) compared to its cytosolic twin (40%), but very low G-content in the D-loop. The melting temperature was determined to 59 °C, which is much lower than that of bacterial transcripts with >70 °C (Kelley et al., 2000). tRNA^{Ile} lacks most of the characteristically conserved sites for tertiary structure folding, like the canonical 9A-12A/U-23U/A nucleotides. Only the tertiary interaction T54-A58 is present (Helm et al., 2000). Amongst others, to stabilize the apparently weak structure, the molecule is six times modified, with the methylation m^1G9, the double methylation m^2_2G26, the both pseudouridines Ψ27 and Ψ28 and the threonylcarbamoylation t^6A37 (Suzuki et al., 2011). Modifications of tRNA^{Ile} are essential for efficient aminoacylation of the molecule (Degoul et al., 1998).

1.3 Mitochondriopathies

Mitochondrial diseases are characterized by mitochondrial dysfunction, which are caused by mutations in either the nuclear or the mitochondrial genome. Frequently, mutations result in symptoms concerning the neuromuscular system, but in the end any kind of tissue or organ can be affected. Diverse clinical symptoms can present. According to their high energy demand, muscle and nerve cells highly depend on functioning of the respiratory chain. Therefore, they are more frequently affected. Patients (1) can express complex multisystem disorders, including besides neuropathies and myopathies, e.g., deafness, diabetes, headache or seizures, (2) can show widespread lesions including myopathies, encephalomyopathies, or cardiopathies, or (3) can develop single organ disorders, e.g., an isolated cardiomyopathy or LHON (Leber's hereditary optic neuropathy), affecting exclusively

the optic nerve. The disease can present at any age, in childhood as well as in adulthood, and can be caused by nuclear and mitochondrial mutations, given the dual genetic origin of the respiratory chain and the solely nuclear origin of all other mitochondrial molecules (Munnich and Rustin, 2001; Zeviani and Di Donato, 2004). Biochemical and morphological indications are in many cases detectable, like a dysfunction of respiratory chain subunits or the typical red ragged fibres (RRFs), an accumulation of abnormal mitochondria under the sarcolemmal membrane, which appear red, when the muscle is stained with Gomori trichrome stain (Engel, 1963). Characteristically, the RRFs are combined with COX-negative staining, due to an impaired respiratory chain (Dimauro and Davidzon, 2005).

Currently, it is established to speak of mitochondrial diseases if a mutation, either present in the nuclear or the mitochondrial genome, interferes with the respiratory chain. The disease causing mutation may also have an effect on mitochondrial systems like the citrate cycle or β-oxidation, but they are assigned to another category, the metabolic diseases, and are not further discussed in this work.

The respiratory chain diseases may be caused by mutations, which affect the respiratory chain directly or else indirectly. Mutations in polypeptide subunits of the respiratory chain or mutations, which affect the assembly of the OxPhos complexes, count as direct effects, whereas an indirect impact of mutations attack the stability of mtDNA or the intramitochondrial protein translation (Park and Larsson, 2011; Schon and DiMauro, 2007). Both kinds of consequences can originate from mutations in nuclear or mitochondrial DNA, given the mosaic genetic origin of the respiratory chain and the mitochondrial translation machinery, and the genetically nuclear origin of respiratory chain assembly factors or other mitochondrial factors for, e.g., maintenance.

1.3.1 Nuclear DNA Mutations

Mitochondrial disorders follow a Mendelian inheritance, when the pathogenic mutations are present in the nuclear genome (Calvo et al., 2006; Zeviani and Klopstock, 2001), more precisely in the approximately 1500 genes, whose products are imported into mitochondria (Spinazzola and Zeviani, 2009). The mutations can comprise those in subunits of the respiratory chain subunits, in proteins responsible

for the assembly of the complexes (Diaz et al., 2011), in proteins required for the biogenesis or maintenance of either mitochondria themselves, like OPA1, a main player in mitochondrial fusion (Duvezin-Caubet et al., 2006), or mtDNA, like mutations in polymerase gamma, which is the core enzyme of the mitochondrial replisome (Hudson and Chinnery, 2006). Moreover, they comprise proteins, which are required in tRNA metabolism by affecting tRNA modification, processing, expression or functioning in translation, e.g., in case of mutated aminoacyl-tRNA-synthetases (Suzuki et al., 2011).

1.3.2 Mitochondrial DNA Mutations

In contrast to nuclear mutations, which are inherited according to the Mendelian rules, mitochondrial mutations are maternally inherited solely (Giles et al., 1980). That means, an affected mother passes the mutation on to all her children, but only the daughters will transmit the mutation to their children. Unusual cases were reported, in which mtDNA was inherited paternally in mice over several generations of interspecific backcross, and paternal inheritance of mtDNA was also detected in humans (Schwartz and Vissing, 2002). But in fact, mtDNA copy number declines strongly during spermatogenesis. The molecular mechanism of this reduction process is still unclear. Recently, it was shown in *Drosophila melanogaster* that an endonuclease is involved in this active mechanism (DeLuca and O'Farrell, 2012). In cow and monkey, it was shown that paternal mitochondria are tagged by the recycling marker ubiquitin after fertilization, suggesting an additional active elimination mechanism (Sutovsky et al., 1999).

The prevalence of mitochondrial disorders is estimated to 1:8500 on average (Chinnery and Turnbull, 2001). A study, in which the prevalence of 10 different pathogenic mtDNA mutations was analyzed, revealed that 1 in 200 newborns carried at least one of the 10 mutations, with the potential to pass the mutation on to their offspring or to develop a mitochondrial disease theirselves (Elliott et al., 2008).

Mutations in the mitochondrial genome had first been described in 1988 (Holt et al., 1988; Wallace et al., 1988; Zeviani et al., 1988). They may occur in every mitochondrial gene, the 13 mitochondrial encoded subunits of the respiratory chain, the 22 tRNAs and the 2 rRNAs. Effects on respiratory chain activity are obvious,

because the tRNAs and rRNAs are players in the intramitochondrial protein synthesis, translating the 13 mRNAs into respiratory chain subunits. As consequences of mutations, the ATP production can be impaired, the ratio of the reduction equivalents NADH/NAD^+ can be destabilized as well as the Ca^{2+} homeostasis, or increased ROS can be produced (Munnich and Rustin, 2001). Follow up effects of the mutations beyond affecting the respiratory chain functionality are conceivable. In mice, it was shown that an amino acid changing mutation in a protein coding gene can lead to degradation of the respective respiratory chain subunit, and that the resulting peptides can reach the cell surface, thereby developing to novel histocompatibility antigens (Loveland et al., 1990; Morse et al., 1996). Another interesting study associated cytosolic and mitochondrial tRNAs with apoptosis (Mei et al., 2010b). The researchers found a tRNA dependant regulation of cyt*c* induced apoptosis, which is accomplished by tRNA binding to cyt*c*, an electron carrier of the respiratory chain and pro-apoptotic stimulator when released from mitochondria to the cytosol. Mutations in mitochondrial tRNAs might affect the tRNA:cyt*c* binding and contribute to the pathogenesis of a mitochondrial disorder, where no failure of the respiratory chain can be detected. However, this is only a discussed, but not proven hypothesis (Mei et al., 2010a).

MtDNA mutations can show as point mutation or as large scale rearrangements (partial deletions or duplications), the latter frequently causing KSS (Kearns-Sayre syndrome), PEO (progressive external ophthalmoplegia) or PS (Pearson syndrome). Whereas point mutations can be a spontaneous event or be inherited, large scale rearrangements are usually not inherited but occur sporadic at the germ-cell level or the very early development of the embryo (Zeviani and Di Donato, 2004). Concerning the point mutations, the literature differentiates between mtDNA mutations located in protein coding genes and those affecting mitochondrial protein synthesis. The latter are point mutations located in RNA coding genes (tRNA or rRNA). Typical diseases caused by point mutations and affecting translation are MELAS (mitochondrial encephalomyopathy, lactic acidosis and stroke-like episodes) or MERRF (myoclonus epilepsy and ragged-red fibers). Point mutations in protein-coding genes frequently cause LHON (Leber's hereditary Optic Neuropathy), Leigh syndrome or NARP (neuropathy, ataxia, retinitis pigmentosa). Nevertheless, clinical features are overlapping and therefore not very suitable to discriminate the possible groups of mutations, e.g., MELAS was also found to be caused by mutations in several

protein-coding genes and MELAS causing tRNA mutations were also associated with other syndromes (Brandon et al., 2005; McFarland et al., 2007). A broad spectrum of diseases is associated with mtDNA mutations (Larsson and Clayton, 1995; Munnich and Rustin, 2001; Zeviani and Di Donato, 2004). What makes their classification not easier is that different mutations can result in the same clinical pattern (Masucci et al., 1995; Rossmanith et al., 2008), while the same mutation in different probands can cause different clinical presentations. MtDNA mutates at a high frequency, and the majority of the mutations are silent polymorphisms without any pathogenic appearance. Hence, pathogenicity criteria have been constituted to prove the status of a new mutation (DiMauro and Schon, 2003). The mutation should be absent in a large control group of the same haplogroup and should locate at a conserved site with obvious functional importance. Furthermore, it should cause an impairment of the respiratory chain activity or the intramitochondrial translation in tissues or in a cybrid cell line. Based on the threshold effect, the degree of heteroplasmy (the contingent of mutated mtDNA molecules relative to the wild type mtDNA) should alter the clinical phenotype and the cell pathology. The degree can be determined in single muscle fiber analysis. The last rule indeed counts only for heteroplasmic mutations, and most of the pathogenic mutations are numbered among them. Homplasmic mutations are more difficult to diagnose, because they often escape the classical criteria. Furthermore, some mutations cause tissue-specific respiratory chain defects, which then cannot be easily demonstrated by available cell types like blood, muscle or fibroblasts (DiMauro and Schon, 2003). To establish a unique evaluation of mitochondrial mutations, a program was provided in 2004 that gives a defined pathogenicity score for a mutation (McFarland et al., 2004). The program was revised in 2011 (Yarham et al., 2011).

1.3.2.1 Homoplasmic Mutations

Homoplasmic mutations in mtDNA often cause stereotypical diseases with tissue specific diseases, often neurological symptoms, also if the mutation is present in different tissues. Thus, other factors must play a role in pathogenesis, like tissue-specific molecular mechanisms during development or an interaction with other genetic or epigenetic factors. Typical homoplasmic diseases are cardiomyopathy or LHON, the latter is in more than 90% of all cases caused by either the 11778G>A, the 3460A>G or the 14484T>C mutation in complex I genes of mtDNA (Zeviani and

Di Donato, 2004). Homoplasmic LHON-causing mutations (heteroplasmic LHON mutations have also been described) are transmitted to all offspring, but 50% of the male and only 10% of the female offspring develop the disease. The outcome must therefore be linked to nuclear genetic factors (Taylor and Turnbull, 2005). The homoplasmic 1555A>G mutation in the 12S rRNA gene caused deafness after exposure to aminoglycoside antibiotics, which demonstrated the possibility of an environmental impact (Prezant et al., 1993). Further studies of this homoplasmic mutation shed light on the pathological mechanism of the tissue-specific disease: multiple tissues of a mouse model showed increased methylation of the mitochondrial 12S rRNA. This hypermethylation caused ROS-dependent activation of the nuclear proapoptotic transcription factor E2F1 and apoptosis only in cell types of the inner ear. The mice developed a progressive E2F1-dependent hearing loss (Raimundo et al., 2012).

But still, the field of homoplasmic mtDNA mutations is not well understood, and the molecular mechanisms that determine the clinical phenotype, i.e., the pathogenesis in a specific tissue, remain to be discovered.

1.3.2.2 Heteroplasmic Mutations

Up to several thousand copies of the mitochondrial genome can be present in one cell. Based on this fact, mutations are frequently present in a heteroplasmic state, that is, wild type and mutant mtDNA coexist in one cell. In many cases, mitochondriopathies show up, when a distinct threshold is exceeded, thus a certain percentage of the mitochondrial genomes carry the disease causing mutation (the “threshold effect”). The threshold varies between different tissues, depending on the individual energy demand, and depends also on the kind of mutation. The bottleneck effect of the female germline is the reason for a varying degree of hetroplasmy in the offspring. Only a small fraction of all mtDNA copies in the germ cells is transmitted to the oocyte, and thereby can shift the genetic pattern (Jenuth et al., 1996). Given that the replication of the mitochondrial genome occurs randomly and independently of the cell cycle (Bogenhagen and Clayton, 1977), the “mitotic segregation” can sometimes change the clinical phenotype (Schon and DiMauro, 2007). Thus, a single mutation may expand clonally or can be lost during cell division and accordingly shift the phenotype, when an individual grows older.

Typical heteroplasmic diseases are MELAS (mitochondrial encephalomyopathy with lactic acidosis and stroke-like episodes), MERRF (myoclonic epilepsy with ragged red fibers), NARP (neurogenic weakness, ataxia and retinitis pigmentosa), CPEO (chronic progressive external ophthalmoplegia), Leigh syndrome or Leigh-like encephalopathies. Many symptoms, which are caused by heteroplasmic mutations, overlap with symptoms caused by homoplasmic mutations, like deafness, diabetes or myopathies (Taylor and Turnbull, 2005).

1.3.3 tRNA Mutations

tRNAs appear to be particular frequently affected by pathogenic mtDNA mutations. Since the first pathogenic mitochondrial mutation had been described in the end of the 80's, the number increased to more than 220. More than 150 of them are located in tRNA sequences, although tRNA genes comprise only 9% of the mitochondrial genome (Brandon et al., 2005; Stewart et al., 2008a). Pathogenic tRNA mutations are associated with various diseases and symptoms, e.g., encephalopathy, encephalomyopathy, Leigh syndrome, myopathy or chronic progressive external ophthalmoplegia.

As the main function of tRNAs is the transfer of the correct amino acid to the growing peptide chain located at the ribosomal complex, pathogenic tRNA mutations consequently affect the intramitochondrial translation, leading to an impairment of complexes I, III, IV or V or a combined failure (Smeitink et al., 2001). It can be evoked by different impairments in tRNA metabolism: a reduced tRNA stability (Glatz et al., 2011), impaired tRNA synthesis (Toompuu et al., 2002), a failure in tRNA precursor processing (Toompuu et al., 2004), reduced aminoacylation (Koga et al., 2011), missing modifications (Yasukawa et al., 2005) or a reduced interaction with EF-Tu (Hino et al., 2004), often accompanied by an altered structure of the tRNA (Hao and Moraes, 1997; Jones et al., 2008; Wittenhagen and Kelley, 2003). The mutations can appear in a homoplasmic state, resulting more in tissue-specific diseases with stereotyped syndromes, or in a heteroplasmic state, with diverse clinical phenotypes, depending on the mutation load, the location of the mutation and the affected tissue. Even cells within the same tissue show varying degrees of mutation load, resulting in a mosaic respiratory chain deficiency in affected tissues.

Although in all 22 mitochondrial tRNAs pathogenic mutations have been identified, their number differs, with $tRNA^{Leu(UUR)}$, $tRNA^{Ile}$ and $tRNA^{Lys}$ apparently being hot-spots for pathogenic mutations (http://www.mitomap.org/MITOMAP). MELAS is caused by $tRNA^{Leu(UUR)}$ mutations in 80% of the cases, which evidently manifests in the most frequently diagnosed tRNA mutation 3243A>G in the D-loop at a highly conserved site of $tRNA^{Leu}$. This mutation alters the structure and prevents modification of the Wobble position, resulting in an impaired aminoacylation (Li and Guan, 2010). The 8344A>G mutation in the T-loop of $tRNA^{Lys}$ leads to another typical mitochondrial disease: MERRF. It is caused by a defect in tRNA aminoacylation and hinders taurine modification in the anticodon-loop, thereby impairing codon-anticodon interactions (Enriquez et al., 1995). $tRNA^{Ile}$ is another hot-spot of pathogenic mutations, and the known mutations are described in the next paragraph.

1.3.4 $tRNA^{Ile}$ Mutations

To date, mutations at 22 different nucleotide positions in $tRNA^{Ile}$ have been linked to diseases (http://www.mitomap.org/MITOMAP), listed in *table 1.1* with their associated clinical patterns. When we started the project, only 13 mutations had been described. The huge number of meanwhile additionally detetcted mutations underline the hot-spot character of this tRNA. Only $tRNA^{Leu(UUR)}$ harbors more pathogenic mutations and $tRNA^{Lys}$ is similarly frequented, with 20 different nucleotide positions, according to the Mitomap database. The primary diseases caused by $tRNA^{Ile}$ mutations are cardiomyopathy and CPEO (chronic progressive external ophthalmoplegia). Of the 21 $tRNA^{Ile}$ nucleotide positions found mutated, nine are associated with cardiomyopathy. Among them, the 4300A>G mutation was found twice in two independent families, with heart being the only clinically affected organ (Casali et al., 1995; Taylor et al., 2003). In the other cases, cardiomyopathy was accompanied by a multiorgan disease (4269A>G, (Taniike et al., 1992)), a motoneuron disease (4274T>C, (Borthwick et al., 2006)), deafness (4277T>C and 4316A>G, (Chamkha et al., 2011; Perli et al., 2012)), a multisystem disorder (4284G>A, (Corona et al., 2002)), exercise intolerance or weakness (4295A>G, 4317A>G

Table 1.1. *Mutated nucleotide positions in $tRNA^{Ile}$ with their particular diagnosed diseases, detected homoplasmic or heteroplasmic states, i.e. 100% mutant mtDNA or mixed wild type and mutant mtDNA, and original references. hom=homoplasmic; het=heteroplasmic; CPEO=chronic progressive external ophthalmoplegia.*

nucleotide change	hom/het	disease	reference
4263A>G	hom	hypertension	(Wang et al., 2011)
4267A>G	het	myopathy, ataxia, deafness	(Taylor et al., 2002)
	het	CPEO	(Smits et al., 2007)
4269A>G	het	multiorgan disorders including cardiomyopathy	(Taniike et al., 1992)
4274T>C	het	CPEO	(Chinnery et al., 1997)
	het	motoneuron disease including cardiac and metabolic syndromes	(Borthwick et al., 2006)
4277T>C	hom	hypertrophic cardiomyopathy, deafness	(Perli et al., 2012)
	hom	hypertension	(Zhu et al., 2009)
4281A>G	het	recurrent myoglobinuria, rhabdomyolysis	(Emmanuele et al., 2011; Patchett and Grover, 2011)
4284G>A	het	multisystem disorder including cardiomyopathy	(Corona et al., 2002)
	het	MERRF	(Hahn et al., 2011)
4285T>C	het	CPEO, exercise intolerance	(Silvestri et al., 1996)
4290T>C	hom	encephalopathy	(Limongelli et al., 2004)
4291T>C	hom	metabolic syndromes including hypertension	(Wilson et al., 2004)
4295A>G	het	hypertrophic cardiomyopathy, exercise intolerance	(Merante et al., 1996)
	hom	hypertension	(Zhu et al., 2009)
	het	occipital stroke	(Finnila et al., 2001)
	hom	nonsyndromic deafness	(Gutierrez Cortes et al., 2012)
4296G>A	het	Leigh syndrome	(Cox et al., 2012)
4298G>A	het	rhabdomyolysis, myoglobinuria, myalgias	(Crimi et al., 2004)
	het	CPEO, multiple sclerosis	(Taylor et al., 1998)
4300A>G	hom	cardiomyopathy	(Casali et al., 1995)
	hom	cardiomyopathy	(Taylor et al., 2003)
4302G>A	het	CPEO, diabetes, multiple lipomas,	(Berardo et al., 2010)
4308G>A	het	CPEO, hyperCKemia	(Souilem et al., 2011)
	het	CPEO, exercise intolerance	(Schaller et al., 2011)
4309G>A	het	CPEO	(Franceschina et al., 1998)
	het	PEO, deafness, exercise intolerance	(Campos et al., 2002)
4314T>C	hom	hypertension	(Zhu et al., 2009)

del4315A	hom	CPEO	(Kornblum et al., 2008)
4316A>G	het	hypertrophic cardiomyopathy, deafness	(Chamkha et al., 2011)
4316A>TA		hypertension	(Zhu et al., 2009)
4317A>G	?	cardiomyopathy, weakness	(Tanaka et al., 1990)
	hom	hypertension	(Zhu et al., 2009)
4320C>T	het	hypertrophic cardiomyopathy, encephalopathy	(Santorelli et al., 1995)

(Merante et al., 1996; Tanaka et al., 1990)) and encephalopathy (4320C>T, (Santorelli et al., 1995). The 4316A>G mutation was found together with a 3395A>G missense mutation in the mitochondrial ND1 gene, and the authors suggest a synergistically effect of the two mutations, causing a cumulative negative effect (Chamkha et al., 2011). Eight different mutant nucleotide positions caused ophthalmoplegia, of which two were found twice in independent cases, the 4308G>A (Schaller et al., 2011; Souilem et al., 2011) and the 4309G>A mutation (Campos et al., 2002; Franceschina et al., 1998). The 4308G>A mutation was accompanied by hyperCKemia (Souilem et al., 2011) or exercise intolerance (Schaller et al., 2011). The 4309G>A mutation was reported to cause isolated CPEO in the first report (Franceschina et al., 1998), but additionally deafness and exercise intolerance in the second patient, which harbored also a second mitochondrial mutation in the 12S rRNA gene, 1555A>G (Campos et al., 2002), and again a cumulative effect of the both mutations is belike. The other patients showed nucleotide exchanges at positions 4267A>G (Smits et al., 2007), 4274T>C (Chinnery et al., 1997), 4285T>C combined by exercise intolerance (Silvestri et al., 1996), 4298G>A combined with multiple sclerosis (Taylor et al., 1998), 4302G>A combined with multiple lipomas and diabetes (Berardo et al., 2010) and a 4215A deletion, which was accompanied by another tRNA 5835G>A mutation (Kornblum et al., 2008). All the CPEO causing mutations were heteroplasmic in the patients, except for the deletion at position 4315, which however was accompanied by another tRNA mutation.

Apparently, hypertension is also frequently associated with $tRNA^{Ile}$ mutations: by screening the mitochondrial genome of a patient cohort suffering from hypertension, six $tRNA^{Ile}$ mutations were detected: 4263A>G, 4277T>C, 4295A>G, 4314T>C, 4216A>TA, 4217A>G and in the case of 4263A>G confirmed as pathogenic (Wang et al., 2011; Zhu et al., 2009). Besides this study, hypertension combined with further syndromic features was diagnosed for one additional mutation, 4291T>C (Wilson et

al., 2004). Deafness and encephalopathies are further pathologies of $tRNA^{Ile}$ mutations, found in more than one case.

1.3.5 Model Systems

For the purpose of studying the pathologies of mitochondrial mutations and their underlying disease mechanisms, appropriate model systems were desirable. Presently, no transfection system exists for mammalian mitochondria. This limits the possibilities in creating mouse models for mitochondrial disease. In some studies, naturally appearing mtDNA mutations were introduced into mouse embryos or mouse embryonic stem cell lines to generate transmitochondrial mito mice (Fan et al., 2008; Kasahara et al., 2006; Marchington et al., 1999; Nakada and Hayashi, 2011; Sligh et al., 2000), whereas in others nuclear genes were manipulated, which control or interact with mitochondrial DNA (Wallace, 1999).

Much effort has been made to create a mammalian *in vivo* model for mitochondrial diseases. Trifunovic et al. were successful in creating an mtDNA mutator mouse with a deficient proofreading function of polymerase gamma, which results in an accumulation of acquired point mutations (2004). Another group generated a similar mouse model and suggested that not the accumulation of mtDNA mutations, but large deletions of mtDNA molecules cause the phenotype of premature aging (Kujoth et al., 2005). It is highly discussed, whether the mutator mouse is an appropriate model for mitochondrial diseases or a model of ageing showing a premature ageing syndrome (Edgar and Trifunovic, 2009; Khrapko et al., 2006; Larsson, 2010). Mitochondriopathies are triggered by a monoclonal expansion of one single type of mutation, whereas ageing is accompanied by an accumulation of different mitochondrial mutations at lower levels. In fact, the mutator mouse model was helpful in throwing light on evolutionary questions concerning mtDNA mutations. Stewart et al. analyzed the maternal transmission of random point mutations of mutator mice, and they found that mutations in tRNA and rRNA genes are much better tolerated than amino acid replacement mutations, which are strongly sorted out (2008b). An appropriate mouse model is especially helpful in studying tissue specific diseases. A recently published study is a nice example: the authors analyzed the pathogenic mechanism of a tissue-specific disease caused by the homoplasmic mutation

1555A>G in the 12S rRNA. The authors were able to show that the deafness was caused by a hypermethylation of the mitochondrial 12S rRNA by the methyltransferase mtTFB1 (Raimundo et al., 2012). Transgenic-mtTFB1 mice also showed this hypermethylation in multiple tissues, whereas the thereby caused activation of the nuclear proapoptotic transcription factor E2F1 only was found in cell types of the inner ear. The mice developed a progressive E2F1-dependent hearing loss. To uncover the nuclear genes involved in the pathogenic mechanism, they at first used patient-derived 1555A>G cells, which were cybrid cell lines, another well-established model, described in the following chapter.

1.3.5.1 The Cybrid Model

A fundamental milestone was achieved in 1989, when King and Attardi established a new model for studying mitochondrial disease by repopulating human cells lacking mtDNA with exogeneous mitochondria, and thereby changing the respiratory phenotype of the host cell (1989). This cytoplasmic hybrid cell model is commonly used to analyze mtDNA mutations (Vithayathil et al., 2012). Cybrids are generated by fusion of patient cells, harboring a suspected pathogenic mutation in the mitochondrial genome, to a *rho*^{0} host cell line, which is depleted of mitochondrial DNA by prolonged ethidium bromide treatment. Nuclear markers allow the selection of cells containing the host cell's nuclear background, and determination of the mitochondrial genotype of different clones allows selection of cells, which carry the mitochondrial mutation. Respiratory chain disturbances in these cybrid cell lines, containing a nuclear background different from the patient's one, definitely confirm the pathogenic character of the mitochondrial mutation and exclude the responsibility of the nuclear genome. These cybrid cell lines moreover allow the characterization of the molecular and cellular mechanisms of mtDNA mutations. In case of heteroplasmic mutations, the generation of homoplasmic cybrids makes it possible to analyze the pathogenesis on homogeneously mutated cells, without an impact of wild type mtDNA on the phenotype. Furthermore, the introduction of a neutral nuclear background facilitates a direct comparison of the effects caused by different mtDNA mutations. The cybrid technology has also been used to study the involvement of mitochondria in cancer development (Kaipparettu et al., 2010) or neurodegenerative disorders like Alzheimer disease (Onyango et al., 2006) or Parkinson disease (Esteves et al., 2010).

The classical host cell to study mitochondrial diseases is the 143B TK^- osteosarcoma cell line. The neuronal cell lines NT2 and SH SY5Y are primarily used to study neurodegenerative diseases. The osteosarcoma cell line is thymidine kinase-negative and therefore cannot incorporate the toxic thymidine analogue bromodeoxyuridine (BrdU), which is deployed as selection marker. The 143B206 TK^- osteosarcoma cell line is the corresponding *rho*^{0} cell line, depleted of mitochondrial DNA and nevertheless viable, but reliant on pyruvate and uridine supplement (King and Attardi, 1989). The pyruvate dependence is based on an elevated conversion of pyruvate into lactate by anaerobic glycolysis, which is catalyzed by lactate dehydrogenase. During this step, $NADH/H^+$ is regenerated into NAD^+, which is required for glycolysis. Additionally, due to elevated pyruvate consumption in *rho*^{0} cells, the citrate cycle is deprived of pyruvate, leading to a constricted function. Exogeneous pyruvate addition helps to maintain this metabolism. Uridine addition is necessary, because the enzyme dihydroorotate dehydrogenase, catalyzing a step in pyrimidine synthesis, is dependent on a functional respiratory chain. This enzyme cascade is not present in mtDNA-less cells, and cells are therefore reliant on an external pyrimidine source (Moraes et al., 2001).

Platelet cells of the patient frequently serve as mtDNA donor, because they do not contain a nucleus. Other cell types have to be enucleated to obtain cytoplasts, before they are fused to the host cell line. After fusion, a nuclear marker in the host cell allows selection against the donor cell nuclear DNA. After selection, the resulting cybrid cell pool represents a mixture of homoplasmic and heteroplasmic cells. Genotyping of different clones allows the selection of the desired cell species, which only contain mutated mtDNA or solely wild type mtDNA molecules.

The homoplasmic clones contain the nuclear background of the chosen host cell and the mitochondrial genome of the patient. This technique provides a model system, which makes it possible to analyze the effects of different mtDNA mutations comparably in a uniform nuclear background (Vithayathil et al., 2012).

2. Aim of the Project

Mitochondrial diseases show a huge variability and heterogeneity of tissue-specific and multisystemic symptoms. This also true for clinical patterns caused by mutations in the same mitochondrial gene, and the pathogenic mechanisms are largely unknown. The $tRNA^{Ile}$ gene is frequently affected by pathogenic mutations, which mainly cause ophthalmoplegia or cardiomyopathy. We comparatively analyzed five $tRNA^{Ile}$ mutations in the 143B osteosarcoma cybrid cell model.

4281A>G caused ophthalmoplegia and exercise intolerance, 4284G>A a multisystemic disorder including cardiomyopathy, 4290T>C and 4296G>A caused neurological disorders and 4300A>G isolated cardiomyopathy.

The goal of our study was first, to describe and characterize the unpublished mutations 4281A>G and 4296G>A on a cellular and molecular level. Second, we wanted to gain a better understanding of the different molecular mechanisms, which underlie pathogeneses, by analyzing molecular and cellular consequences of the five mutations comparatively.

3. Case Reports

The clinical pictures caused by the mutations 4284G>A (Corona et al., 2002), 4290T>C (Limongelli et al., 2004) and 4300A>G (Casali et al., 1995; Davidson et al., 2009; Taylor et al., 2003) were previously described. The 4284G>A mutation resulted in a multisystem disorder, the 4290T>C mutation caused a neurological disorder and the 4300A>G mutation isolated cardiomyopathy.

The other two mutations 4281A>G and 4296G>A were recently characterized in collaboration with Reginald Bittner, Michael Freilinger and Vassiliki Konstantopoulou, and the cases are unpublished, albeit both mutations have meanwhile been independently found in other patients (Cox et al., 2012; Emmanuele et al., 2011). The patient, who carried the 4281A>G mutation was diagnosed a different disease with similar symptoms to our patient and the clinical pattern caused by the 4296G>A substitution was also similar in both cases.

3.1 m.4281A>G

The mutation 4281A>G was found in a girl suffering from CPEO, a chronic progressive external ophthalmoplegia, and general exercise intolerance. Apart from that, she developed normal. The mitochondrial myopathy was diagnosed when she was 7 years old. Staining of a muscle biopsy showed numerous RRFs (ragged red fibers) and COX-negative fibers, and a biochemical analysis indicated a complex impairment of the respiratory chain. By screening of the mitochondrial genome, the heteroplasmic 4281A>G transition was detected, with 78% of the genomes affected in muscle and 15% in blood. In single muscle fiber PCR analysis, cytochrome *c* oxidase deficiency strictly correlated with high levels of the mutation. The A to G

transition was also detected in hair cells, urine sediment and mucosa of the patient. The mutation is a sporadic one, as neither the parents nor the siblings of the patient carried it. The blood count further revealed a slight anemia, increased creatine kinase, pyruvate and lactate levels, typical indicators for mitochondrial disease.

Emmanuele et al. described a recurrent myoglobinuria in a patient carrying the same mutation (2011). The mutation was heteroplasmic, showing a mutation load of 46% in muscle biopsy. The clinical symptoms were comparable, and the mutation was not found in family members.

3.2 m.4284G>A

In brief reflection, the hetroplasmic 4284G>A transition caused a multisystem disorder in a family (Corona et al., 2002). The proband showed a pure spastic paraparesis, while his brother died at 27 years of age of heart failure. Besides the rapidly progressive cardiomyopathy developing from age 25, the brother suffered from petit mal epilepsy, myoclonic jerks of the facial muscles, diverse neurological symptoms, hearing loss, a change of mood and personality, mental deterioration, diabetes mellitus type 2, a lipoma on the back of the neck and a hypogonadal appearance. The muscle biopsy did not show RRFs (ragged red fibers), but biochemical assays disclosed a dramatic decrease of complex IV activity and a slight decrease of complex I and V activity. The probands' mother also suffered from hearing loss, type 2 diabetes mellitus, a complex neurological syndrome, proximal muscle weakness, severe ophthalmoparesis and a mild mental deterioration. Biochemical analysis of the muscle biopsy revealed a combined reduction of complex I and IV activities. The mutation load was 55% in the proband's muscle, 80% in his mother's and 90% in his brother's muscle. Additional family members of the mother's lineage developed diabetes mellitus type 2, hearing loss, muscle dystrophy or encephalopathy.

3.3 m.4290T>C

The homoplasmic 4290T>C transition was found in sisters, causing a bilateral necrotizing encephalomyelopathy (Limongelli et al., 2004). The mutation was detected in muscle, fibroblasts and lymphocytes. The patient developed a blurred vision, diplopia, headache, vertigo and a general malaise and weakness at age of 16. During a few weeks she gained more than 10 kg of body mass and showed hypertension with impaired glucose tolerance. In muscle biopsy, neither RRFs nor COX-depleted fibers were detected, but biochemical assays revealed a reduced complex I and IV activity. The younger sister developed a similar clinical pattern already at age of 6, with a more severe phenotype. Additionally, she showed developmental delay with impaired cognitive and fine motor skills. Diverse neurological symptoms followed in the subsequent years. The younger sister died at age of 21 of respiratory failure. Muscle biopsy neither showed specific changes in this patient, but the biochemical analysis also showed an impairment of complex I and IV. A third and elder sister died unexpectedly at age of 1 year of respiratory arrest after a minor viral infection. An autopsy showed a degeneration of the brainstem with abnormalities in the mesencephalon. Surprisingly, the mother of the three sisters did not show neurological symptoms, changed neurological parameters in the physical examination or alterations in the muscle biopsy, although she was a mutation carrier. The homoplasmic mutation was present in her fibroblasts and skeletal muscle and almost homoplasmically expressed in her lymphocytes (97%), and complex I and IV of the respiratory chain showed reduced activities.

3.4 m.4296G>A

The patient harboring the 4296G>A mutation showed a Leigh-like slowly progressive neurodegenerative encephalopathy. He showed first symptoms at the beginning of adolescence (11 years old) with a progressive extrapyramidal cognitive pathology. His concentration, memory and perception capability were decreased, with a massive detraction of cognitive functions, a paresis (ophthalmoplegia) and rigor of limbs. In

his case, muscle biopsy did not reveal any histochemical or biochemical mitochondrial deficiencies. The level of the 4296G>A mutation was nearly homoplasmic in muscle (95%) and heteroplasmic in skin (84%) and blood (66%). Neither his siblings nor his parents carried the mutation. During the start of this study, it was not clear whether this mutation could really be assigned to be pathogenic. Cybrid studies can be helpful in the declaration of pathogenic mutations. The same mutation was found in another patient. She showed the same clinical pattern (Cox et al., 2012) but with an earlier onset (the physical examinations started when she was 16 months old). Biochemical analysis showed a strongly reduced respiration of cultured fibroblasts. The mutation load was 85% in the fibroblasts and 78% in the proband's blood and present less than 5% in blood, cheek cells and urine sediment of the asymptomatic mother and sister.

3.5 m.4300A>G

Two independent families, carrying the 4300A>G mutation, showed an isolated cardiomyopathy, with heart as the only clinically effected organ (Casali et al., 1995; Taylor et al., 2003). In the first description in 1995, the initial patient was a 36-year-old male and several family members suffered from maternally transmitted hypertrophic cardiomyopathy. While the mutation was described to be heteroplasmic in the initial patient, with a load of >95% in skeletal muscle, heart and blood presenting almost homoplasmic (Casali et al., 1999), a repeated analysis of this family confirmed the pure homoplasmic character of the mutation in blood and fibroblasts of symptomatic and asymptomatic individuals (Taylor et al., 2003). The muscle biopsy showed RRFs, while biochemistry of the electron transport chain did not reveal any alterations. In the second family, two brothers died at age 1 and 5 of cardiac failure, whereas two other brothers were asymptomatic. The mutation was homoplasmic in muscle, blood, heart, fibroblasts and myoblasts. Many COX-negative heart cells were diagnosed post-mortem, while the muscle cells showed normal COX activity and did not show any histological alterations like RRFs. Analysis of the respiratory chain revealed severe defects of complex I and IV in cardiac samples,

whereas the activity in muscle, fibroblasts and myoblasts was normal. In heart and skeletal muscle tissue, a significant decrease of the steady-state levels of $tRNA^{Ile}$ was found as well as in cultured skin fibroblasts and myoblasts.

4. Results

4.1 Cellular and Biochemical Phenotype of 143B Cybrid Cells

In our project, the five mutations 4281A>G, 4284G>A, 4290T>C, 4296G>A and 4300A>G of the mitochondrial $tRNA^{Ile}$ gene were comparatively studied in the 143B osteosarcoma cybrid cell system.

Homoplasmic 4281A>G and 4296G>A cybrid cells and their respective wild types lines were generated in our laboratory by fusion of the patients' platelets with the 143B206 *rho*^{0} cell line, which is depleted of mtDNA, and subsequent selection. The mitochondrial genomes were sequenced to exclude additional pathogenic mutations. Homoplasmy of the clones was confirmed by real-time PCR. Due to the severe phenotype caused by the 4281A>G mutation, it was difficult to obtain 100% homoplasmic mutant cell lines harboring this mutation. Therefore, selected heteroplasmic cybrid clones with a high frequency of the mutation were subcloned after EtBr treatment to reduce the copy number of mtDNA (King, 1996). It was possible to select single clones, which were homoplasmic for the mutation.

Homoplasmic wild type 4284G, mutant 4284G>A and mutant 4290T>C cybrid cells were a kind gift of Valeria Tiranti and Massimo Zeviani, Instituto Nazionale Neurologico Carlo Besta, Milano, Italy. As the latter mutation was homoplasmic in the patients, it was not possible to generate wild type clones from the same patient, and instead, the standard 143B osteosarcoma cell line served as control.

The homoplasmic mutant 4300A>G cybrid cells were provided by Mercy M Davidson, Department of Neurology, Columbia University College of Physicians and Surgeons,

New York. This mutation was also expressed homoplasmically in the patient, and therefore, the 143B cell line was used as wild type control.

The 143B206 *rho*^{0} cell line, which is depleted of mitochondrial DNA, served as negative control in several experiments. *Table 4.1* gives an overview of the number of the different clones (=n), as well as the positive and negative controls. When not described elsewise in the text, the mean of wild type or mutant clones, which harbored the same mutation, was calculated, and p-values were calculated of these means. Alternatively, samples are shown separately, depending on the variability of their experimental outcome.

Table 4.1. *Analyzed cell lines of the five mutations in the nuclear 143B osteosarcoma background, respective wild type and mutant cell clones; including wild type cell line 143B, which was not derived from patient material, and the negative control 143B206, which was depleted of mitochondrial DNA.*

	4281A>G	**4284G>A**	**4290T>C**	**4296G>A**	**4300A>G**
wild type	SN(17-71) SN(47-5)	Bel(1) Bel(3)		PN(1) PN(2) PN(5)	
mutant	SN(17-49/1) SN(47-4) SN(47-9)	Bel(2) Bel(5) Bel(8)	SV(1) SK(3)	PN(3) PN(37) PN(2-2)	FB(106) FB(109)
Wild type host cell line	143B				
(-) control	143B206 *rho*^{0}				

4.1.1 Cell Growth in Galactose Medium

In galactose medium cells are forced to rely on their respiratory chain activity. Consequently, respiratory chain impairments should lead to a diminished capability of the cells to grow under this respiratory stress conditions. As some of the mutated cells acidified the growth medium faster than the wild type cells and grew slower, especially the mutant 4281A>G cells, we measured the cells' ability to grow in galactose medium relative to glucose medium. The same cell number was seeded in glucose or galactose medium at time point zero, and cells were counted after 48 h, which revealed differences in the cells' capability to metabolize galactose (*figure 4.1*).

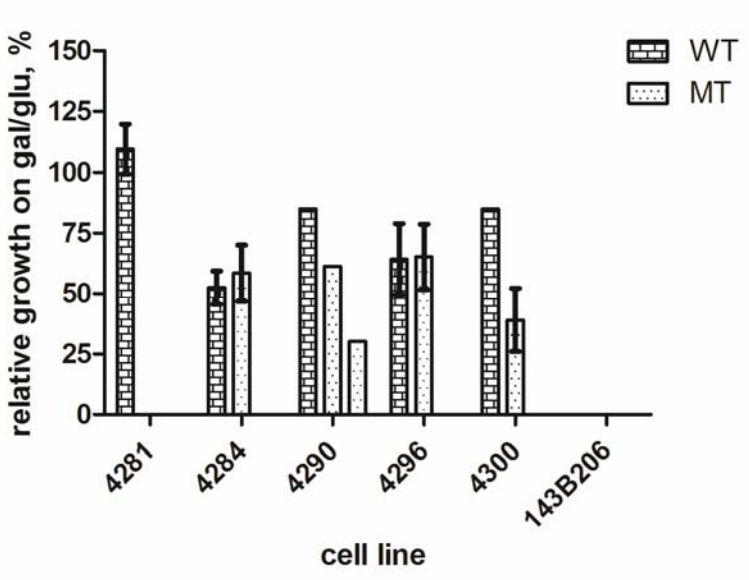

Figure 4.1. *Relative cell growth in galactose/ glucose medium. Cell number in galactose medium after 48 h/ cell number in glucose medium after 48 h, at time point 0 same cell number was seeded. gal=galactose; glu=glucose; WT=wild type; MT=mutant.*

After 48 h cell growth, the wild type 4281A clones grewjust as well in galactose as in glucose medium, whereas the mutant 4281A>G cells did not survive the seeding in galactose medium. Already after 24 h no viable cells could be detected. The mutant 4281A>G clones behaved like the 143B206 cell line in galactose medium, unable to rely on their respiratory chain, which indicated a strong impairment. Apart from the growth analysis in galactose, it was surprising that the mutated 4281A>G cells grew slower than the 143B206 cell line in standard glucose medium (data not shown).

No difference was found in the growth behavior of wild type 4284G and mutant 4284G>A clones under respiratory stress conditions. Also, the wild type 4296G and mutant 4296G>A clones grew at the same rate in both media. Even though wild type and mutant cells behaved the same, we astonishingly detected a reduced growth rate in galactose medium compared to the growth of wild type cells in glucose medium. The growth capability of the 4284G cells was diminished to 50% and of the 4296G cells to 65% in galactose medium. This was not the case for the wild type 4281A cell lines, which showed the same growth rate in both media and therefore a 100% relation.

The 143B cells, which were used as wild-type control for the mutant 4290T>C and 4300A>G cells, proliferated slightly better in glucose than in galactose (in galactose reduced to 85%). The two 4290T>C cybrid lines grew slower in galactose medium compared to 143B cells, but the two cybrid lines showed dissimilar degrees of growth reduction. Also the two mutant 4300A>G clones grew slower than 143B cells in galactose, with 50% less cells after 48 h in galactose medium than in glucose medium.

The disability of the 4281A>G cells to grow in galactose and the reduced capability of the 4290T>C and 4300A>G cells hinted to a decreased activity of the respiratory chain, a typical feature of mitochondrial diseases.

4.1.2 Polarographic Analysis of Cell Respiration

The partly impaired growth in galactose medium was expected to be caused by a deficiency of the respiratory chain (RC), a typical indicator for mitochondrial disease. Therefore, oxygen consumption was measured after successive addition of specific substrates and inhibitors (*figure 4.2*). We monitored the basal cell respiration of the intact cells (*figure 4.2.a*, *br*). Subsequently, we permeabilized the cells and stimulated complex I by glutamate and malate addition (*figure 4.2.a*, *gmIV*) in absence of ADP (state IV respiration). This represents the respiration based on complex I-V interactions. The respiratory chain is coupled to an active ATP synthetase (complex V). Addition of ADP stimulates complex V activity and thereby stimulates the coupled respiration. Glutamate and malate stimulated respiration in presence of ADP (state III respiration) is indicated as *gmIII* in *figure 4.2.a*. Furthermore, complex II was fed by succinate, still in presence of glutamate, malate and ADP (*figure 4.2.a*, *gmsIII*). After inhibition of complex III by antimycin A, the (still coupled) complex IV based respiration by TMPD and ascorbate stimulation was measured (*figure 4.2.a*, *atIII*). In the next step, FCCP addition uncoupled the respiration from complex V activity and allowed to measure the uncoupled and separated activity of complex IV (*figure 4.2.a*, *uncoupled*), to exclude a complex V based impairment of respiration.

Consistently with their inability to grow in galactose medium, the 4281A>G cells did not respire at all, regardless of which respiratory chain complex was stimulated. The marginal oxygen decrease, observed when complex IV was stimulated by TMPD,

was also seen in the negative control, the 143B206 cell line, and can be explained by an auto-oxidation of the substrate. This auto-oxidation should be inhibited by a concurrent addition of the antioxidant ascorbate but cannot be bypassed completely. In contrast to this strong phenotype, the mutated 4284G>A cells respired in the same way like their analog wild type cells. They did not show any defect in respiration, which was consistent with their normal ability to metabolize galactose. The polarographic analysis further revealed an impaired 4290T>C cell respiration in all analyzed modes. Like in the growth rate experiment, the two mutant cell lines showed reductions at different degrees. Whereas clone 1, SV(1), consumed approximately 50% less oxygen than the wild type, clone 2, SK(3), showed an even stronger decrease of oxygen consumption. Error bars do not indicate biological replicas in this case, but experimental repeats of the 143B wild type sample and the two 4290T>C samples. Also, p-values of experimental repeats were calculated in case of the 4290T>C samples. 4296G>A cells showed a slight, yet reproducible general decrease of respiration. Interestingly, these mutants consumed a similar amount of oxygen like wild type cells of the other cell lines. The 4296G wild type cybrids used even more oxygen in total (170-200 pmol O_2/(s x ml) in complex I and II stimulated state III respiration compared to approximately 150 pmol O_2/(s x ml) consumed by other wild types). The 4284G wild type cells took up the lowest amount of oxygen (120-140 pmol O_2/(s x ml) in complex I and II stimulated state III respiration). This could explain their lower growth in galactose medium compared to other wild types. On the other hand, also the 4296G wild type cybrid lines, which consumed the most oxygen in polarographic analysis, showed an impaired growth in galactose medium, albeit less than the 4284G wild type cells. No disturbance of the respiratory chain was found for the 4300A>G cells, although the mutants proliferated slower in galactose than in glucose medium.

A complex V impairment could not be detected for any of the mutations, as the complex IV based oxygen uptake did not increase after uncoupling from complex V activity (*fig. 4.2*). It was not possible to analyze complex V of cells carrying the severe 4281A>G mutation, because complex IV was inactive and did not reduce oxygen to water at all.

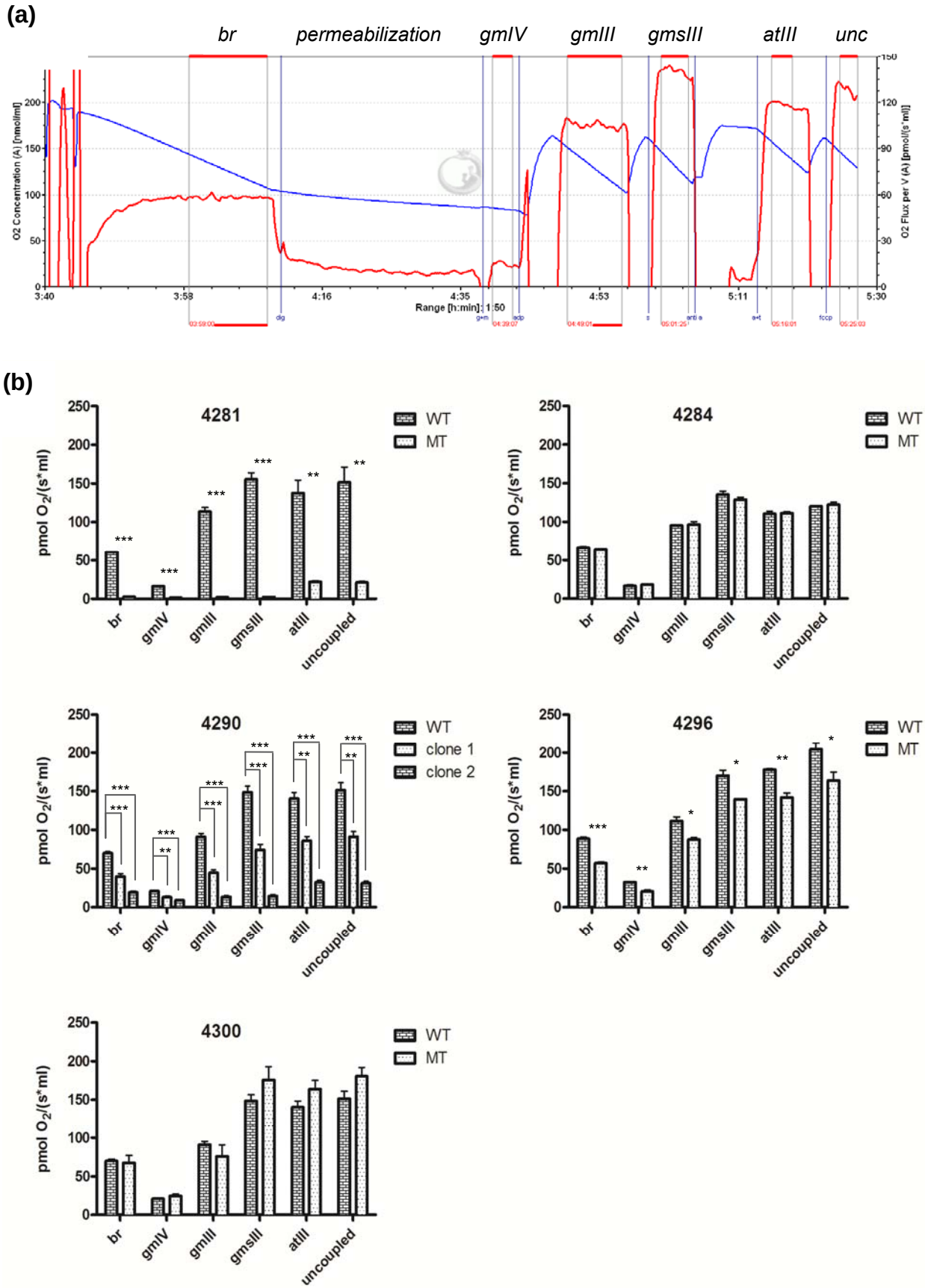
(a)
br
permeabilization
gmIV
gmIII
gmsIII
atIII
unc
O2 Concentration (A) [nmol/ml]
O2 Flux per V (A) [pmol/(s*ml)]
Range [h:min]: 1:50
(b)
4281
4284
4290
4296
4300
WT
MT
clone 1
clone 2
pmol O2/(s*ml)
br
gmIV
gmIII
gmsIII
atIII
uncoupled

Figure 4.2. *Polarographic analysis of cell respiration: measurement of oxygen consumption on permeabilized cells. (a) Experiment output for 4281A wild type cells and the different modi indicated; x-axis (blue): O_2 conc: nmol/ ml, y-axis (red): derived O_2 flux/ vol= pmol/(s x ml). (b) Respiration of all cell lines in comparison. br=basal respiration of intact cells (complex I-V); after permeabilization: gmIV=glutamate+malate stimulated state IV respiration without ADP (complex I-V); gmIII=glutamate+malate stimulated state III respiration (+ADP) (complex I-V); gmsIII=glutamate+malate+succinate stimulated state III respiration (+ADP) (complex I-V); atIII=ascorbate+TMPD stimulated state III respiration (+ADP) in presence of antimycin A (complex IV+V); unc=state III respiration uncoupled by FCCP (complex IV). WT=wild type, MT=mutant; br=basal respiration; unc=uncoupled. Standard deviation and p-values of 4290T>C samples were not calculated of biological replicas, but of experimental repeats. *: p<0.05; **: p<0.01; ***: p<0.001.*

4.1.3 Spectrophotometric Analysis of Respiratory Chain Enzyme Activity

The polarographic assay allowed the analysis of respiration as a result of teamwork of the RC enzyme complexes. This physiological approach can show overall problems in respiration, but does not reveal activities of the single enzyme complexes. Therefore, a spectrophotometric assay on isolated mitochondria was applied to analyze the activity of the respiratory chain complexes I, II, III and IV separately. Independently of the interaction between the complexes, their isolated maximum activity was measured by the change of absorption by substrate turnover, and their activity was normalized to citrate synthase activity (*figure 4.3*). As expected, in case of the 4281A>G mutation, the three respiratory chain complexes I, III and IV were not active, whereas the solely nuclear encoded complex II showed normal activity. Surprisingly, analysis of the 4284G>A clones revealed an isolated complex IV reduction of about 60% remaining activity, although these cells did not display any defect in the polarographic studies. Similarly, the impaired enzyme activity of the 4296G>A mutant clones is focused to complex IV, with a reduction to 80% residual activity on average. This reduction may be the reason for the overall respiration deficiency found in polarographic studies, as complex IV was involved in each analyzed respiration state. However, in case of the 4284G>A mutation, the impaired complex IV activity did not have an effect on the overall respiration of the cells, indicating an alternative pathological mechanism. The two 4290T>C samples showed differing results. Whereas sample one showed decreased complex I and IV activity, sample two showed a stronger activity reduction for all four complexes. The enzyme

activities of the mutant 4300A>G cybrids were normal, which matched well with the normal respiration seen in the polarographic studies. Still, it did not explain the growth delay of these cybrids in galactose medium.

Complex II serves as an internal control, because the subunits are encoded by the nucleus only. We demonstrated a normal complex II activity for the cell lines, but it was decreased in sample 4284G>A, and more sursprisingly, we found a 50% decreased activity in cybrid line 2 of the 4290T>C cells (*figure 4.3.*, complex II, MT2), which cannot be explained as effect of a mutation in mtDNA.

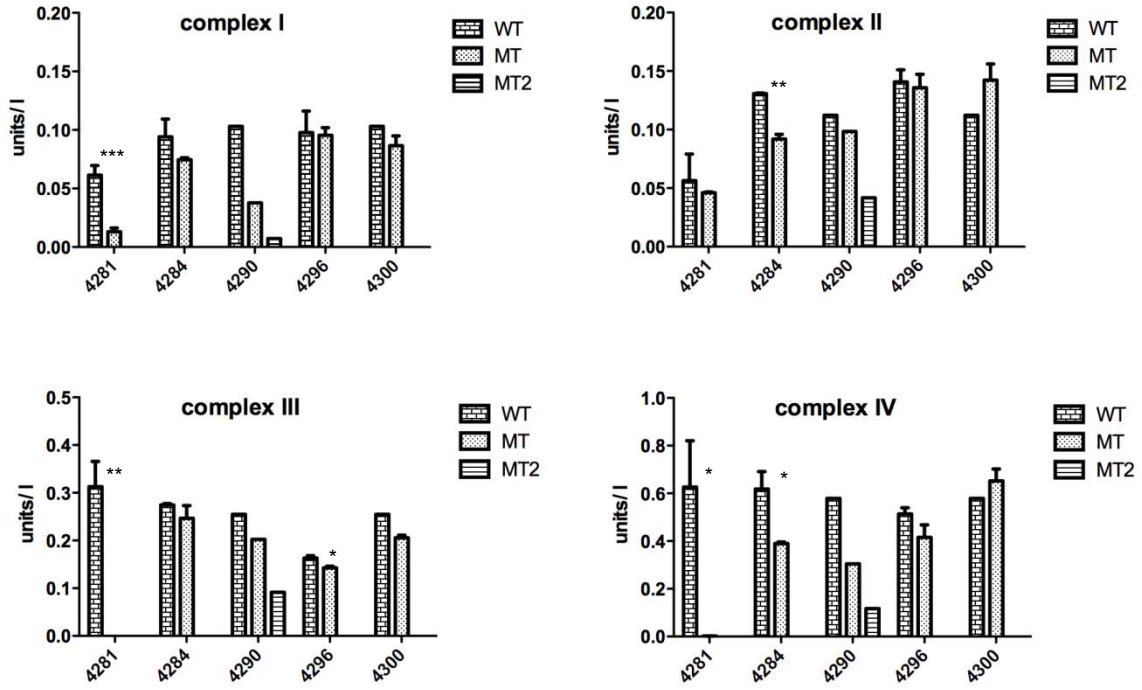

Figure 4.3. *Spectrophotometric analysis of respiratory chain complex activity on isolated mitochondria. Substrate turnover of the complexes was monitored separately by change of absorption. l=liter; cI=complex I; cII=complex II; cIII=complex III; cIV=complex IV; WT=wild type; MT=mutant. Standard deviation and p-values of samples 4290T>C and 4300A>G were not calculated, because no biological replicas were available for the wild type and the separately shown 4290T>C samples. *: p<0.05; **: p<0.01; ***: p<0.001.*

4.1.4 mtDNA Copy Number

To demonstrate that the impairments in cell growth and respiration were not caused by an altered mtDNA content of the cybrid cells, we checked the quantity of the

mitochondrial encoded *ND1* gene relative to the nuclear encoded *18S rRNA* gene by probe-based quantitative real-time PCR.

Except for the 4290T>C cybrid lines, the cell lines do contain the same amount of mtDNA in wild type and mutant clones (*figure 4.4*). Unexpectedly, the 4290T>C cell lines showed a 1.8-fold elevated mtDNA copy number. The standard deviation resulted from a slight difference of the two analyzed cybrid lines: mtDNA of cell line SV(1) was increased 1.65-fold and of cell line SK(3) (showing stronger impairments in many analyses) 1.93-fold.

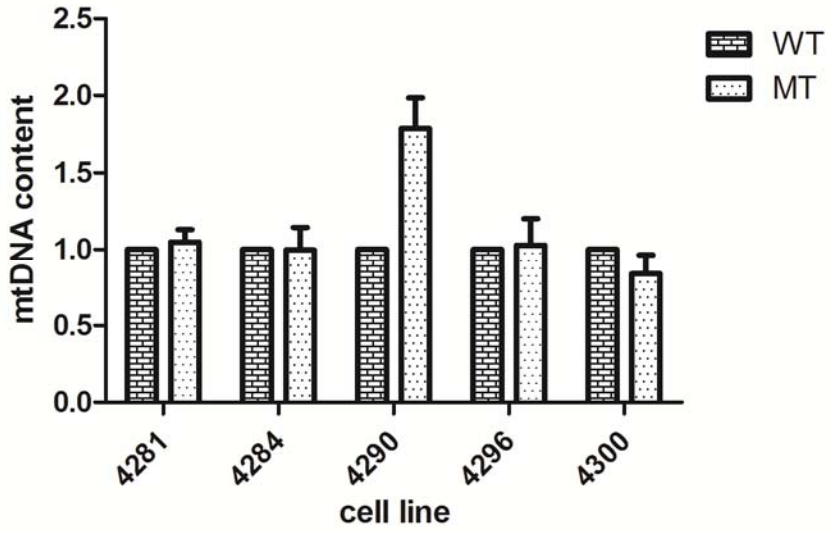

Figure 4.4. *mtDNA copy number of the mutant cell lines relative to wild type cell lines, ND1 gene sequence quantified relative to 18S rRNA gene sequence. WT=wild type; MT=mutant.*

4.1.5 Sequencing of mtDNA

The two 4290T>C cybrid lines frequently showed differing outcomes in the experiments, with cell line SK(3) bearing the stronger effects. We decided to sequence the mitochondrial genome of the two clones to exclude any additional pathogenic mutations in the mitochondrial genome. *Table 4.2* illustrates the detected SNPs of the two cybrid lines.

Table 4.2. *SNP analysis of the two 4290T>C cybrid lines. Positions in bold were only found in one of the two cell lines. Indicated are: nucleotide changes (heteroplasmic at positions 10979 and 11074), amino acid changes for protein-coding genes and SNP report status according to mtSNP database (http://mtsnp.tmig.or.jp/mtsnp/search_mtSNP_e.html) or Mitomap (http://www.mitomap.org/MITOMAP). aa=amino acid; PM=pathogenic mutation; SNP=single nucleotide polymorphism.*

position	SV(1)	SK(3)	location	aa change	Reported
73	A > G	A > G	D-loop	--	SNP
152	T > C	T > C		--	SNP
195	--	**T > C**		**--**	SNP
263	--	**A > G**		**--**	SNP
499	**G > A**	--		--	SNP
514	**insCA**	--		--	SNP
745	A > G	A > G	12S rRNA	--	SNP
750	A > G	A > G		--	SNP
1438	A > G	A > G		--	SNP
1811	A > G	A > G	16S rRNA	--	SNP
2706	A > G	A > G		--	SNP
3204	C > T	C > T		--	SNP
4290	T > C	T > C	tRNA Ile	--	PM
4646	T > C	T > C	ND2	No	SNP
4769	A > G	A > G		No	SNP
5999	T > C	T > C	COX1	No	SNP
6047	A > G	A > G		No	SNP
8818	C > T	C > T	ATPase6	No	SNP
8860	A > G	A > G		Thr>Ala	SNP
10979	**C > T/C**	--	ND4	Pro>Ser	
11074	**C > T/C**	--		no	
11332	C > T	C > T		no	SNP
11467	A > G	A > G		no	SNP
11719	G > A	G > A		no	SNP
12308	**A > G**	--	tRNA Leu(CUN)	--	SNP
12372	G > A	G > A	ND5	no	SNP
12937	A > G	A > G		Met>Val	SNP
14620	C > T	C > T	ND6	no	SNP
14766	C > T	C > T	Cytb	Ile>Thr	SNP
15326	A > G	A > G		Thr>Ala	SNP
15693	T > C	T > C		Met>Thr	SNP

16134	C > T	C > T	D-loop	--	SNP
16301	C > T	C > T		--	SNP
16356	T > C	T > C		--	SNP
16519	T > C	T > C		--	SNP

35 SNPs were found in total, of which 28 homoplasmic SNPs were found in both cell lines and have already been described in the literature as polymorphisms. The seven positions in bold (*table 4.2*) were only detetcted in one of the two cybrid cell lines. Four of them were present in the D-loop, the non-coding region of mtDNA, which is well-known for its high rate of polymorphisms; two were present in protein-coding genes and one in a tRNA gene. Surprisingly, the three mutations in protein and tRNA sequences were present in cell line SV(1), the cell line, which showed the less severe phenotype. Of these three mutations, two apparently heteroplasmic point mutations were located in the *ND4* gene, coding for a subunit of complex I. Thereof, one introduced an amino acid exchange at position 10979, whereas the other one was silent. The tRNA mutation was found at position 12308 in $tRNA^{Leu(CUN)}$ and has been described many times in literature as polymorphism, which frequently accompanied other pathogenic mutations. We did not find additional potentially pathogenic mutations in cell line SK(3), the cell line, which showed the more severe phenotype in our experiments. This is not necessarily surprising: the decreased complex II activity in spectrophotometric analyses led to the assumption of additional defects in the nuclear system.

4.1.6 Structure of Mitochondria

Cells harboring the 4281A>G mutation appeared swollen, they grew very slow and their respiratory chain was defect. Therefore, we supposed an altered mitochondria formation and a disrupted mitochondrial network within the cell. Electron microscopy images confirmed our guess – compared to wild type mitochondria, which exhibited a typical tubular shape, containing many Cristae arranged in parallel (*figure 4.5.A-B*), mutated mitochondria were enlarged with a more circular shape or abnormal structures (*figure 4.5.C-E*). The number of Cristae was strongly reduced, and instead of parallel Cristae they seemed to curl. Their appearance was comparable to those of 143B206 mitochondria, which lack mtDNA (*figure 4.5.F*).

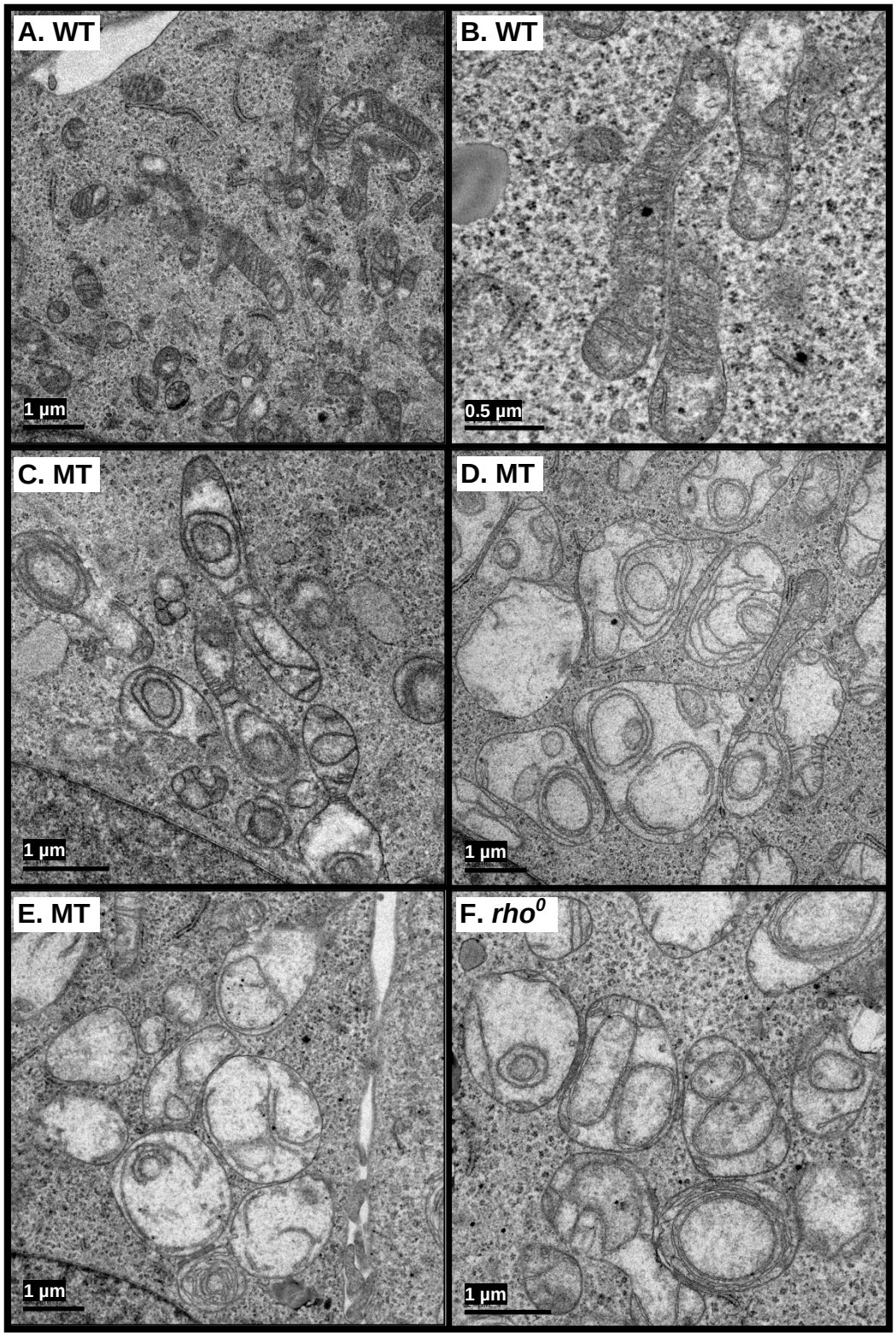

Figure 4.5. *Electron microscopy images of mitochondria in 4281A wild type and 4281A>G mutant cells. A-B: wild type clone SN(17-71); C: mutant clone SN(17-49/1); D: mutant clone SN(47-4); E: mutant clone SN(47-9); F: 143B206 rho^0.*

Furthermore, we stained the 4281 cybrid cells with Mitotracker to visualize the mitochondrial network, and the nucleus was stained with Hoechst staining (*figure 4.6*). Despite a high staining background a defined difference between wild type and mutant cells could be detected. The wild type cells showed a network-like formation (*figure 4.6.A-B, D-E*), whereas the 4281A>G mutated cells showed a dotted structure (*figure 4.6.C,F-H*), indicating a disruption of the network. Mitochondria of mutant cells and 143B206 cells (*figure 4.6.I*) were indistinguishable.

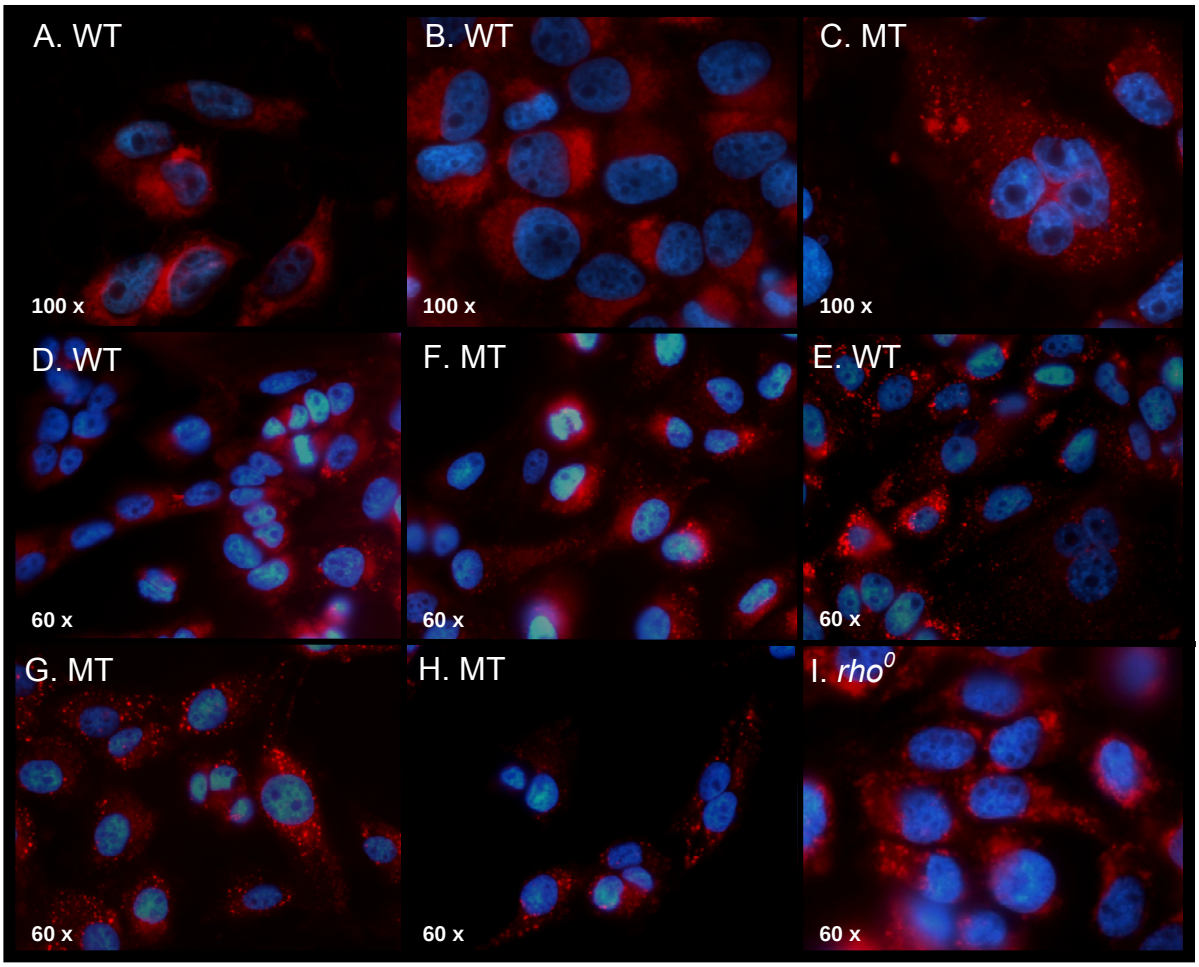

Figure 4.6. *Fluorescence microscopy of wild type 4281A and mutant 4281A>G cells, Mitochondria stained with Mitotracker Red 580 (red) and nuclei with Hoechst dye (blue). A-C: 100x; D-I: 60x. A+D: wild type clone SN17-71); B+E: wild-type clone SN(47-5); C+F: mutant clone SN(17-49/1); G: mutant clone SN(47-4); H: mutant clone SN(47-9); I: 143B206 rho^0. WT=wild type, MT=mutant.*

4.2 Effects of the tRNA^{Ile} Mutations at the Molecular Level

4.2.1 Steady-State Levels of tRNA^{Ile}

A possible consequence of a tRNA mutation is an altered expression of the molecule itself. Therefore, we assayed the levels of the mature wild type tRNA^{Ile} and the corresponding mutants by Northern Blot hybridization. The probe bound to the 3' end of tRNA^{Ile} and did not cover the mutated sites. Results were normalized to 5S rRNA *(figure 4.7)*, but normalization to mt tRNA^{Lys} and mt tRNA^{Arg} gave the same results.

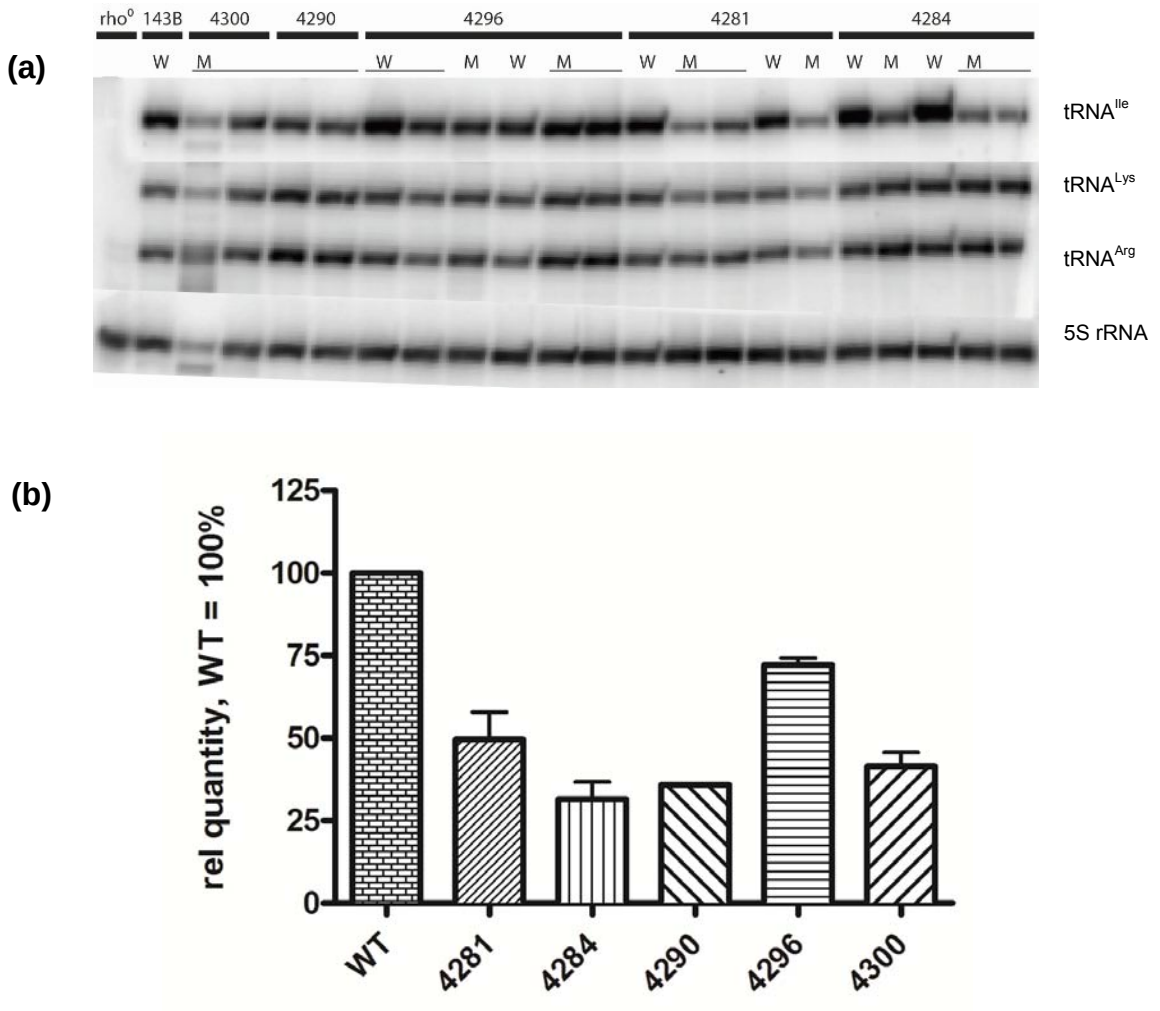

Figure 4.7. *Steady-state levels of mature tRNA^{Ile} in the cybrid cell lines. (a) Northern Blot probed with radioactive oligonucleotides specific for tRNA^{Ile}, tRNA^{Lys}, tRNA^{Arg} and 5S rRNA. (b) Relative quantification of tRNA^{Ile} steady-state levels, normalized to 5S rRNA. M=mutant; W and WT=wild type; rho^0=143B206.*

Each of the five mutations reduced the steady-state level of the mature tRNA. Levels of $tRNA^{Ile}$ containing the mutations 4281A>G, 4290T>C or 4300A>G were reduced to 50%, 36% and 41% compared to the respective wild-type cells. The 4284G>A mutation caused the severest reduction to 31%, whereas the 4296G>A transition merely reduced the $tRNA^{Ile}$ amount to 74%. Results were confirmed by RNase protection assay (*chapter 4.2.2, figure 4.9*).

4.2.2 Steady-State Levels of Precursor $tRNA^{Ile}$

The decreased steady-state levels of the mutated tRNAs could derive from a reduced transcription of the tRNA precursor, impaired precursor processing or instability of the mature molecule. First, the levels of the $tRNA^{Ile}$ precursors were estimated by quantitative real-time PCR using three different primer sets. One was spanning from the 5' extension sequence to the 3' extension sequence of the tRNA (53pI), a second one from the 5' extension sequence to the 3' end of the tRNA sequence (5pI) and a third one from the 5' start sequence of the tRNA sequence to the 3' extension sequence (3pI). Results were normalized to steady-state levels of $tRNA^{His}$, $tRNA^{Val}$, $tRNA^{Glu}$ precursors including 5', 3' or 5' and 3' extensions. Normalization to GAPDH gave similar results.

The strongest effect on the $tRNA^{Ile}$ precursor level was caused by the 4284G>A and 4300A>G mutations, with a respective 12-fold and more than 6-fold increase (*figure 4.8*). Combined with the decreased steady-state levels of the mature tRNAs, we supposed a malfunction of the precursor processing. The 4281A>G mutation was responsible for a weak 1.4-fold and the 4290T>C mutation for an approximately 3-fold precursor accumulation. On the contrary, the $tRNA^{Ile}$ precursor was reduced to 70% in case of the 4296G>A transition (wild type = 100%).

Within one mutation, no remarkable differences were detected in the precursor level by using different primer sets spanning the tRNA with 5' and 3' extensions, the tRNA with only the 5' extension or the tRNA including only the 3' extension. Differences could have given hints towards a processing problem at the 3' end, as in humans, mitochondria 5' processing occurs first, and a disturbed 3' processing should consequently result in the specific increase of the 3pI precursor (tRNA + 3' trailer).

This was not the case. Therefore, we did not expect a problem in 3' processing of the $tRNA^{Ile}$ precursor.

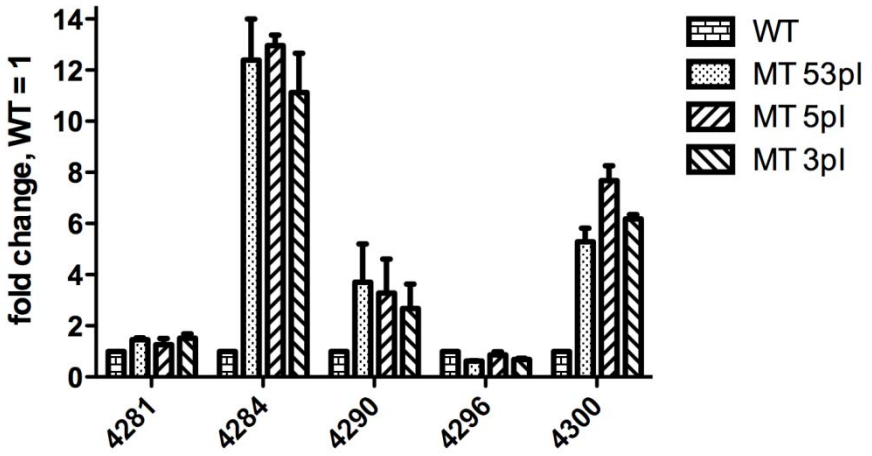

Figure 4.8. *Steady-state levels of $tRNA^{Ile}$ precursor. Fold change of $tRNA^{Ile}$ precursor steady-state levels by probe-based real-time PCR, normalized to $tRNA^{His}$, $tRNA^{Val}$ and $tRNA^{Glu}$ precursors. 53pI= $tRNA^{Ile}$ +5' +3' extensions, 5pI= $tRNA^{Ile}$ + 5' extension, 3pI= $tRNA^{Ile}$ +3' extension. WT=wild type, MT=mutant.*

The results were confirmed by RNase protection assay. We applied two different $tRNA^{Ile}$ precursor probes: phI2 spanned the tRNA including 5' leader and 3' trailer and phI3 spanned $tRNA^{Ile}$ including only the 3' trailer. A probe complementary to $tRNA^{Glu}$ precursor, phE3, served as control. The radiolabeled probes should bind to the precursors and also to the mature tRNAs, allowing to detect both species in the same assay. Subsequently, single strand RNA was digested, and the RNase-protected, double-stranded molecules were denatured and analyzed in a denaturing polyacrylamide gel. *Figure 4.9.a* shows the result for probe phI2, spanning $tRNA^{Ile}$ including 5' leader and 3' trailer, and figure *4.9.b* the control probe phE3. Binding of $tRNA^{Ile}$ probes to $tRNA^{Ile}$ was not affected by the mutations, because no additional bands, as consequence of digestion at the mutated sites, were detected in mutant samples.

The strong precursor accumulation of the 4284G>A tRNA (*figure 4.9.a, lanes 9-11*) and the 4300A>G tRNA (*figure 4.9.a, lanes 21, 22*) was confirmed by the RNase protection assay. Also the increased 4290T>C tRNA precursor was detectable (lanes

12, 13) and a slightly increased 4281A>G tRNA precursor (lanes 4-6), as already shown by quantitative real-time PCR. Likewise, the decreased steady-state levels of mature $tRNA^{Ile}$, detected by Northern Blot analysis, were confirmed by this RNase protection assay: all mutant tRNAs showed decreased levels of mature $tRNA^{Ile}$, with the exception of 4281A>G tRNAs (lanes 4-6), which seemed to be increased a bit. There is no explanation for this difference to the results obtained by Northern blotting.

Figure 4.9.b shows the species of the $tRNA^{Glu}$. Apparently, the precursor was not detectable, which may be due to low amounts. The level of mature $tRNA^{Glu}$ was similar in all cell lines.

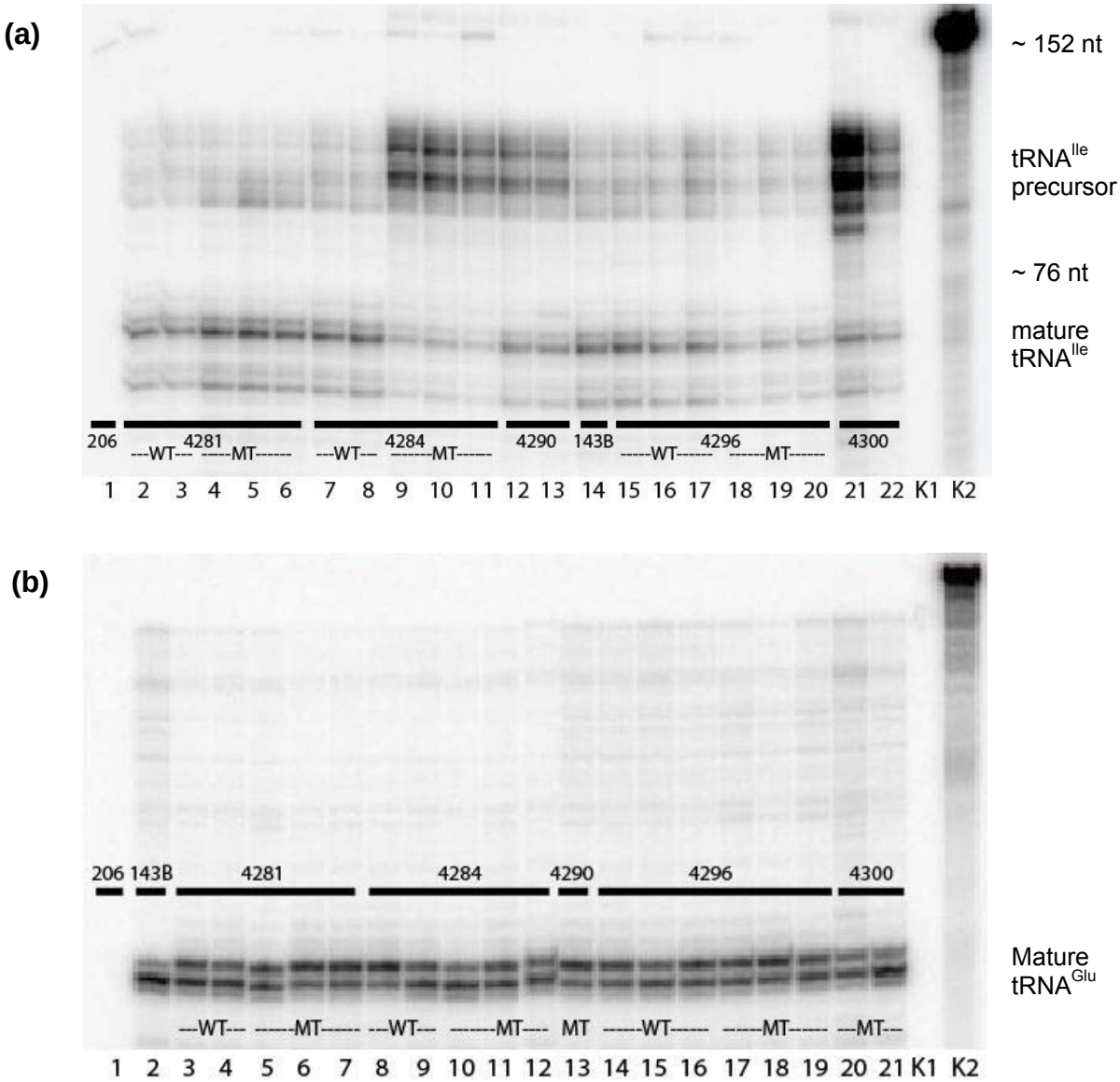

Figure 4.9. *Different species of precursor and mature tRNAs in cybrid cells. (a) Radiolabeled tRNA^{Ile} probe phI2 or (b) radiolabeled tRNA^{Glu} probe phE3 were hybridized with total RNA, single-strand RNA was digested, RNase-protected double-stranded products denatured and resolved in denaturing polyacrylamide gels. K1=probe without sample, digested; K2=probe without sample, without digestion. WT=wild type, MT=mutant, nt=nucleotides, 206=143B206 rho^{0}.*

4.2.3 Processing of the tRNA^{Ile} Precursor in vitro

The combination of tRNA precursor accumulation with a reduction of the mature tRNA level was markedly found for the 4284G>A and 4300A>G mutations and to a lower extent for the 4281A>G and 4290T>C mutations. This findings could originate in an impaired precursor processing, an essential step in tRNA maturation by cleaving the precursor molecule at the 5' and 3' end of the tRNA. As we did not expect a 3' processing impairment (*chapter 4.2.2*), we focused only on 5' processing. *In vitro* transcribed tRNA precursors were 5' processed by an RNase P assay, and the processing activity was estimated by relative quantification of the mutated mature tRNA to the wild type tRNA (*figure 4.10*). The 4263A>G mutation, located in the acceptor stem at the first position of the tRNA^{Ile} 5' end, was additionally included in this study in coorperation with Min-Xin Guan, Cincinnati Children's Hospital Medical Center, Cincinnati.

The precursor processing was reduced to 75% in case of the 4300A>G mutation and to 59% in case of the 4263A>G mutation. The other mutations did not cause differences between wild type and mutant tRNA processing. At least, the strong increase of the 4300A>G tRNA^{Ile} precursor with the concomitant reduction of the mature form could be explained by this result, but not the even stronger 4284G>A tRNA^{Ile} precursor accumulation.

3' processing by RNase Z was not analyzed, because we did not expect a defect, as described in *chapter 4.2.2*. Considering that 3' processing occurs after 5' processing, real-time PCR would have shown a stronger accumulation of the tRNA^{Ile} precursor plus 3' extension sequence in case of an impaired 3' processing. This was not the case.

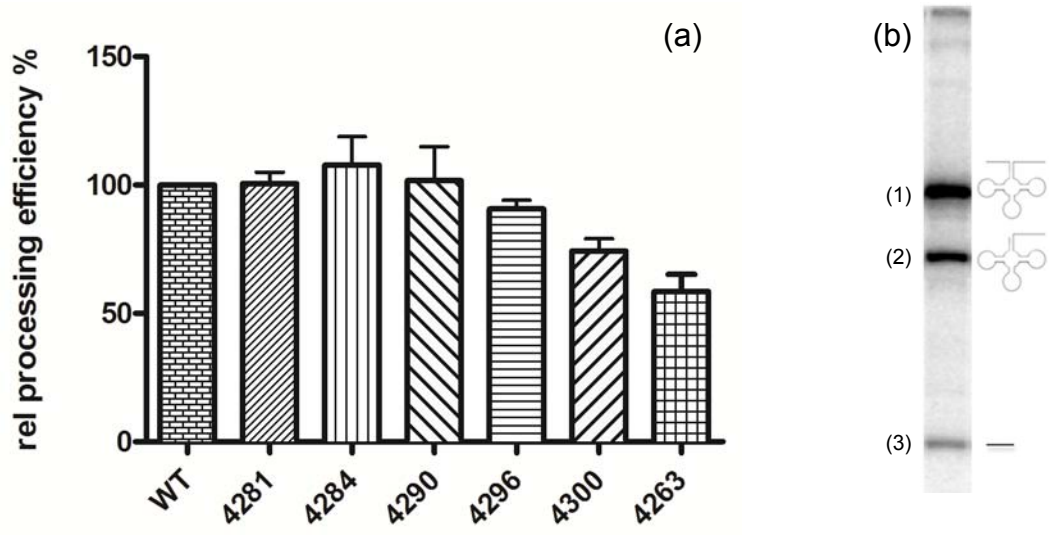

Figure 4.10. *tRNA^{Ile} 5' processing by RNase P. (a) Relative processing efficiency of in vitro transcribed and radiolabeled tRNA^{Ile} precursors by recombinantly expressed RNase P. (b) typical products of an RNase P activity assay, separated on a denaturing polyacrylamide gel: (1) radiolabeled precursor including 5' and 3' extensions, (2) 5' processed precursor carrying the 3' trailer and (3) cleaved leader.*

4.2.4 tRNA^{Ile} Stability and Resynthesis

The altered steady-state level of mutant 4300A>G tRNA could be explained by an impaired 5' processing, but still the strong increase of the 4284G>A tRNA precursor and the reduced steady-state levels of all mutant mature tRNAs cannot be explained. Another cause for the reduced steady-state level of mutant mature tRNA^{Ile} could be instability of the tRNA molecule or a decelerated resynthesis. Stability was tested in a time-course experiment on cells with sustained ethidium bromide treatment to block mitochondrial transcription. Steady-state levels of mature tRNAs were analyzed at different time-points by Northern Blot hybridization with probes binding to the 3' end of tRNA^{Ile} or tRNA^{Lys} and normalized to 5S rRNA. Solely, mutation 4284G>A led to an increased decay of tRNA^{Ile}, which apparently caused the strong steady-state level reduction of 4284G>A tRNA to 30%. Stability of 4281A>G, 4290T>C and 4300A>G tRNAs was not altered, and the mutant 4296G>A clones even seemed to be slightly more stable than the wild type clones. tRNA^{Lys} decay of the same clones was not altered compared to the wild types.

(a)

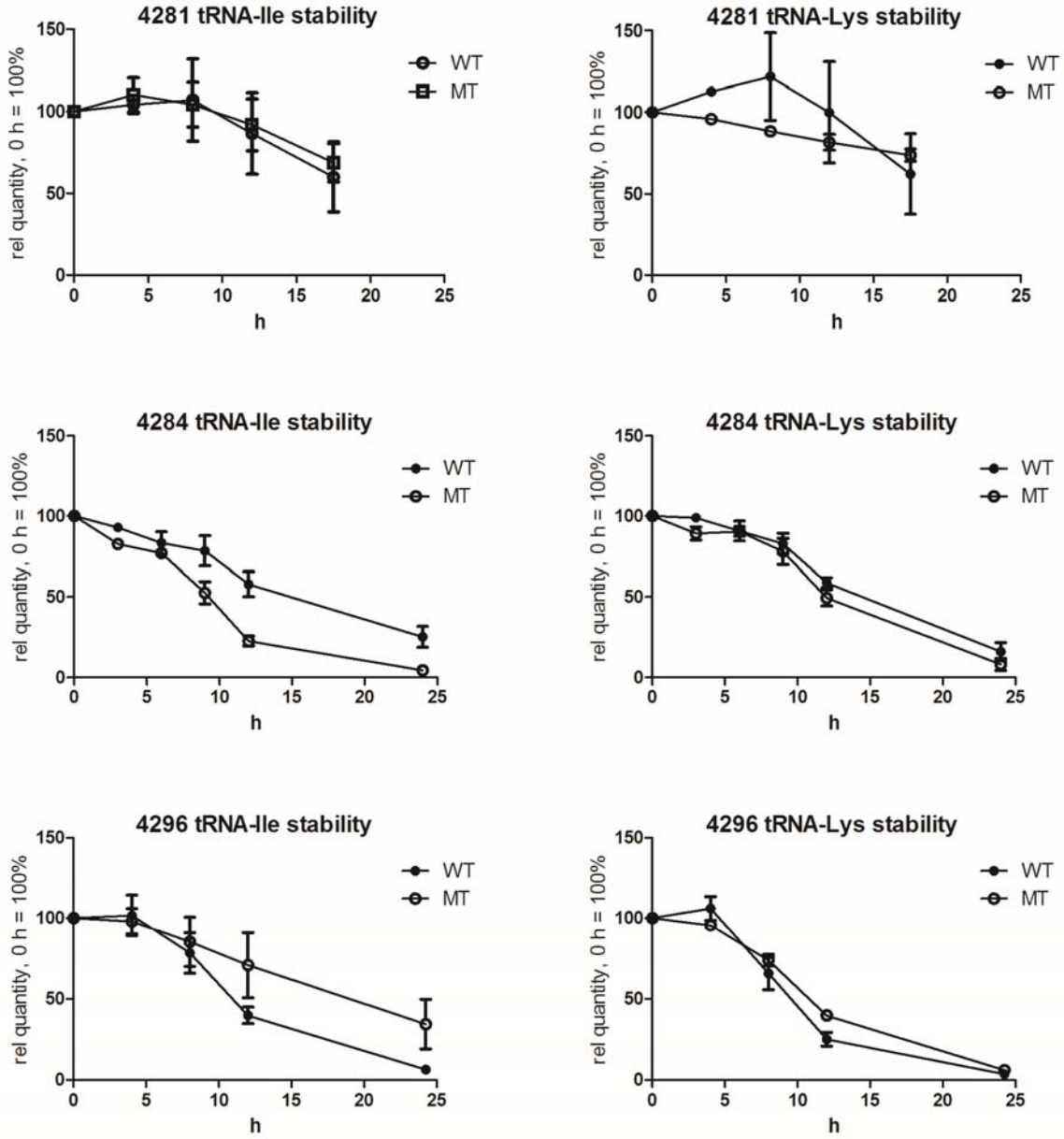
4281 tRNA-Ile stability
4281 tRNA-Lys stability
4284 tRNA-Ile stability
4284 tRNA-Lys stability
4296 tRNA-Ile stability
4296 tRNA-Lys stability
rel quantity, 0 h = 100%
h
WT
MT

(b)

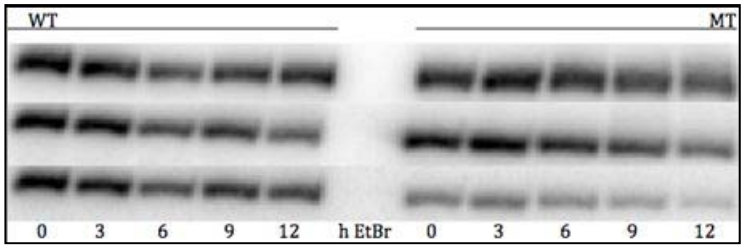
WT
MT
0 3 6 9 12 h EtBr 0 3 6 9 12
5S rRNA
tRNA^Lys
tRNA^Ile

Figure 4.11. *$tRNA^{Ile}$ and $tRNA^{Lys}$ stability in cybrid cells. Mitochondrial transcription was blocked by EtBr treatment, total RNA of different time-points separated on denaturing polyacrylamide gels, and tRNA levels detected by probing Northern Blots with radiolabeled oligonucleotides specific for $tRNA^{Ile}$, $tRNA^{Lys}$ and 5S rRNA. (a) Relative quantity of the $tRNA^{Ile}$ and $tRNA^{Lys}$ compared to the quantity at time-point 0. (b) Northern Blot example for mutant 4284G>A sample. EtBr=ethidium bromide; WT=wild type; MT=mutant.*

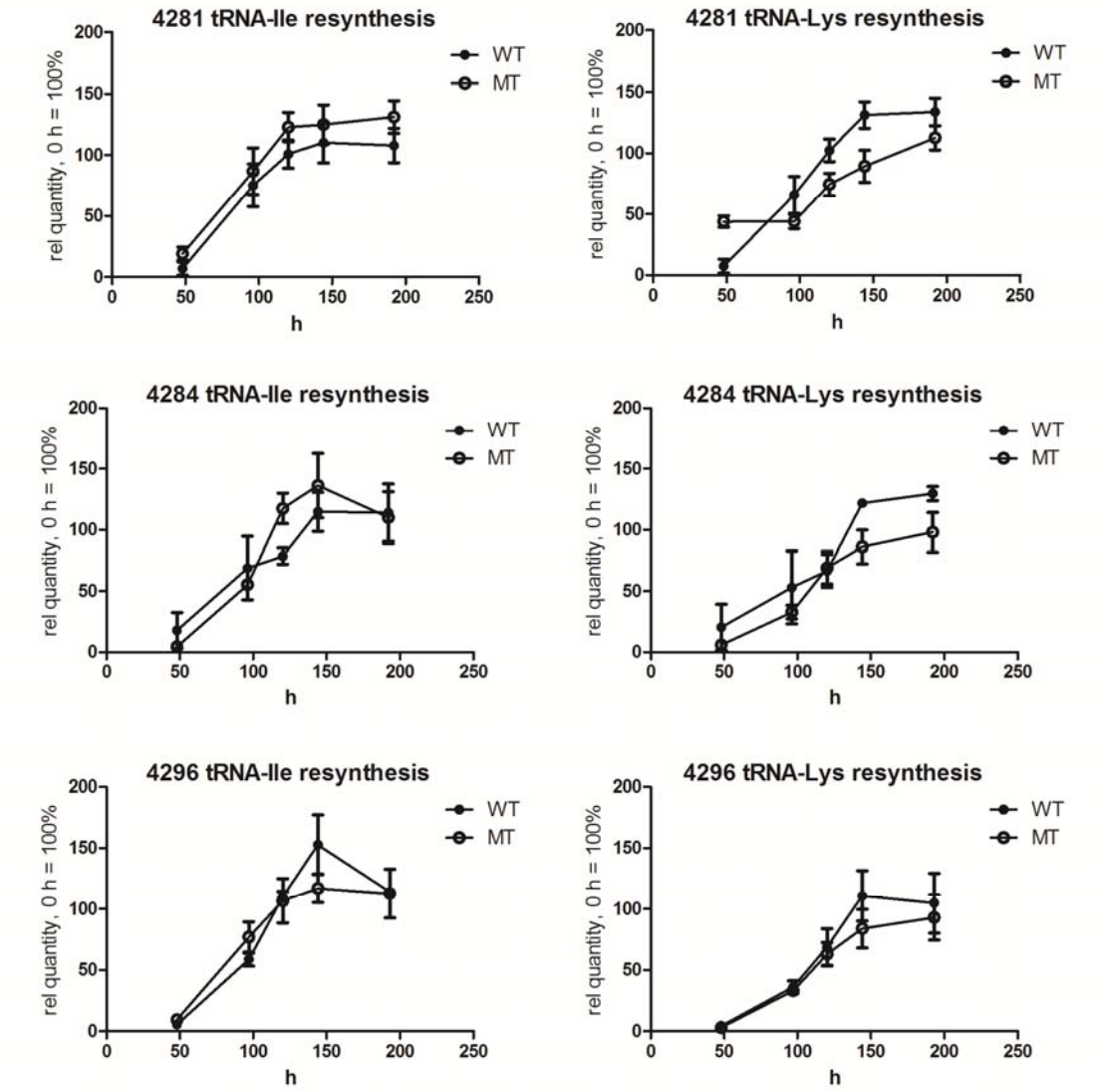

Figure 4.12. *tRNA resynthesis of tRNAIle and tRNALys. After release of transcription block by EtBr, tRNA levels were determined at different time-points by Northern Blot. Relative quantity of the respective tRNA compared to the quantity at time-point 0 prior transcription block is indicated. WT=wild type, MT=mutant.*

To analyze $tRNA^{Ile}$ resynthesis, cells were treated with ethidium bromide, until they almost lacked mitochondrial tRNA. Upon release of this mitochondrial transcription block, recovery of $tRNA^{Ile}$ and $tRNA^{Lys}$ steady-state levels was determined every 24 or 48 hours for eight days. Total RNA was isolated and resolved in denaturing polyacrylamide gels. Northern Blot hybridization monitored the same recovery rate for $tRNA^{Ile}$ and $tRNA^{Lys}$, and compared to the wild type samples, $tRNA^{Ile}$ resynthesis was not impaired in any of the mutations. *Figure 4.12* shows the results for 4281A>G, 4284G>A and 4296G>A tRNA resynthesis.

4.2.5 $tRNA^{Ile}$ Aminoacylation in Cybrid Cells

To fulfill their task, i.e., the transfer of the appropriate amino acid to the translation machinery at the ribosomal site, tRNAs have to be aminoacylated adequately with isoleucine by isoleucyl-tRNA synthetase. Dysfunction of the respiratory chain, as impressively detected in the 4281A>G cells, may originate from a decreased tRNA aminoacylation. We assessed the aminoacylation status of $tRNA^{Ile}$ by an acid gel approach, in which the pH maintains the amino acid-loading of the tRNAs (Enriquez and Attardi, 1996; Kohrer and Rajbhandary, 2008). Northern Blot hybridization with specific tRNA probes should theoretically visualize two tRNA species: the unloaded tRNA and the slower migrating aminoacylated tRNA. In practice, additional bands appeared frequently (*figure 4.13*), possibly indicating different tRNA conformations, which may be present under this not perfectly denaturing conditions. The additional bands made the quantification more difficult, but it was possible to separate the bands sufficiently. A deacylated control fraction was run in parallel and allowed to assign the bands representing deacylated tRNAs. Wild type $tRNA^{Ile}$ was almost completely aminoacylated.

Mutation 4281A>G had the strongest impact on $tRNA^{Ile}$ aminoacylation: no aminoacylated form could be detected, but only bands migrating at the level of the deacylated mutant control sample (*figure 4.13.a*). The 4284G>A mutation also affected $tRNA^{Ile}$ aminoacylation, albeit much milder: the aminoacylated tRNA fraction was reduced to ~75% (*figure 4.13.b*). Calculated numbers are mentioned with reservation, because the weak band separation in acid gels did not allow a clear interpretation. We also saw a ~50% reduced aminoacylation on average in the

mutant 4296G>A samples (*figure 4.13.c*). The decreased aminoacylation of these two mutants, 4284G>A and 4296G>A, may be the reason for the isolated impairment of complex IV activity, which we had detected in respiratory chain analyses. The mutant 4290T>C tRNA was aminoacylated like wild type tRNA (*figure 4.13.d*), and aminoacylation of the mutant 4300A>G tRNA was also unchanged (*figure 4.13.d*), coinciding with the cell line's normal respiration.

The mutated tRNAs showed a mobility shift compared to their respective wild type forms. While mutated 4281A>G and 4290T>C tRNAs migrated faster, 4296G>A tRNA migrated slower, and 4284G>A and 4300A>G tRNAs seemed to migrate a bit slower than the corresponding wild type tRNA, too. This migration shift may indicate an alteration of the tRNA structure (*see chapter 4.2.9*). Therefore, we could not exclude that the 4281A>G tRNA bands, which were apparently completely deacylated, actually represented a mixture of aminoacylated and deacylated tRNAs, which migrate equally. To exclude such a bias, we moreover analyzed tRNA aminoacylation by an alternative method.

4.2.6 $tRNA^{Ile}$ Aminoacylation "in Organello"

An *in organello* approach on isolated mitochondria was applied to confirm the results of the acid gel approach, as the different bands were difficult to interpret and calculate. The aminoacylation process occurred in isolated mitochondria, with addition of ^{14}C-labeled isoleucine and the other 19 unlabeled amino acids. Total mitochondrial RNA was separated in polyacrylamide gels under acidic conditions to maintain isoleucylation and then blotted to a Nylon membrane. Accordingly, this approach only visualized the radioactive amino acid, but not the tRNA, thus indicated the loaded tRNA solely.

The assay confirmed that the 4281A>G tRNA was not aminoacylated (*figure 4.14*), only the wild type tRNAs carried the radioactive isoleucine. The "*in organello"* approach also confirmed the reduced aminoacylation level of 4284G>A tRNAs. Of course, one should consider the decreased tRNA steady-state levels, which contributed to the diminished signal (total mitochondrial RNA was applied on the acid gel). Therefore, the reduction of the aminoacylation signal appeared even stronger in case of reduced tRNA levels.

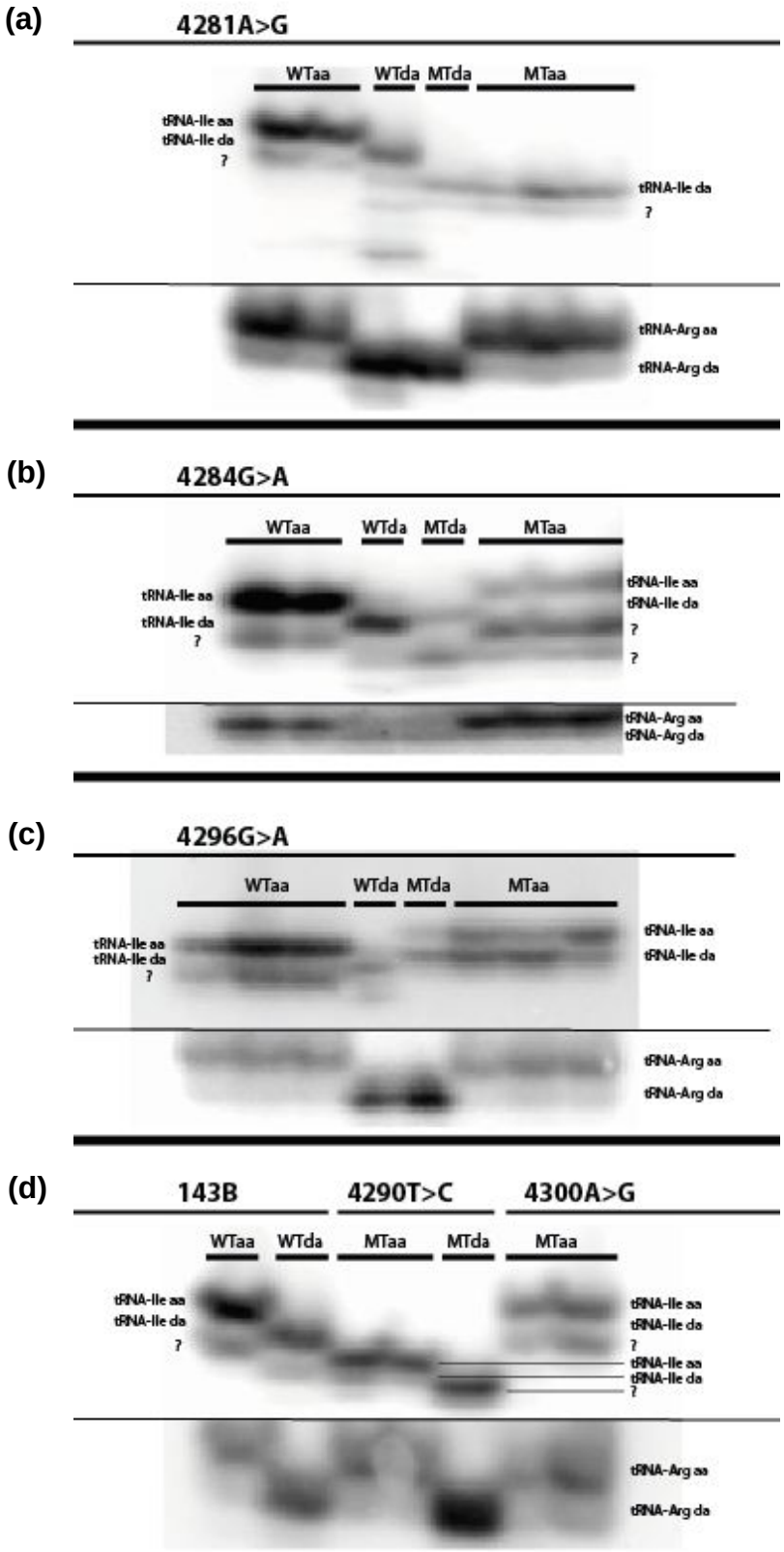

Figure 4.13. *$tRNA^{Ile}$ aminoacylation in cybrid cells. Northern Blot analysis of total RNA samples, which were run on acid 8 M urea 8% polyacrylamide gels pH 4.5 and probed with radiolabeled oligonucleotides specific for $tRNA^{Ile}$ or $tRNA^{Arg}$. Control RNA was deacylated at pH 8.5. Aminoacylated tRNAs showed shift in migration. aa=aminoacylated; da=deacylated; WT=wild type; MT=mutant.*

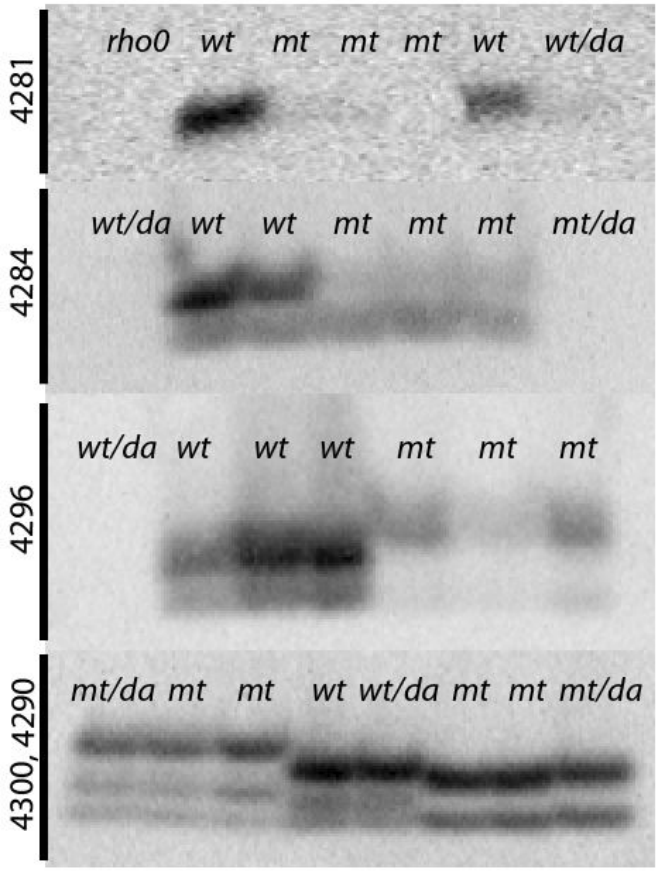

Figure 4.14. *"in organello" aminoacylation. Analysis of aminoacylation in isolated mitochondria by ^{14}C-isoleucine labeling, separated in acid 8 M urea 8% polyacrylamide gels at pH 4.5 to maintain aminoacylation and blotted to Nylon membranes. Wt=wild type; mt=mutant; da=deacylated.*

We could reproduce the reduced amount of aminoacylated 4296G>A tRNA^{Ile} by the "*in organello"* approach, too. In this case, the mutant aminoacylated tRNAs migrated slower than the wild type aminoacylated tRNAs, as also did the 4300A>G mutated tRNAs. Except for the 4281 sample, the aminoacylated tRNAs of the 4284, 4290 and 4296 samples appeared as double bands, of the 4300 even as three bands, possibly representing different conformations.

4.2.7 Mitochondrial Protein Synthesis

A reduced or even lacking aminoacylation, like in case of the 4281A>G $tRNA^{Ile}$, should have a strong impact on mitochondrial translation. We analyzed translation by pulse-labeling of cybrid cells with ^{35}S-methionine/cysteine in presence of emetine, an inhibitor of cytosolic translation. The products were resolved in SDS polyacrylamide gels (*figure 4.15*). Indeed, we detected an overall strong reduction of the 13 mitochondrial translation products in the 4281A>G cells (*figure 4.15.a+e*). Albeit at reduced levels, the 13 products were actually expressed, which is not consistent with the lacking aminoacylation of tRNAs harboring the 4281A>G mutation. The discrepancy could be explained by a very low aminoacylation level, which may actually be present, but could not be detected by the aminoacylation assays due to a detection limit. Mutant cybrid line 2 of the 4290T>C cells, SK(3), also showed a generally reduced translation of mitochondrial polypeptides (*figure 4.15.b*). The other mutations did not affect translation, only a very slight reduction of translation products was found for 4296G>A mutant clone 3 (*figure 4.15.b*). 143B206 *rho^0* cells, which are lacking mitochondrial DNA, did not express mitochondrial proteins (*figure 4.15.a*). We checked for balanced protein loadings on SDS polyacrylamide gels by Coomassie staining (*figure 4.15.c+d*).

4.2.8 Steady-State Levels of Mitochondrial Proteins

All 13 mtDNA encoded proteins are subunits of the respiratory chain. We analyzed the impact of the five $tRNA^{Ile}$ mutations on the steady-state levels of these proteins by immunoblotting with specific antibodies. Except for the two antibodies against mitochondrial encoded complex IV subunit 1 (COX1) and complex IV subunit 2 (COX2), only antibodies against nuclear encoded subunits worked specifically. We tested available antibodies against mitochondrial encoded subunits of complex I, but they did not work specifically, as they showed signals in the negative control (143B206 *rho^0* cell extract). Antibodies against nuclear encoded subunits were specific for complex I β subcomplex subunit 8, complex II 70 kDa subunit, complex III core 1 subunit, complex IV subunit 4 (COX4) and complex IV subunit 5a (COX5) and complex V subunit a.

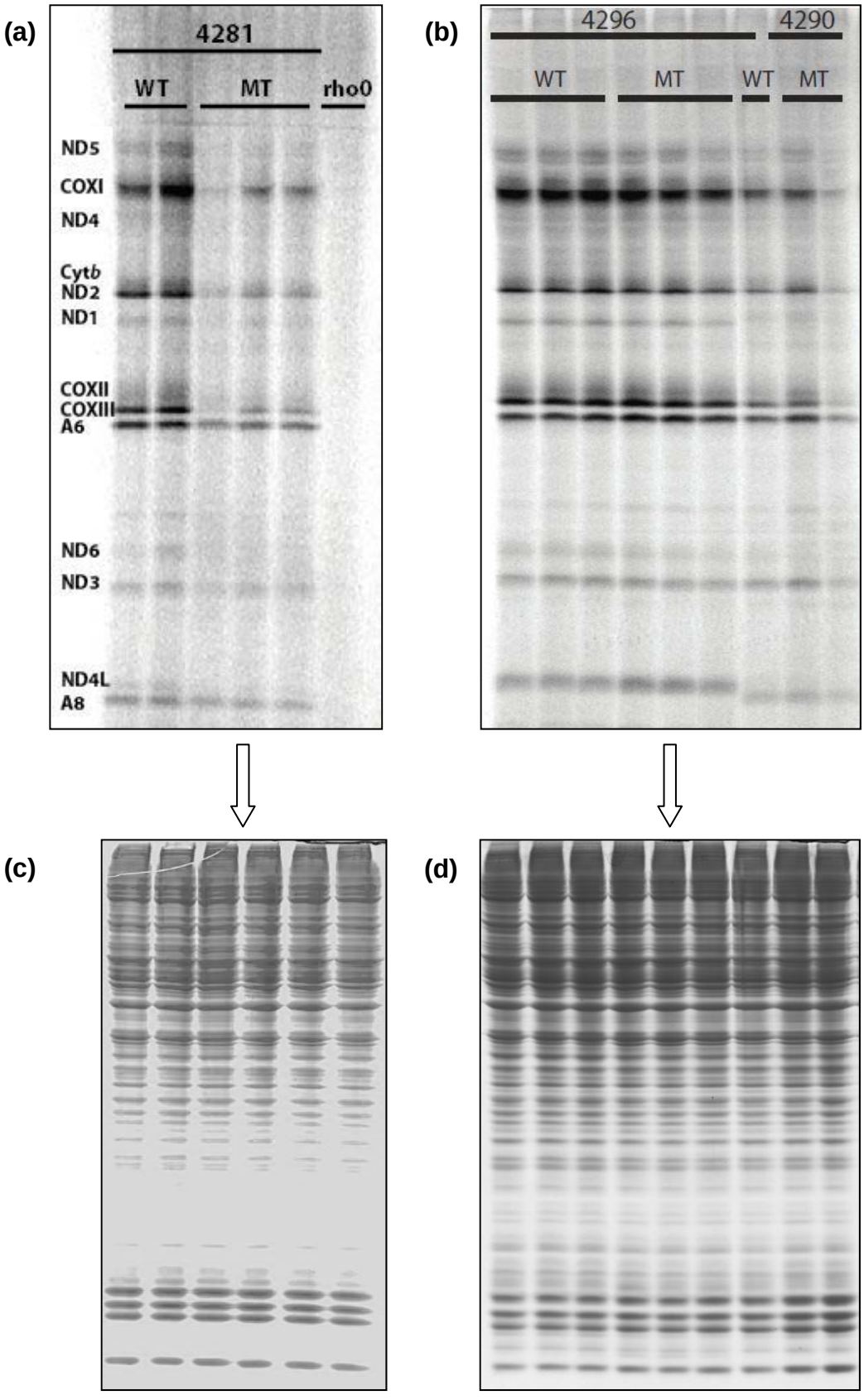
(a)
4281
WT
MT
rho0
ND5
COXI
ND4
Cyt*b*
ND2
ND1
COXII
COXIII
A6
ND6
ND3
ND4L
A8
(b)
4296
4290
WT
MT
WT
MT
(c)
(d)

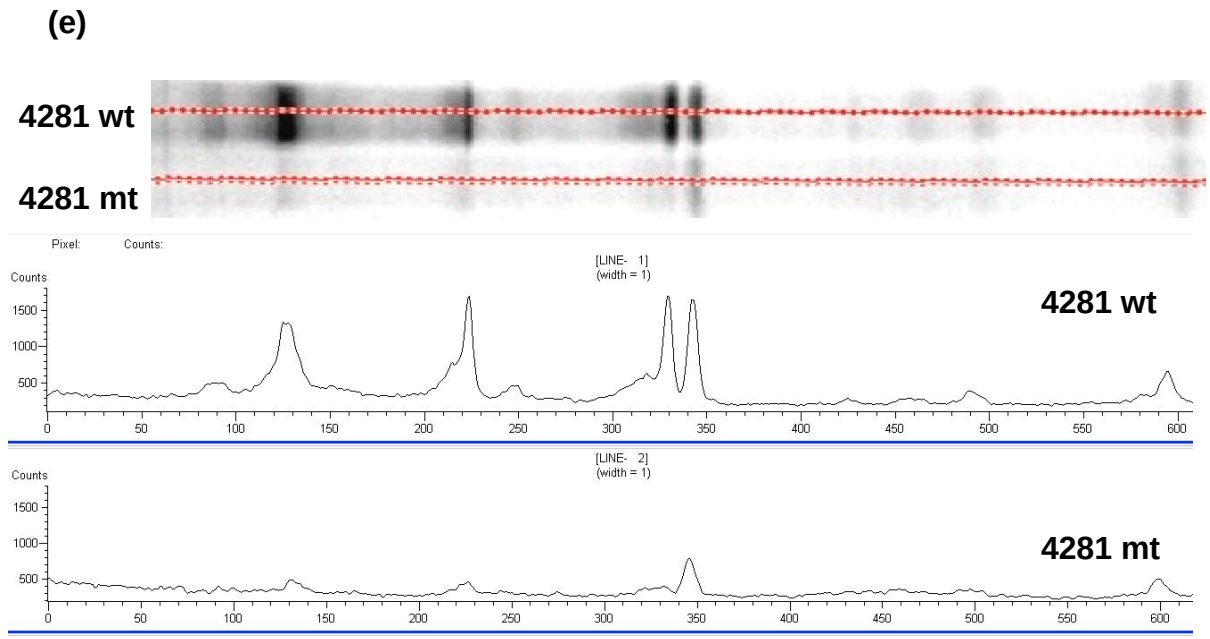

Figure 4.15.a-e. *Mitochondrial protein synthesis. During block of cytosolic translation by emetine, the mitochondrial translation products were labeled by incorporation of ^{35}S-methionine and separated on a 15% SDS polyacrylamide gel. (a) 4281 cell lines; (b) 4296, 4290 cell lines; (c) sample 4281, protein loading control by Coomassie staining; (d) samples 4296, 4290, protein loading control by Coomassie staining; (e) histogram of 4281A and 4281A>G polypeptides. ND1, ND2, ND3, ND4, ND4L, ND5 and ND6 are subunits of complex I; Cytb of complex III, COXI, II and III of complex IV; A6 and A8 of complex V; WT=wild type; MT=mutant.*

4281A>G cell lysates were absolutely negative for the mitochondrial encoded subunits COX1 and COX2 (*figure 4.16, 4281, c IV 1 and c IV 2*), which was consistent with the lacking respiration and the strongly reduced mitochondrial translation of the mutants. This cell lysates were also strongly reduced in their nuclear encoded subunit of complex I (*figure 4.16, 4281, c I*), with 6% residual expression relative to the wild type cell lysates. The other nuclear encoded proteins were not affected by the mutation, but a reproducible reduction of complex III subunit to 40% relative expression was surprisingly found for mutant clone SN(17-49/1), only (*figure 4.16, 4281, c III, MT1*).

In their respiratory chain, the mutant 4284G>A cells showed reduced complex IV activity, only, and therefore, we specifically analyzed the complex IV subunits COX1 and COX2 (mitochondrial encoded) and COX4 and COX5 (nuclear encoded) (*figure 4.16, 4284, c IV 1,2,4 and 5*). Two of the three mutant clones did not show

alterations, but the third mutant, Bel(8), expressed mitochondrially encoded subunits 50% less. This explains the higher error bars of the mutant samples, especially for COX2 (*figure 4.16, 4284, c IV 2*). As expected, the additionally analyzed expression of the complex I subunit was not affected by the mutation (*figure 4.16, 4284, c I*).

For the two mutant 4290T>C cybrid lines, also the Western Blots showed differing results. While expression of complex I, III and all four complex IV subunits was normal in cell line 1, SV(1), it was reduced to approximately 50% or more in cell line 2, SK(3). This reduction was consistent with the photometrically detected reduced activity of the respiratory chain complexes, the slow cell growth in galactose medium and the reduced translation of the 13 mitochondrial proteins.

The 4296G>A transition exclusively affected complex IV activity in respiratory chain analysis, and the Western Blots showed consistent results: reduced levels of mitochondrial encoded complex IV subunits COX1 and COX2 (*figure 4.16, 4296, c IV 1 and c IV 2*), but normal levels of nuclear encoded subunits COX4 and COX5 (*figure 4.16, 4296, c IV 4 and c IV 5*).

The normal respiring 4300A>G mutants showed regular protein expressions. Neither complex I, nor the complex IV subunit COX1 expression was altered. *Figure 4.16* shows complex I and COX1 only.

4.2.9 Secondary Structure Prediction of tRNA^{Ile}

We studied the predicted secondary structures of wild type and the five mutant tRNA^{Ile} sequences by the software module RNAfold of the Vienna RNA package, based on minimal free energy calculations (*figure 4.17*). The software is available on the website http://www.tbi.univie.ac.at/~ivo/RNA/man/RNAfold.html. Wild type tRNA and four of the five mutations, 4284G>A, 4290T>C, 4296G>A and 4300A>G folded into cloverleaf-like structures, whereas the 4281A>G transition led to an alternative stem-loop structure. In case of the 4281A>G mutation, at least the T-stem, -loop and acceptor stem were maintained but the anticodon stem and –loop and the D-stem and –loop melted into this peculiar stem-loop structure.

(a)

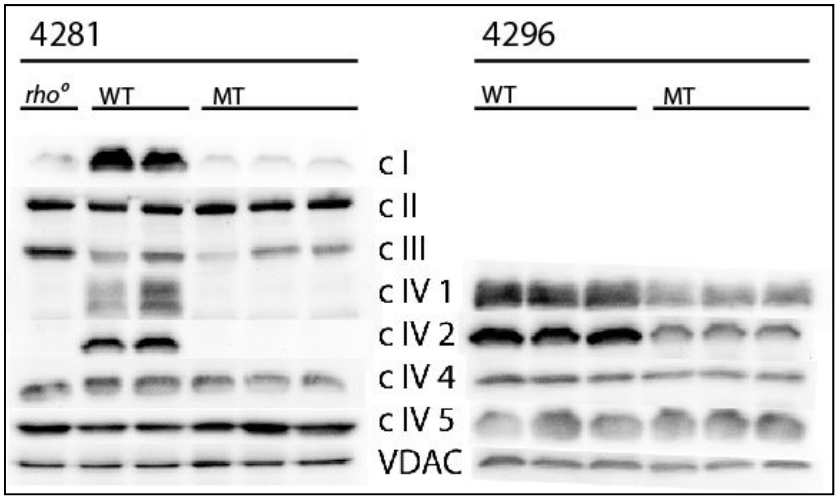
4281
4296
rho°
WT
MT
WT
MT
c I
c II
c III
c IV 1
c IV 2
c IV 4
c IV 5
VDAC

(b)

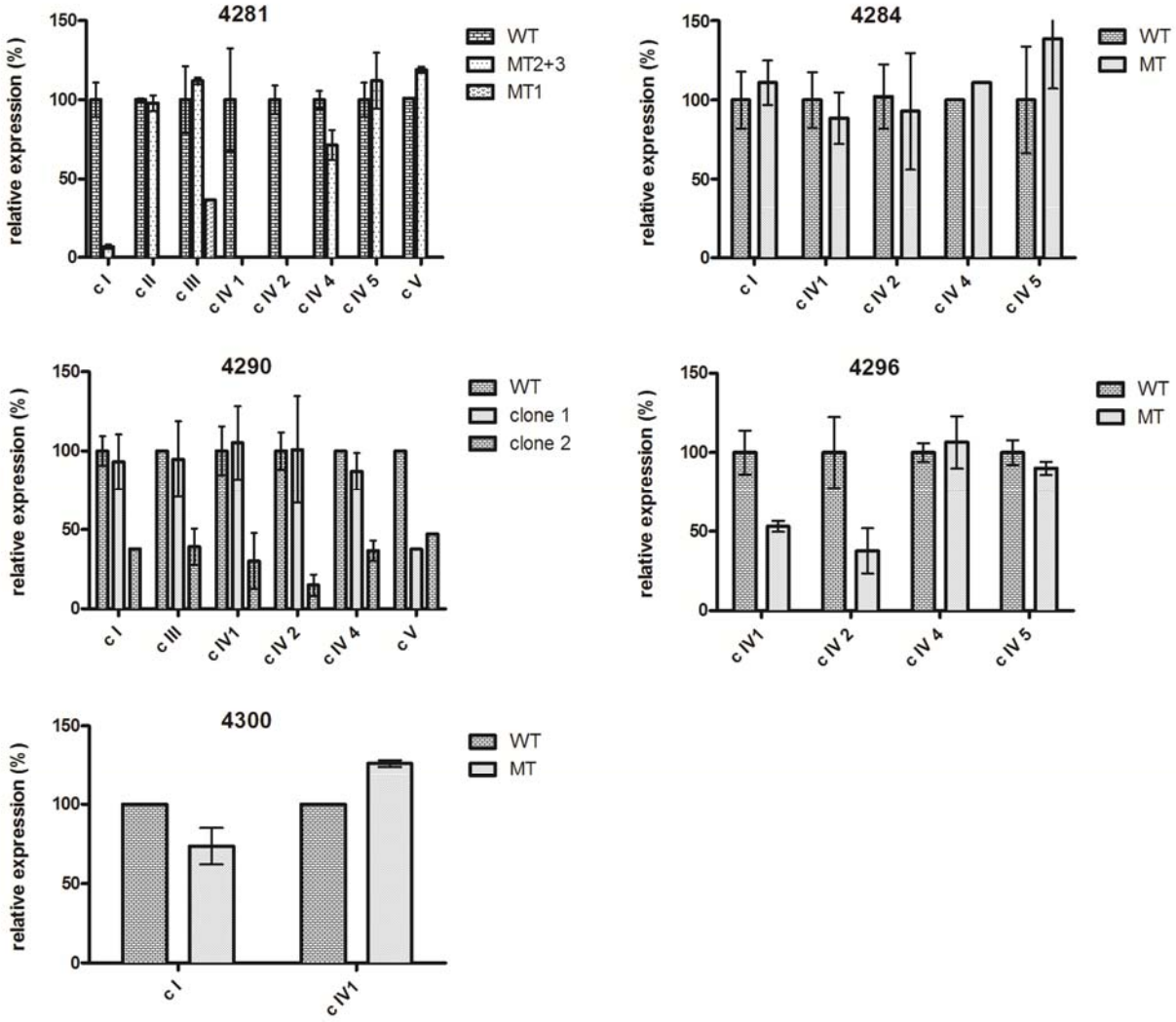
4281
relative expression (%)
WT
MT2+3
MT1
c I
c II
c III
c IV 1
c IV 2
c IV 4
c IV 5
c V
4284
relative expression (%)
WT
MT
c I
c IV1
c IV 2
c IV 4
c IV 5
4290
relative expression (%)
WT
clone 1
clone 2
c I
c III
c IV1
c IV 2
c IV 4
c V
4296
relative expression (%)
WT
MT
c IV1
c IV 2
c IV 4
c IV 5
4300
relative expression (%)
WT
MT
c I
c IV1

Figure 4.16. *Expression of protein subunits of the respiratory chain analyzed on cell extracts by Western Blot, normalized to GAPDH (glycerinaldehyde-3-phosphate dehydrogenase) or VDAC (voltage dependant anion channel). (a) Western Blot examples for samples 4281 and 4296; (b) quantification of expression of respiratory chain complexes in mutant cell lines relative to wild type cell lines. C I=complex I β subcomplex subunit 8; c II=complex II 70 kDa subunit; c III= complex III core 1 subunit; c IV 1= complex IV subunit 1 (COX1); c IV II= complex IV subunit 2 (COX2); c IV 4= complex IV subunit 4 (COX4); c IV 5= complex IV subunit 5a (COX5); c V= complex V subunit a; WT= wild type; MT= mutant.*

The mutant 4284G>A tRNA perfectly showed the cloverleaf-structure like wild type tRNA, only the base pair probabilities of D-loop and –stem, anticodon stem and the mutated position itself changed. The 4290T>C mutation also caused altered base pair probabilities of the same areas, the strongest applying to the anticodon stem and –loop. In the calculated structure, the mutated 4290T>C nucleotide base-paired with guanine at the opposite site in the anticodon loop, which is position 4296. This additional base-pair also allowed base-pairing of the neighboured positions 4291 and 4295, which are located next to the anticodon triplet. In this scenario, the size the anticodon loop is reduced to the only three bases, which is the anticodon triplet. The 4296G>A mutation induced similar alterations, with an additional base-pairing of the mutated 4296G>A nucleotide with uridine at the opposite site in the anticodon loop. The anticodon loop still consisted of five bases in this calculation: the anticodon triplet and the two adjacent nucleotides. The 4300A>G mutation did not affect the anticodon loop of the tRNA, but opened the upper part of the anticodon stem from a total of five base-pairs to only three. The mutated guanine at position 4300 could not, like in wild type $tRNA^{Ile}$, pase-pair with G at position 4286, and thereby opened the anticodon stem. Structural alterations of tRNAs may be the reason for functional impairments.

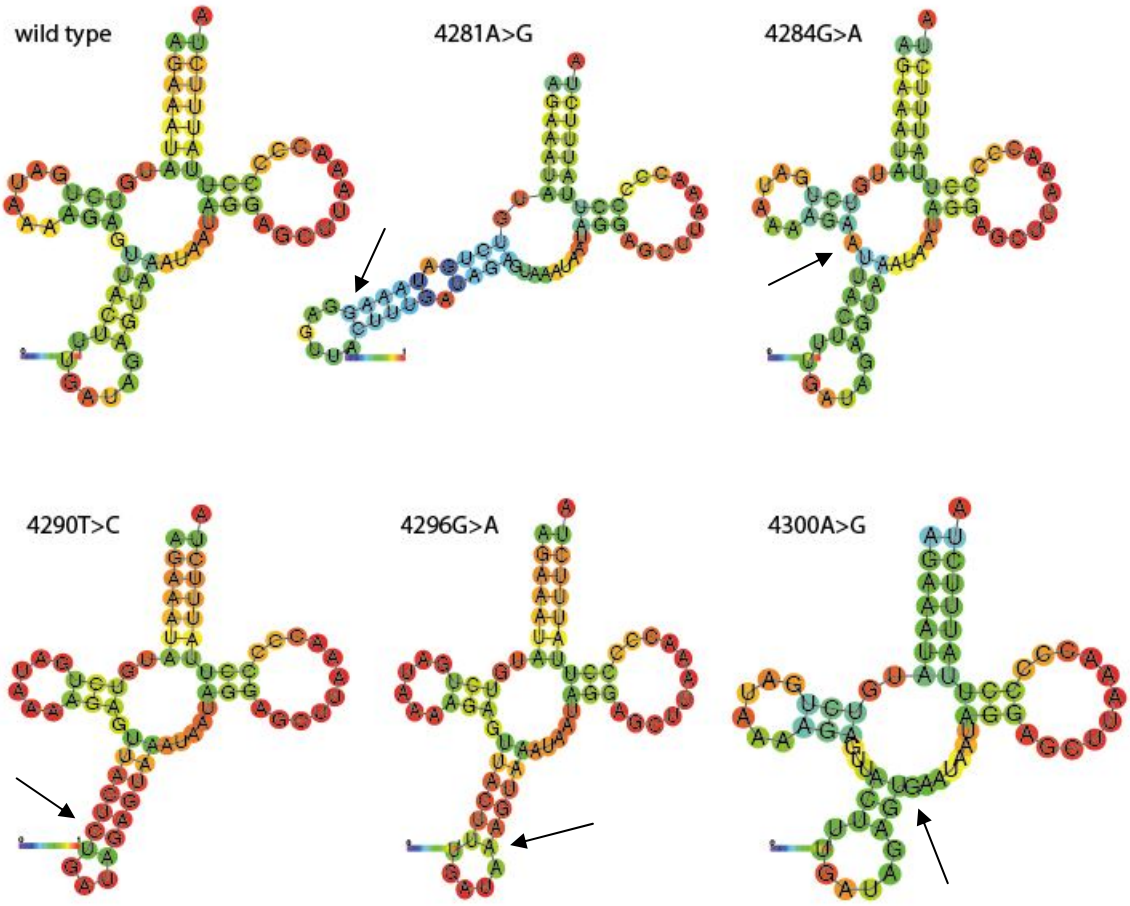

Figure 4.17. *Secondary structure prediction of wild type tRNA^{Ile} and mutated tRNA^{Ile} harboring the five mutations. Calculation by the RNAfold modul of the Vienna RNA package. Arrows indicate the mutated nucleotides; colors indicate the base pair probabilities, with blue=0 and red=1.*

5. Discussion

5.1 Aim of the Study

The purpose of our study was on the one hand to characterize the molecular and cellular phenotypes of the two $tRNA^{Ile}$ mutations 4281A>G and 4296G>A in the osteosarcoma cybrid model. Both were unknown mutations, when we started the project, and had been found and characterized in collaboration with Michael Freilinger, Vassiliki Konstantopoulou and Reginald E. Bittner. The molecular mechanism was not analyzed so far. On the other hand the aim was to compare the molecular and cellular consequences of all five mutations in the cybrid model. Three of the mutations, including a few cybrid studies, had been published before, but their molecular impact was not analyzed extensively.

5.2 The Cybrid Model

Cybrid cells are a useful and easy to handle model, because mtDNA mutations can be studied in a controlled system. Several factors can be excluded, which may be responsible for a high variability of the phenotypes, e.g., heteroplasmy, the ratio of mutated to wild type cells, or the nuclear genotype of the patient. The cybrids of our study were homoplasmic, thus excluding a mixed phenotype caused by wild type and mutant mtDNA molecules. They carried the mitochondrial mutations of the patients, but the nuclear background of the same cell type, 143B osteosarcoma, and should therefore enable a direct comparison of the phenotype, caused by the five mutations.

Cybrid cells allow the analysis of virtually unlimited amounts of biological material, which is a problematic factor in case of patient material or primary cell culture.

On the other hand, the model bears disadvantages. Some mutations, especially the homoplasmic ones, often result in tissue-specific diseases. The differentiation type and the epigenetic background of the cybrid cells do in most cases not correspond to the affected tissue, and therefore cybrid studies do not pay regard to the impact of nuclear modifier genes, which appear to influence the pathogenesis (Cock et al., 1998; Davidson et al., 2009). We accepted this disadvantage in favor of the possibility to compare the consequences of the five mutations directly. The nuclear genotype affects the mitochondrial phenotype (Cock et al., 1998), because almost all of the mitochondrial proteins are encoded by the nuclear genome, and other unknown regulatory factors are possibly involved. The 143B osteosarcoma cybrid model has been used in most studies of pathogenic mtDNA mutations (Vithayathil et al., 2012), but in some cases also HeLa or lung carcinoma cells served as host cells (El Meziane et al., 1998; Yasukawa et al., 2005). The constriction to transformed tumor cell lines is a weakness of the system, but it allows analyses in a defined system. Indeed, it would be desirable to analyze mutations, which cause tissue-specific diseases, in corresponding cell lines, i.e., to analyze a mutation causing isolated cardiomyopathy in heart cell culture. However, in our study the comparability of the cybrid cell lines had priority.

Depending on the severity of the mtDNA mutation's impact, it can be a challenge to generate viable homoplasmic mutant cybrid cells. This was the case for mutation 4281A>G. Gottfried Stegfellner from our lab, who generated the cybrid lines from the patients' platelets, only obtained heteroplasmic cybrids, due to a better fitness of these cells compared to the homoplasmic mutant cybrids. A further selection by ethidium bromide treatment, subcloning of heteroplasmic mutants and genetic screening of hundreds of clones was necessary to generate homoplasmic mutants (King, 1996).

Usually, cancer cell lines are used as host cells for cybrid generation. One should consider critically the possible aneuploidy of these ell lines. In addition, the process of cybrid generation may have an influence on the chromosomes, and one should also take into account the different sources of the host cell, i.e. the varying culture conditions in different laboratories. Differences in the karyotype can have an impact on the phenotype, which is a possible reason for variance of different clones carrying

the same mitochondrial mutation. We saw strong discrepancies between the two mutant 4290T>C cell lines, although they should theoretically contain the same nuclear and mitochondrial genome. It could be explained by the seven mitochondrial polymorphisms, which distinguished the two cybrid lines. However, the decreased complex II activity of cybrid line 2, SK(3), hinted to an underlying alteration of this cell line's nuclear genome. A less obvious variance was also found in mutant 4281A>G cells. The evident reason is that the three homoplasmic mutant cell lines were generated by subcloning of two different heteroplamic clones. Particularly, we obtained one homoplasmic mutant clone, SN(17-49/1), by subcloning of one heteroplasmic clone and two additional homoplasmic mutant clones, SN(47-4) and SN(47-9), by subcloning of another heteroplasmic clone. The three mutant cybrid lines behaved quite similar, but for example complex III activity was only decreased in clone 1, SN(17-49/1), but not in the others, SN(47-4) and SN(47-9), and mitochondrial translation was weaker in clone 1, too. Nevertheless, the three clones showed equal results in all other experiments. A different behavior of cybrid clones was also reported in other studies (Toompuu et al., 1999). However, the use of several clones showing slight variability is a basis for good statistics, because differences between wild type and mutant cell lines base on the analysis of biological replicas and not only on experimental repeats.

5.3 Characterization of the Molecular and Cellular Phenotypes of Individual Mutations

5.3.1 m.4281A>G

The heteroplasmic mutation 4281A>G caused CPEO and mild exercise intolerance starting in early childhood. Although the patient had been showing a benign course of the symptoms for ten years, the mutation caused the most severe phenotype in the cybrid system, with devastating impacts on tRNA function and consequently the cells' viability. The mutation is a paradigm of classical mtDNA mutations: it presented heteroplasmic in the patient, and in muscle tissue-staining, up to 25% of the fibers

showed a RRF-like appearance and were COX-negative. Biochemistry of muscle tissue showed a strongly reduced respiratory chain activity. The mutation is located at a highly conserved site of the tRNA, which has not been described as polymorphism, and the clinical pattern, ophthalmoplegia, is a symptom frequently associated with $tRNA^{Ile}$ mutations.

The 4281A>G transition in the D-arm (*fig. 1.3*) disrupted an A-U base pair at a highly conserved site, and in silico calculations predicted an alternative stem-loop secondary structure (*chapter 4.2.9, fig. 4.17*). This position, which is nucleotide number 23 referring to the standard tRNA numbering, is presumably engaged in tertiary structure folding. Although wild type $tRNA^{Ile}$ does not hold the classical and highly conserved 9A-12A/U-23U/A nucleotides, which show long-range interactions in classical tRNA tertiary structures (Helm et al., 2000), it instead contains $9m^1G$-12U-23A nucleotides in wild type $tRNA^{Ile}$, a base triplet which may interact similarly. Messmer and colleagues analyzed tertiary structure interactions of these three bases in human mitochondrial $tRNA^{Asp}$ (Messmer et al., 2009). Their cybrid cells contained a mutated G at position 9. By introducing the variant A at position 23, the 9-12-23 triplet is identical to the triplet bases found in wild type $tRNA^{Ile}$ (which is G-U-A). Containing these nucleotides, $tRNA^{Arg}$ does not hold the typical L-shape. They discuss that the structural neighborhood of this triple could have an influence to the structure. Either wild type $tRNA^{Ile}$ does not contain the classical tertiary base interaction 9-12-23, or the neighboring bases of the triplet allow an interaction of the triplet in $tRNA^{Ile}$. A fundamental investigation of the tertiary structural interaction and the possible involvement of positions 9-12-23 remain to be conducted.

An altered tRNA structure is additionally implied by our aminoacylation studies: mutated tRNAs migrated faster than their wild type counterparts in acid polyacrylamide gels (*fig. 4.13.a*). A recently described mutation at the same position in the D-arm of $tRNA^{Ala}$ (5636T>C) also caused CPEO (Pinos et al., 2011). In this case, secondary structure prediction showed the typical cloverleaf-like structure not only for the wild-type, but also for the mutated tRNA, albeit a relevant loss of free energy in the D-domain of the tRNA was calculated. This may allow an altered conformation of the secondary structure *in vivo*.

In the cybrid system, the 4281A>G mutation resulted in 50% decreased $tRNA^{Ile}$ steady-state levels and a slighty increased tRNA precursor level (*fig. 4.7 and 4.8*), but neither 5' processing by RNase P (*fig. 4.10*) nor stability of the mature molecule were altered (*4.11*). Since precursor tRNA plus 3' trailer was present in an equal amount like precursor tRNA plus 5' leader (see *chapter 4.2.3*), we concluded that 3' processing was not impaired. 5' processing was analyzed on *in vitro* transcripts, and we cannot exclude a slightly reduced processing *in vivo*. A strong impact of the mutation was found in aminoacylation experiments: we could not detect any aminoacylated mutant $tRNA^{Ile}$ (*fig. 4.13 and 4.14*), albeit we saw a weak translation activity in these cell lines (*fig. 4.15*). This discrepancy can be due to a technical quantification limit of the aminoacylation analysis. Nevertheless, the translation was very weak, and also, no expression of the mitochondrial encoded proteins could be detected (*fig. 4.16*). Additionally, the nuclear encoded subunit of complex I was strongly decreased, hinting to an accelerated decay of this polypeptide, which is unable to assemble into its destination complex. Surprisingly, we found the expression of the nuclear encoded subunit of complex III decreased in mutant clone 1, but unaltered in the other two. Different clones containing the same mutation should theoretically behave the same, but in this case they did not. Even more divergent results were obtained for the two cybrid cell lines containing mutation 4290T>C. This is one of the possible difficulties with cybrid studies as discussed in *chapter 5.2*. The differences between the 4281A>G cells may be due to polymorphisms in the nuclear genome. The mitochondrial genome was sequenced and contained the same polymorphisms. However, the lack of mitochondrial encoded proteins led to cell species, which did not respire (*fig. 4.2*); only the fully nuclear encoded complex II showed activity (fig. *4.3*). This is why they were not able to grow in galactose medium (*fig. 4.1*), but made use of glycolysis to survive, albeit with a worse fitness compared to wild type cells. They showed a strongly reduced growth rate and a swollen and vacuolated cell appearance. The structure of mitochondria was also swollen, and the Cristae formation was abnormal (fig. *4.5*), resulting from the malfunction of the OxPhos proteins. We conclude from the data that the A to G mutation at the conserved site 4281 apparently altered $tRNA^{Ile}$ structure, and thereby prevented aminoacylation of the molecule by isoleucyl-tRNA-synthetase. We cannot conclude whether this is caused by a hindered binding of the enzyme to the tRNA or the inability to aminoacylate $tRNA^{Ile}$. Mitochondrial translation relies on functional

$tRNA^{Ile}$, as no other isoacceptor for isoleucine exists in the mitochondrial system. Consequently, the 13 mitochondrial polypeptides could not be expressed and the complexes I, III, IV and V of the respiratory chain not be assembled. The cells were not able to respire and to generate their energy by oxidative phosphorylation. Despite their bad cell appearance, the mutated cells contained the same amount of mtDNA like wild type cells (*fig. 4.4*). Apparently, mtDNA maintenance is important for the cells' homeostasis, apart from its function in oxidative phosphorylation. During the studies, it was surprising that *rho*^{o} cells, which did not contain any mtDNA, grew faster and showed a healthier appearance than the 4281A>G cells. This could be due to the higher energy demand of the 4281A>G cells to maintain their mtDNA molecules, including mitochondrial translation and transcription, or due to an unknown negative effect of the mutated $tRNA^{Ile}$ on the cell system.

In addition, mutation 4281A>G was found in another patient, who suffered from myoglobinuria, which mainly affected the same tissue: the muscle (Emmanuele et al., 2011). The muscle biopsy revealed similar characteristics, several RRFs and COX-negative fibers. In contrast to our patient, the disease developed later in the adult age (39 years old, whereas our patient was a 6-year-old girl) and the respiratory chain activity was normal in muscle tissue. The mutation load was 65% in COX-negative muscle fibers and 45% in COX-positive fibers. In our patient, the mutation load was 89% in COX-negative fibers and 34% in COX-positive fibers. A threshold effect in the symptom development is obvious. Apparently, the wild type load of the mitochondrial genomes compensated the potential disastrous effect of the mutated ones. Thereupon, a more severe disease pattern, including an effect on respiratory chain activity, could develop in case of an increasing ratio of mutated to wild type mtDNA molecules. The same mutation was described in a second article (Patchett and Grover, 2011), but apparently it is same patient as described by Emmanuele et al. (2011). The patient description is surprisingly similar, and the authors held the identical clinic affiliation during the case observation.

In wild type $tRNA^{Ile}$, adenine at D-stem position 4281 (position 23 in standard tRNA numbering) base-pairs with uridine at position 4274. This position corresponds to position 12 of the classical nucleotide numbering and is therefore part of the discussed 9-12-23 triple, which is possibly involved in tertiary interactions (Messmer et al., 2009). Transitions at position 4274, which also disrupt base-pairing of

nucleotides 12 and 23, have been reported twice (Borthwick et al., 2006; Chinnery et al., 1997). Interestingly, the first report in 1997 described not only a phenotype similar to our case (mutation 4274T>C also caused CPEO), but also similar pathological impacts: the patient developed symptoms in the childhood, her muscle biopsy showed RRFs and COX-negative fibers, the activity of the respiratory chain complexes I and IV were strongly decreased and of complex III at least weak. The mutation was present at a level of 95% in COX-negative fibers and 68% in COX-positive fibers, with 81% prevalence in muscle homogenate. Aminoacylation kinetics revealed a strongly reduced *in vitro* aminoacylation activity of 6% for this mutant tRNA, compared to wild type $tRNA^{Ile}$ (Kelley et al., 2000). The authors found K_{cat} strongly reduced ($4 \times 10^{-3} s^{-1}$ compared to $1.3 \times 10^{-1} s^{-1}$ for wild type tRNA) but K_m only slightly (3.7 µM compared to 4.3 µM for wild type tRNA), and they concluded that the altered structure of mutated $tRNA^{Ile}$ allowed binding to aaRS, but hindered the aminoacylation reaction. In consequence, mutated tRNAs competed with wild type tRNAs in heteroplasmic cells, and therefore acted as inhibitors of aminoacylation. The same may be true for mutation 4281A>G, as both nucleotide positions are involved in the same secondary and probably tertiary interactions. Both mutations seemed to have similar effecst on tRNA structure, and consequently on the aminoacylation reaction. Kelley et al. (2000) further analyzed the double mutation 4274T>C/ 4281A>G, which restored almost 50% of the activity loss. This is an additional indicator for a structural defect caused by these mutations.

Levinger et al. (2003) analyzed the 3' processing activity on *in vitro* transcripts containing mutation 4274T>C, and they found a 4.2-fold reduction of processing efficiency. In this work, they compared 3' processing efficiency of 10 different $tRNA^{Ile}$ mutations, and mutation 4274T>C was one with milder effects on processing activity. They concluded that the mutants, which result in strong aminoacylation deficiencies, show a weaker effect on 3' processing and *vice versa*. This was the case for mutation 4274T>C mutation and in the same way counted for the mutated base-pair partner 4281A>G: we found a strong effect on aminoacylation (no aminoacylated tRNA species, *fig. 4.13.a and 4.14*), but processing was not impaired. (5' processing was not altered *in vitro* and we did not find precursor accumulation).

Of the ten described patients harboring a $tRNA^{Ile}$ mutation and suffering from CPEO (*table 1.1*), nine carried a heteroplasmic $tRNA^{Ile}$ mutation. Also mutation 4281A>G

was heteroplasmically expressed. The del4315A was the only homoplasmic mutation, however this mutation was accompanied by another heteroplasmic $tRNA^{Tyr}$ mutation and the correlation of the both mutations was not further analyzed. It was discussed that the pathogenesis of ophthalmoplegia bases on structural fragility, leading to functional defects of $tRNA^{Ile}$ (Kelley et al., 2000). In case of mutation 4281A>G in the D-stem, we were able to underline this assumption. The mutation apparently caused an alternative structural conformation, thereby hindered functionality of $tRNA^{Ile}$, and moreover introduced an anaerobic cell metabolism in the homoplasmic cybrid cells. The patients suffering from ophthalmoplegia tolerate the strong effect of the mutation by carrying a mixture of mutated and wild type mtDNAs.

5.3.2 m.4284G>A

The 4284G>A mutation affected the connector nucleotide between D-stem and anticodon stem (*fig. 1.3*), a poorly conserved position, and until now nothing is known about the structural and functional consequences of this mutation (Corona et al., 2002; Hahn et al., 2011). The position is modified to N2,N2-dimethylguanosine (m^2_2G).

Hitherto, the rare 4284G>A mutation was found in three independent cases (Corona et al., 2002; Hahn et al., 2011; Valente et al., 2009). We used the cybrid cells generated by Corona and colleagues for our studies. They described a family with heterogeneous disorders. The proband showed a neuronal disease and a mutation load of 55% in muscle. His brother and their mother showed a multisystem disorder, with a mutation load of 90% and 80% in muscle. The brother with the higher mutation load died of cardiomyopathy. While the activity of the RC complexes I and IV was decreased in the brother's and mother's muscle homogenate, the proband's muscle homogenate showed normal activity, resulting from a compensating effect of the higher wild type load. Consequently, the homoplasmic mutant cybrids derived from this proband showed decreased COX activity and decreased respiration compared to the patient's heteroplasmic muscle homogenate (Corona et al., 2002). We also detected reduced complex IV activity in the cybrid cells, but not the decrease in respiration, without any explanation for this discrepancy.

In the second case, the 27 years old patient suffered from spastic paraparesis (Valente et al., 2009). The skeletal muscle morphology was normal and biochemical analysis did not reveal any respiratory chain deficiencies. Within this study, several potentially pathogenic mtDNA mutations were detected in different patients. As the 4284G>A mutation had already been described, the authors did not follow studies on this mutation and no further information was given.

The third patient described recently was an 8-year old girl suffering from a MERRF-like phenotype without RRFs (Hahn et al., 2011). In muscle homogenate, complex I activity was reduced and complex IV weak. The mutation was present at 80% in the girl's blood and 20% in her mother's blood, who did not show clinical symptoms. Together with this description, the 4284G>A mutation was one of the few cases, in which $tRNA^{Ile}$ mutations did not result in the classical $tRNA^{Ile}$ diseases cardiomyopathy or CPEO.

On the molecular level, our cybrid studies showed reduced steady-state levels of mutant mature $tRNA^{Ile}$ to 30%; whereas the $tRNA^{Ile}$ precursor was increased 12-fold (fig. *4.7 and 4.8*). The mtDNA content in the cells was not altered (*fig. 4.4*), but the stability of $tRNA^{Ile}$ was decreased (fig. 4.11), possibly explaining the reduced level of the mature form. In consideration of the high precursor level, we expected an impaired 5' precursor processing, but this was not the case (fig. 4.10). Initially, we excluded an impaired 3' precursor processing, because the levels of different possible processing intermediates was the same (*chapter 4.2.3*). However, the strongly increased tRNA precursor levels indicated processing impairments and should be clarified. Although steady-state levels of mature $tRNA^{Ile}$ were reduced to 30%, and this small amont was less aminoacylated (approximately 75%, *fig. 4.13 and 4.14*), neither mitochondrial protein synthesis nor protein expressions of respiratory chain complexes I and IV were affected (*fig. 4.15 and 4.16*). Nonetheless, the isolated activity of respiratory chain complex IV was decreased (fig. 4.3), but not the activity of the respiratory chain as a whole (measured by oxygen consumption, *fig. 4.2*). Mutant cells showed unchanged respiration, and they were able to grow normal in galactose medium (*fig. 4.1*). This does not necessarily surprise, as complex IV is described to possess an excess capacity. Its reduced activity may be sufficient to fulfill the redox reactions, which are necessary for the full function of the redox partners (Gnaiger et al., 1998). The low amount of mature $tRNA^{Ile}$ and the even lower

amount of loaded $tRNA^{Ile}$ species is apparently sufficient to translate mitochondrial proteins, at least COX1 and COX2 of complex IV. Unfortunately, only antibodies against these mitochondrial encoded proteins worked specifically. We don't know the expression level of COX3, the third mitochondrial encoded complex IV polypeptide. Possibly, the level of solely this protein was reduced. Alternatively, other unknown regulatory functions of the loaded or unloaded $tRNA^{Ile}$ might impact on complex IV assembly or function, and thereby caused its reduced activity. Though speculative, other regulatory functions of tRNAs beyond amino acid transfer cannot be excluded, and if so, altered tRNA steady-state levels can result in malfunction of respiratory chain complexes or act beyond, without having an effect on the classical transfer function. For instance, the binding potential of mitochondrial tRNAs to cytochrome *c*, which impacts on apoptosis susceptibility, was shown recently (Mei et al., 2010b).

The predicted $tRNA^{Ile}$ secondary structure was not altered (*fig. 4.17*). However, the structure prediction software disregarded any modifications, and mutation 4284G>A is located at a dimethylated position. Therefore, we could not exclude an alternative tRNA folding *in vivo*. As modifications, which are not located in the anticodon loop, are probably involved in tRNA folding and stability (Motorin and Helm, 2010), one could assume a defect on this point. The decreased stability of mutant $tRNA^{Ile}$, which we had found, substantiates this assumption. Yasukawa et al. (2000) described another $tRNA^{Ile}$ mutation, 4269A>G, which also caused instability of $tRNA^{Ile}$. They analyzed the stability of unmodified *in vitro* transcripts and the sensitivity of native, modified tRNAs to degradation in a mitochondrial extract. The unmodified tRNAs were more sensitive to degradation, suggesting a protective contribution of post-transcriptional modifications.

Altogether, the mutation of the modified connector between D-stem and anticodon stem had a destabilizing effect on $tRNA^{Ile}$. In combination with accumulated precursors and impaired functionality of $tRNA^{Ile}$, a strongly reduced amount of mature $tRNA^{Ile}$ 4284G>A was detected, leading to an isolated decrease of complex IV activity. This specific defect of the respiratory chain did not cause diminished respiration, but may be involved in pathogenesis by other (regulatory) mechanisms.

5.3.3 m.4290T>C

Mutation 4290T>C is located at position 32 (according to the international standardized tRNA numbering), two bases upstream of the anticodon in the anticodon loop (*fig. 1.3*). Hitherto, the mutation has been reported in two independent cases (Limongelli et al., 2004; Valente et al., 2009). Limongelli et al. described a family with two affected sisters, suffering from a Leigh-like disease, while their mother, who also carried the homoplasmic mutation, astonishingly did not show any symptoms. No biochemical abnormalities were detected in muscle homogenate, but reduced activities of the respiratory chain complexes I and IV were detected in fibroblasts of the two sisters and surprisingly also the mother, who did not show any clinical symptoms. It is still unknown why homoplasmic mutations can show variable penetrance in different family members, i.e., causing pathological phenotypes in some individuals, while in others not. Limongelli et al. (2004) generated homoplasmic cybrids and were able to reproduce the reduced complex I and IV activity. They moreover found a reduced translation of ND4 and ND5, which are subunits of complex I, and COX1, which is a subunit of complex IV of the respiratory chain. Studies on cytochrome *c* oxidase assembly revealed an approximately 50% increased presence of immature subcomplexes of complex IV. The second report of the 4290T>C mutation told a similar pattern (Valente et al., 2009): the authors described a 16-year-old patient suffering from severe encephalopathy, with normal skeletal muscle morphology and reduced complex I and IV activities in muscle homogenate. We used two different cybrid cells, generated by Limongelli et al. (2004), for further investigation on this mutation. The two cybrid lines are derived from each of the two sisters.

In homoplasmic cybrid cells, steady-state levels of mature mutant $tRNA^{Ile}$ were reduced to 35%, while steady-state levels of the precursors were elevated three times (*fig. 4.7 and 4.8*). We neither found alterations in 5' processing (*fig. 4.10*) nor in stability or resynthesis of $tRNA^{Ile}$ (*chapter 4.2.4*). Like in case of the mutated $tRNA^{Ile}$ 4284G>A, quantification of the precursor steady-state levels, specifically $tRNA^{Ile}$ plus 5' extension, $tRNA^{Ile}$ plus 3' extension and $tRNA^{Ile}$ plus 3' and 5' extensions, showed the same levels. The precursor, which consisted of tRNA plus 3' extension, was not particularly increased. Therefore, we excluded defects in 3' processing.

Notwithstanding, a constrained processing seemed to be the only logical explanation for the increased precursor level and the concomitant decrease of the mature tRNA level. Aminoacylation of the mutated tRNA worked as fine as with the wild type control, we did not find differences (*fig. 4.13 and 4.14*). Further studies on translation (*fig. 4.15*), mitochondrial protein expression (*fig. 4.16*), OxPhos activity (*fig. 4.2 and 4.3*) and growth in galactose medium (*fig. 4.1*) brought astonishing outputs, because the two cybrid lines reproducibly showed divergent results. While cell line one, SV(1), showed approximately 50% reduced complex I and IV activity and thereby reflected the results described by Limongelli et al. (2004), cell line two, SK(3), showed much stronger deficiencies of these complexes and additionally of complex II and III. Cybrid line one showed a translation pattern similar to wild type cells, and the second one an overall reduced translation. Consistently, expressions of complex I and IV subunits were normal in cybrid line SV(1) and about 50% or more reduced in cybrid line SK(3). Also the cell growth of cybrid line SK(3) in galactose medium was more decelerated than the cell growth of cybrid line SV(1), which is not surprising, considering the strongly impaired respiratory chain activity. Recognizing the decreased complex II activity in SK(3) cells, we assumed an impact of the nuclear genome to the stronger phenotype of this cybrid line. It was beyond our possibilities to analyze the nuclear genome within this project; we therefore focused on sequencing the mitochondrial genomes to exclude additional pathogenic mutations. The mtDNA sequences of the two cybrid lines deviated from the mtDNA reference sequence (Andrews et al., 1999) at 35 positions (*table 4.2*). 28 SNPs were present in both cybrid lines and homoplasmic. Thereof, one was the 4290T>C mutation and the others were already described polymorphisms (*table 4.2)*. The other seven polymorphisms were only present in one of the two cybrid lines. This is an unexpectedly high number of deviations between the two sequences, considering that the two cybrid lines contained mtDNA of two sisters. Reasons for these differences are unknown. Of the seven SNPs, only two were detected in cybrid line SK(3), which were both already known homoplasmic polymorphisms in the D-loop at position 195 and 263 (http://mitomap.org/MITOMAP). Surprisingly, cybrid line SV(1), which showed the less severe phenotype, harbored five SNPs: two homoplasmic mutations were present in the D-loop and already reported as polymorphisms, while two heteroplasmic transitions at positions 10979 and 11074 in the ND4 gene were unknown until now. 10979C>T/C heteroplasmically changed a proline to a serine

codon, and the second one was silent. The fifth SNP in SV(1) cybrid cells was a homoplasmic 12308A>G transition in $tRNA^{Leu(CUN)}$. It was formerly described as polymorphism, which frequently accompanied pathogenic mutations in the mitochondrial genome (Crimi et al., 2003; Grasso et al., 2001; Zifa et al., 2008), but was also described as pathogenic mutation (Moraes et al., 1993). Furthermore, this mutation serves as marker for defining haplogroup U, and its presence is supposed to be a risk factor for strokes (Finnila et al., 2001; Pulkes et al., 2000). We found this mutation only in one of the two 4290T>C cybrid cell lines. As the 4290T>C cybrid lines were generated with mtDNA of two sisters, we can exclude different haplogroups. Therefore, we assume that 12308A>G is rather a random mutation in case of cybrid line SV(1). We only can speculate about the impact of this mutation on the cells' phenotype. It could act synergistically with the pathogenic 4290T>C mutation. Alternatively, mutation 12308A>G could to some part rescue the phenotype caused by the 4290T>C mutation. This would explain the less severe phenotype of cybrid line SV(1) (containing 4290T>C and 12308A>G) compared to cybrid line SK(3) (containing only 4290T>C), although the rescue mechanism is not obvious to us. Rescue of a pathogenic phenotype by additional mitochondrial mutations was previously described in other cases and can even own the capacity to revert a pathogenic phenotype to a wild type-like phenotype (El Meziane et al., 1998). The theory of a rescue effect of the 12308A>G mutation would explain the less severe phenotype of cybrid line SV(1), but on the other hand abstracts away from the low activity of the nuclear encoded complex II in 4290T>C cell line 2, SK(3) (*fig. 4.3*). The reduced activity of the nuclear encoded OxPhos complex II makes a nuclear contribution to the severe phenotype of the SK(3) cybrid line more likely. This, maybe combined with a rescue effect of those additional mutations in cell line SV(1), may explain the differing results of the two 4290T>C cybrid lines.

Limongelli et al. (2004), who provided us these cybrid lines, mentioned the presence of 18 polymorphisms in the mitochondrial genome of the patients' cells, which were uniform in all probands. Whether the additional mutations in the cybrid cells have developed during the long procedure of cybrid generation or later on, is unknown. The additional mutations in the cybrid cells were apparently homoplasmic (with exception of the two mutations in gene *ND4* of cell line SV(1)), which provides

evidence of a mutation event during the procedure of cybrid generation; otherwise we would expect a mixture of mutated and wild type genomes.

The mtDNA content in the 4290T>C mutants was 1.8-fold increased (*fig. 4.4*). This amplification could be seen as compensation attempt to counterbalance the pathogenic effects of the mutation. 4290T>C cybrid cells from the same source were also analyzed by another group, which found the same ratio of mtDNA (Moreno-Loshuertos et al., 2011) and also a decreased respiration rate in the mutant cell lines. They assumed a partly alternative conformation of mature $tRNA^{Ile}$, because they found a second $tRNA^{Ile}$ band in acid polyacrylamide gels during aminoacylation analyses, which did not disappear by deacylation. In our case, the mutant tRNA migrated faster than wild type tRNA in acid polyacrylamide gels (*fig. 4.13.d and 4.14*), indicating an alternative structure of the mutated molecule, which was probably more compact. This would coincide with the predicted secondary structure of the mutated molecule (fig. 4.17). The mutated site potentially bound the opposite site in the anticodon loop, position 4296 (position 38, international tRNA standard numbering, *fig. 1.3*), tightly, and thereby allowed base-pairing of the two bases adjacent to the anticodon. In this scenario, the anticodon loop only consisted of the anticodon. Admittedly, the modification at position 4295 (position 37, international tRNA standard numbering, *fig. 1.3*), a threonylcarbamoylation (t^6A37), was ignored in this model. This modification probably hinders base-pairing of the two nucleotides adjacent to the anticodon, and thereby protects the anticodon's ability to read the codon during translation. Other studies on *E. coli* demonstrated that the positions 32 and 38, which correspond to positions 4290 and 4296 in human mitochondrial $tRNA^{Ile}$, are conserved and ensure accurate decoding in $tRNA^{Ala(GGC)}$ (Ledoux et al., 2009; Murakami et al., 2009). Deviating nucleotides at these positions led to misaminoacylations (Schimmel and Guo, 2009). Possibly, this is the case for the severely affected cybrid line SK(3). Its mutation 4290T>C may lead to misaminoacylation, which would consequently destabilize mitochondrial proteins and explain their decreased steady-state levels (*fig. 4.16*), the weak cell respiration (*fig. 4.2 and 4.3*) and the slow growth rate in galactose medium (*fig. 4.1*). In case of the milder affected cybrid line SV(1), the additional polymorphisms may rescue the phenotype by unknown mechanisms. Another group analyzed the structural and functional role of nucleotide 32 in yeast mitochondrial $tRNA^{Ile}$ (corresponding to

position 4290 in human mitochondrial $tRNA^{Ile}$ (Montanari et al., 2011). Humans and yeast carry the same wild type nucleotide at this position. They introduced a T>C base substitution at this position in *S. cerevisiae* and found a severe phenotype. The cells did not respire and were not able to grow on nonfermentable substrates. $tRNA^{Ile}$, but also other mitochondrial tRNAs and the mitochondrially translated COX3 were absent in the cells. They showed a stronger defect than our mutant human cell lines, which showed a decreased $tRNA^{Ile}$ steady-state level to 35% (*fig. 4.7*). Overexpression of different aaRS rescued the growth defect of the yeast cells, with IleRS bearing the highest rescuing efficacy. Moreover, overexpression at least partially rescued mitochondrial tRNA levels and protein expression. The phenotype was not rescued by overexpression of EF-Tu, which was expected, as EF-Tu does not bind to anticodon nucleotides. We did not conduct any rescue experiments, but based on the overall strong similarities between yeast and human mitochondrial $tRNA^{Ile}$, these studies on yeast can deliver helpful predictions. Mutant yeast $tRNA^{Ile}$ migrated faster than wild type $tRNA^{Ile}$ in acid polyacrylamide gels, like human mt $tRNA^{Ile}$ did in our hands. This further indicated similar conformational changes. Montanari et al. (2011) analyzed several available three-dimensional tRNA structures and sequences, and their studies revealed a strong conservation of nucleotide positions 32 and 38. In mitochondrial $tRNA^{Ile}$, most frequently T32 and G38 are present, like in case of the human molecule, and these two nucleotides are 100% conserved in mammalian mitochondrial $tRNA^{Ile}$. The authors assumed that in case of a mutated position 32, hydrogen bond interactions between positions 32 and 38 could be altered. This would probably lead to conformational changes of the anticodon loop. They further discuss that position 32 does not interact with class I aaRS (like IleRS), and aminoacylation deficiencies may therefore be unlikely. Consistently, in our studies on mutation 4290T>C, we did not find an effect on tRNA isoleucylation. Olejniczak et al. (2005) demonstrated that the conservation of nucleotides 32 and 38 are necessary for proper binding to the ribosome in *E. coli*. If applicable to the human mitochondrial system, this may be the reason for the decreased protein synthesis in our cybrid cells containing mutation 4290T>C (corresponding to position 32).

5.3.4 m.4296G>A

Mutation 4296G>A is located in the anticodon loop at a highly conserved site (*fig. 1.3*). Due to the absence of histo- or biochemical mitochondrial deficiencies in the patient's muscle tissue, it was not clear whether the mutation could be assigned as pathogenic one. Further evidence was provided by a description of a second patient carrying the same mutation (Cox et al., 2012). The 4296G>A mutation was additionally detected as somatic mutation in oncocytic pituitary adenoma (Porcelli et al., 2010).

We discovered biochemical deficiencies in homoplasmic 4296G>A cybrid cells, which is an indication of pathogenecity. The cybrid cells showed an isolated reduction of complex IV activity to 80% (*fig. 4.3*) and a slightly reduced respiration (*fig. 4.2*). The normal respiratory chain activity in the patient's muscle tissue could result from a compensatory effect of the low number of wild type mtDNA (approximately 5%), while the homoplasmic mutant cybrid cells could not compensate the deficiency. In case of the second patient, who harbored the same mutation (Cox et al., 2012), the mutation load was not measured in muscle tissue. Fibroblasts carried "only" 85% mutated mtDNA and developed a strongly reduced respiration. Blood cells showed a mutation load of 78%. In our patient, mutation load was 95% in muscle, 84% in skin and 66% in blood cells. This discrepancy between the respiratory chain activities of the two patients' cells can be due to the different cell types (muscle and fibroblasts), experimental conditions, epigenetic factors or to an impact of the patient's genotype, e.g., presence of a compensating, but otherwise silent, polymorphism.

The diminished complex IV activity of the homoplasmic cybrid cells caused a slight decrease of respiration (*fig. 4.2*), but cell growth in galactose medium was normal (*fig. 4.1*). The steady-state levels of $tRNA^{Ile}$ precursors and mature $tRNA^{Ile}$ were reduced to 70% (*fig. 4.7 and 4.8*), and aminoacylation of $tRNA^{Ile}$ reduced to 50% (*fig. 4.13 and 4.14*). Despite this reduction, we could not detect an effect on mitochondrial translation; only a faint reduction of translation products in mutant line 3 (PN(2-2) was seen (*fig. 4.15*). The fact that we could not detect a significant reduction in translation does not necessarily surprise. In other studies, strongly decreased steady-state levels of mutant tRNAs did not always lead to decreased translation (Janssen et al., 1999). Anyhow, expressions of the mitochondrial encoded proteins COX1 and COX2,

which are subunits of complex IV, were reduced to 40-50%, whereas expression of nuclear encoded complex IV subunits was unchanged (*fig. 4.16*). Mutation 4296G>A may affect the translation of these proteins, which could not be detected by metabolic ^{35}S-labeling of mitochondrial proteins (*fig. 4.15*). The reduced expression can also be due to instability of the mitochondrial proteins, possibly by incorporation of non-cognate amino acids into the mitochondrial proteins by mutated tRNA^{Ile} (although we did not detect additional or alternative protein bands in the translation assay, *fig. 4.15*). Alternatively, they can be due to other unknown regulatory effects of the tRNA.

In the predicted secondary structure of mutant 4296G>A tRNA^{Ile} (*fig. 4.17*), the mutated adenine base-paired with uridine at position 4290, which is located in the opposite site of the anticodon loop, with two nucleotides distance to the anticodon. Thereby, the size of the anticodon loop was reduced from seven to five unpaired nucleotides (fig. 4.17). The altered structure of this area may possibly have caused the decreased aminoacylation, which we observed.

Moreno-Loshuertos et al. (2011) recently described the generation and characterization of a tRNA^{Ile} mutation in a mouse cell line, which corresponded to the pathogenic 4296G>A mutation in human cells. The mutation was induced by random mutagenesis in mouse cell culture, and transmitochondrial mouse cells were generated thereof. In this cybrid cells, the steady-state levels of mature tRNA^{Ile} were reduced to 80%. In acid polyacrylamide gel analyses, the authors found a proportion of the mutated tRNA alternatively folded, which appeared as second band and was shown to be a non-chargeable form of tRNA^{Ile}. Such an additional band was also present in our studies, and we supposed an alternative tRNA conformation (*fig. 4.13.c*). However, the additional band was also present in wild type samples, and therefore could not be regarded as consequence of the mutation. Moreover, we saw a mobility shift of the total fraction of mutated tRNAs compared to wild type tRNAs, and therefore supposed an altered conformation of the mutated molecule. Mutant 4296G>A tRNAs generally migrated slower than the wild type counterpart. Furthermore, aminoacylation of mutant tRNA^{Ile} was reduced about 50%, but still, this tRNA showed aminoacylation in our hands (*fig. 4.13.c and 4.14*). The different observations can be due to technical parameters: the authors analyzed the aminoacylated tRNA fraction in presence of 4 M urea (we used 8 M urea), a condition which is less denaturing. Consequently, additional non-chargeable tRNA^{Ile}

conformations could be denatured in our assays. The mouse cybrid cells showed a reduced respiration (average reduction of 46%) with decreased activity of all those complexes, which contain mitochondrial encoded subunits. Doubling time in galactose medium was almost 30% increased. This is a stronger effect than in our cybrid cell lines, which showed an isolated reduction of complex IV activity (*fig. 4.3*) and normal growth in galactose (*fig. 4.1*). The reasons causing this difference are unknown, but we can speculate about different regulatory mechanisms of mouse and human cell lines or a possible impact of polymorphisms in the cell lines. The mutation affected respiration in mouse cells more severely than in the human cells, but nevertheless, the authors were also not able to monitor a translation defect. Like in our case, they speculated about limitations of the method, which probably allows the detection of severe translation defects, only. Despite an apparently functional translation, they found the assembly of respiratory complexes reduced and detected non-mature subcomplexes in mutant cells. This is a point, which we also assumed for complex IV in our human cybrid cell line. Moreno-Loshuertos et al. (2011) discussed that the OxPhos deficiency caused by mutation 4296G>A is moderate and therefore tolerated in the homoplasmic cell line. To explain the different outcome in family members carrying the same mutation, they proposed a “functional epistasis model”. It says that severe effects of tRNA mutations in homoplasmic cells can be compensated by either increased mitochondrial biogenesis, induced by ROS production, or by emergence of a second “epistatic” mutation in the same molecule, which would present as polymorphism. Differences in the amplitude of this hypothetical cell response could be modulated by gene context or environmental factors, and thereby change the clinical pattern. In their mouse cells, they indeed detected a two-fold increase in mtDNA content. The mtDNA content in human 4296G>A cybrid cells was not altered compared to wild type cybrid cells (*fig. 4.4*). Hence, mitochondrial biogenesis could in our case not be the reason for the milder deficiencies.

Recent studies on *E.coli* $tRNA^{Ala(GGC)}$ provided strong evidence, that the highly conserved nucleotides at positions 32 and 38 in the anticodon loop (which correspond to the positions 4290 and 4296 in $tRNA^{Ile}$) are responsible for translation fidelity (Ledoux et al., 2009; Murakami et al., 2009). They showed that mutations at these positions highly increased the tRNA’s capability of misreading other near-

cognate codons, so that the wrong amino acid could be inserted into the growing polypeptide chain. Overexpression of tRNAs, which carried transitions at these two positions, was toxic to the cells (Murakami et al., 2009). Schimmel and Guo discussed a connection between mitochondrial diseases and translational infidelity, caused by either mutations at conserved tRNA sites or in the editing center of tRNA synthetases (Schimmel and Guo, 2009). It was shown that mischarged tRNAs can lead to neurodegeneration and ataxia in mice (Lee et al., 2006). The authors reported that misfolded proteins can accumulate intracellularly and cause neuronal death. Our patient suffered from neurological disease. Given the fact that we were not able to observe a defect in translation in the mutant 4296G>A cells, despite a reduced expression of mitochondrial encoded COX subunits (*fig. 4.15 and 4.16*), one could consider translation infidelity; although we did not detect any mobility shift of the mitochondrial proteins in the translation assay. Montanari et al. (2011) analyzed the structure and sequence of yeast mitochondrial $tRNA^{Ile}$. They compared mutant 32T>C tRNAs (which corresponds to 4290 in human mt $tRNA^{Ile}$) and wild type $tRNA^{Ile}$ and discussed that the geometry of the 32-38 base pair (which correspond to 4290 and 4296 in human mt $tRNA^{Ile}$) may be altered by mutations at both positions. Furthermore, they mentioned an interaction of position 38 with the ribosome and class I aaRS (like IleRS), which can contribute to a reduced translation rate. This could hypothetically be the reason for the reduced protein levels of complex IV, which we found in the mutant 4296G>A cybrid cells (*fig. 4.3*).

In general, the 4296G>A mutation appeared more like a typical homoplasmic mutation to us. Despite its heteroplasmic state, the mutation's frequency was rather high in the patient's muscle, with a load of 95%, and it caused a tissue-specific, purely neurological disease. Furthermore, the homoplasmic mutant cybrid cells did not show a strong phenotype. The mutation only had a slight effect on the tRNA amount. Indeed, aminoacylation of $tRNA^{Ile}$ was reduced, but only respiratory chain complex IV showed less activity, and cells grew and respired well, despite their homoplasmic mutation. It means that the cells could stand the effect of the mutation. It was not surprising to us, because the model is a tumor cell line, which mainly relies on glycolysis. Thus, minor alterations in the respiratory chain don't necessarily have a strong influence on cell viability. The molecular pathological mechanism is not yet clear. The cybrid cells grew normal under respiratory stress conditions in galactose,

in which they were forced to use their respiratory chain. Thus, we did not assume increased ROS levels, although we did not analyze this point. The decreased complex IV activity probably caused a stronger effect in the postmitotic nerve tissue of the patient, albeit the possibly underlying regulatory mechanisms are unknown.

5.3.5 m.4300A>G

The 4300A>G transition is located in the anticodon stem of $tRNA^{Ile}$ (*fig. 1.3*). Hitherto, the mutation was found in two different families (Casali et al., 1995; Taylor et al., 2003). In both families, the mutation was homoplasmic in different tissues of symptomatic and asymptomatic individuals, albeit heart was the only clinical affected organ. Only in cardiocytes, severe defects of respiratory chain complexes I and IV were detected, whereas OxPhos activity was normal in muscle, fibroblasts and myoblasts. The steady-state levels of mature $tRNA^{Ile}$ were significantly decreased to approximately 10% in heart and skeletal muscle tissue, and in cultured skin fibroblasts and myoblasts to a lesser extent.

Our studies likewise revealed reduced $tRNA^{Ile}$ steady-state levels in 4300A>G cybrid cells. While mutant cells contained only 40% of the mature $tRNA^{Ile}$ of wild type cells, the precursor transcript was increased 6-fold (*fig. 4.7 and 4.8*). RNase P processing activity on the mutated tRNA precursor was reduced to 75% (*fig. 4.10*), and this is probably the reason for the altered steady-state levels of immature and mature $tRNA^{Ile}$. Mutant $tRNA^{Ile}$ showed a similar stability like wild-type tRNA, it was correctly aminoacylated (*fig. 4.13.d and 4.14*), mitochondrial translation worked normally (*chapter 4.2.7*) and mitochondrial proteins were expressed (*chapter 4.2.8*). 3' processing of the $tRNA^{Ile}$ precursor and aminoacylation was analyzed *in vitro* by another group (Levinger et al., 2003), and they found that the 4300A>G mutation barely affected both reactions, consistent with our results. Despite wild type-like respiration of our mutant 4300A>G cells (*fig. 4.2*) and normal activity of all respiratory chain complexes (*fig. 4.3*), the cells surprisingly grew worse in galactose medium (*fig. 4.1*). After 48 h growth in galactose medium, the cell number of mutant cells was less than half of the number of wild type cells. Similar results were obtained by another group (Perli et al., 2012). Also in their hands, the mutant 4300A>G cells grew like wild type cells in glucose medium, but decelerated in galactose medium. Moreover,

they found increased ROS production and apoptosis in cells grown in galactose medium, which was not the case in glucose medium. In previous studies, ROS increase, as answer upon tRNA mutations, was described as regulatory mechanism to stimulate mtDNA expression and thereby compensate the deficits caused by the mutation (Moreno-Loshuertos et al., 2011). The enforced reliance on the respiratory chain activity in galactose medium in case of the 4300A>G mutation revealed adverse effects, which did not show in altered OxPhos activities. Possibly, the delayed growth in galactose was caused by increased ROS generation, resulting in enhanced apoptosis. ROS levels of mutant 4300A>G cells were not analyzed, but should be clarified. Though, the speculated mechanism, which may connect tRNA mutation 4300A>G and the resulting decreased tRNA amount with increased ROS production, is unknown. Herein, a hitherto unknown regulatory function of tRNA may play a role. tRNAs bear other functions than only transferring amino acids and can apparently also regulate apoptotic mechanisms by binding to cytochrome *c* (Mei et al., 2010b). Similarly, ROS are not only toxic byproducts, but play an important role in cellular signaling pathways (Hamanaka and Chandel, 2010). An impaired balance of ROS generation can have disastrous effects on cell metabolism, and this regulation may be the reason for tissue-specific effects of deregulation.

Perli et al. (2012) analyzed the 4300A>G cybrid cells in comparison to another $tRNA^{Ile}$ mutation, the homoplasmic 4277T>C mutation in the D-loop, which also caused cardiomyopathy and showed variable penetrance. They were able to detect upregulation of IleRS in fibroblasts and muscle cells of the patient's mother. She also was a mutation carrier, but did not show any symptoms of disease. Hence, they discussed the upregulated IleRS expression as a compensatory effect to rescue the phenotype. They were not able to reproduce this regulatory mechanism for the 4300A>G mutation, as no healthy mutation carrier was available for studies. Like in our study, aminoacylation of $tRNA^{Ile}$ was not changed, and overexpression of the enzyme IleRS, which is responsible for this reaction, may therefore hold other functions than aminoacylating the tRNA, but rather act as chaperone, i.e., stabilizing the probably altered three-dimensional structure of $tRNA^{Ile}$ (Perli et al., 2012). Studying IleRS levels and further consequences could be helpful to understand pathogenesis and may also be helpful in understanding why mutations can show variable penetrance.

Secondary structure prediction revealed a shorter anticodon stem with three base pairs instead of the five (*fig. 4.17*). This apparently relaxed structure may be the reason for the slower electrophoretic mobility of mutant tRNA in acidic polyacrylamide gels (*figure 4.13.d* and *4.14*), and can impact on tRNA function, although aminoacylation was normal in our studies. Mutant cells contained 80% mtDNA molecules compared to wild type cells (fig. 4.4). This represents only a slight reduction and apparently had no effect on cell respiration and viability.

The normal cell respiration did not surprise, since only heart cells of the patient, but not other cell types like muscle cells showed a respiratory deficiency, although all analyzed cell types harbored the mutation and showed decreased steady-state levels of mature $tRNA^{Ile}$. Obviously, the decreased level may have had pathogenic effects, e.g., decreased OxPhos activities, only in heart cells. A nuclear modifier gene, which is recessive autosomal, was recently discussed (Davidson et al., 2009). They compared cardiomyocyte cybrid cells containing either wild type cardiomyocyte nuclei or cardiomyocyte nuclei of a patient suffering from cardiomyopathy, combined with either wild type mtDNA or 4300A>G mtDNA of the patient. Only when the heart cells contained the nucleus of the patient and mutant 4300A>G mtDNA, they were complex I and IV deficient. When the mitochondrial mutation came along with a neutral heart cell nucleus, the cells did not show deficiencies. A nuclear modifier gene, which in case of carrying one or more polymorphisms is contributing to pathogenesis, could explain the variable penetrance in a family. It would also mean that homoplasmic mutations *per se* (without influence of nuclear modifier genes) are less severe than heteroplasmic mutations, which show their pathogenic character when reaching a specific threshold level. In contrast, carrying a homoplasmic mutation rather means to either develop a disease or not, possibly depending on the impact of tissue-specific modifier genes. This means that the 143B cybrid cell system is not the appropriate model to analyze the specific underlying pathogenic mechanisms of homoplasmic mutations, and another model should be used for this purpose. Nevertheless, this cell system is a practical and adequate model to analyze molecular and cellular differences caused by homoplasmic mutations, albeit the presenting phenotype of the cells are probably weaker than the phenotype of the affected tissues of the patient.

Nuclear encoded subunits of the respiratory chain can present as different isoforms. In mammals, heart cells and muscle cells express a certain heart-type isoform of cytochrome *c* oxidase subunit 7a (Huttemann et al., 2012). In a knock-out model, lack of this isoform caused cardiomyopathy, which was also the case in heterozygous mice. Hypothetically, mitochondrial tRNA mutations can have regulatory effects on nuclear encoded subunits of the respiratory chain. In case of an isoform-specific effect, this would lead to a tissue-specific disease pattern, like cardiomyopathy.

5.3.6 m.4263A>G

Mutation 4263A>G was additionally included in this study in cooperation with Min-Xin Guan (Wang et al., 2011). The homoplasmic mutation caused hypertension in a large Chinese family with variable penetrance. The mutation is located at the very first 5' position of mature $tRNA^{Ile}$ (*fig. 1.3*), and therefore, effects on 5' end processing seemed to be possible. Indeed, we found a decreased RNase P processing efficiency (*fig. 4.10*), which explained the reduced steady-state levels of $tRNA^{Ile}$ and subsequently a weaker mitochondrial translation compared to wild type cells (Wang et al., 2011). Consequently, respiration was diminished in mutated cells and ROS levels were increased.

5.4 Molecular Pathogenesis in Comparison

The overview of the diseases caused by different mitochondrial $tRNA^{Ile}$ mutations (*table 1.1*) shows that cardiomyopathy and ophthalmoplegia are the most frequently observed symptoms (Chinnery et al., 1997; Perli et al., 2012; Smits et al., 2007; Taniike et al., 1992; Taylor et al., 2003). Nevertheless, mutations in mitochondrial $tRNA^{Ile}$ have also caused other diseases, like encephalopathies (Cox et al., 2012; Limongelli et al., 2004; Santorelli et al., 1995), hypertension (Wang et al., 2011) or MERRF (Hahn et al., 2011).

Diseases caused by mutations at the same positions in other mitochondrial tRNAs do not correlate to the $tRNA^{Ile}$ phenotypes. For example, mutation at position 4281, which caused CPEO in our case, was also found as 3254C>G transition in the D-stem of $tRNA^{Leu(UUR)}$, but caused myopathy including cardiomyopathy (Kawarai et al., 1997) and additionally found as 10010T>C mutation in $tRNA^{Gly}$, where it caused encephalomyopathy. Mutation 4300A>G in the anticidon stem of $tRNA^{Ile}$, which caused cardiomyopathy, was found as 3273T>C transition in $tRNA^{Leu(UUR)}$ and caused ocular myopathy (Campos et al., 2001), to list some examples. This observation is consistent with the fact that even mutations at the same position in the same tRNA can cause different diseases, albeit in many examples they cause similar diseases, like cardiomyopathy in the families carrying mutation 4300A>G, encephalopathy in both patients carrying mutation 4296G>A or muscle disease in both patients harboring mutation 4281A>G in $tRNA^{Ile}$. In different tRNAs, mutations at corresponding positions lead to other pathogenic mechanisms and pathogenic outcomes. The consequence depends on the impact of the mutation on the tRNA structure. The 22 human mitochondrial tRNAs do not show canonical structures, and therefore, structural consequences can be very different for each. tRNA expressions can differ widely in different tissues, this is why a structural defect can show a tissue-specific effect (Dittmar et al., 2006). Moreover, individual tRNAs may bear different regulatory functions, and structural defects of individual tRNAs may have other impacts on the regulatory network of cells.

Our goal was to shed light on the molecular pathogenesis of different diseases caused by mutations in the same tRNA gene, the gene for $tRNA^{Ile}$. A clarified pattern of pathogenesis would help not only in understanding the mechanism of mitochondrial diseases, but on the long run also in setting up treatment strategies.

The results on the one hand provide basic knowledge of cellular and molecular pathologies, which are caused by the five mutations in the same cellular background. By use of the cybrid cell model, our attempt was to generate the same cell surrounding for the five mitochondrial mutations and to distinguish them only by the specific $tRNA^{Ile}$ mutation. Most of the biological replicas, i.e., clones harboring the same mutation, indeed showed identical or at least very similar results. But we had to realize that the model system does not guarantee uniformity, e.g., divergent results were detected for the two 4290T>C cybrid lines.

For the homoplasmic mutations 4290T>C and 4300A>G and the almost homoplasmic mutation 4296G>A, the 143B osteosarcoma cybrid cells do not seem to be the best model to reflect the disease causing molecular mechanisms, paying regard to the tissue-specificity of the disease. Presumably, the specific cell types of the affected tissue, but also specific modifier genes or polymorphisms are components involved in the specific clinical outcome (Davidson et al., 2009; Pierron et al., 2012).

Nevertheless, our studies showed a specific molecular pattern also for these homoplasmic mutations. This was in both cases a reduced mature $tRNA^{Ile}$ level, which in case of the 4290T>C mutation resulted in reduced respiratory chain activity and upregulation of the mtDNA content in the cells. The low $tRNA^{Ile}$ amount in mutant 4300A>G cells, probably caused by processing impairments, did not lead to an altered respiratory chain activity in the cybrid cells, but the cells grew worse in galactose medium. It may result from increased ROS production and consequently elevated apoptosis under this condition, which forced them to rely on respiratory chain activity. If this is the case, it would need further analysis to answer the questions which molecular changes exactly induce ROS production and why this pathology only presents in heart cells. An effect on tissue-specific isoforms of nuclear encoded respiratory chain subunits could be one possible underlying reason (Huttemann et al., 2012). Another study proved the tissue-specific organization of the mitochondrial translation system, which could be an obvious reason for tissue-specific outcomes (Antonicka et al., 2006).

In case of homoplasmic mutations, one can conclude that nuclear modifier genes may play a critical role for the development of pathogenic mechanisms, possibly explaining tissue specificity and/ or variable penetrance. Optionally, an influence of other polymorphisms in the nuclear or mitochondrial genome may contribute as well as a lack of rescue effects, e.g., overexpressed aaRS, or other factors. Tissue-specific molecular regulations of the affected tissues are probably part of the disease causing mechanism. In case of heteroplasmic mutations, reasons for the outbreak are rather the random segregation of the mutation during development and a threshold excess of mutated mtDNA molecules. In contrast to the hypothesis of random segregation, it was shown that the nuclear genome influenced mtDNA segregation in a tissue- and age-dependent manner in mice, which may be an

important factor in the pathogenesis of heteroplasmic dieseases (Battersby et al., 2003). Impacts of epigenetic factors or polymorphisms in the nuclear or mitochondrial genome were discussed (Pierron et al., 2012), which can segregate randomly, but also selectively in some tissues (Jenuth et al., 1997), and make the characterization of mitochondrial diseases more difficult. Actually, a selective segregation of mitochondrial mutations, depending on the patients' genotype, instead of a random segregation, could also be the reason why heteroplasmic mutations cause different diseases in many cases, meaning that the same mutation can affect different tissues in different patients. In the second step, tissue-specificity is probably caused by interactions of tissue-specific regulatory mechanisms with the molecular downstream effects of mitochondrial mutations.

Molecular effects of heteroplasmic mutations seem to be the more severe. Homoplasmic expression of these mutations showed a strong molecular phenotype in cybrid cells. Homoplasmic expression in the patients' tissues would probably cause lethality, because the organism would not be able to compensate all the deficiencies. On the contrary, homoplasmic mutations can express at 100% in different tissues in patients. The pathogenic effects of these mutations seem to be less severe, and the consequences are endured by patients even at a full expression of the mutation.

Consequently, the heteroplasmic mutations showed a more severe phenotype in the cybrid cell lines in our studies, as they are expressed homoplasmically. In case of mutation 4281A>G (heteroplasmic in the patient), homoplasmic mutant cells were very difficult to generate, they showed an anaerobic metabolism, and they grew very slow. In contrast, homoplasmic 4284G>A cells (heteroplasmic in the patient) grew quite well, but nevertheless showed a clear phenotype, including reduced mature $tRNA^{Ile}$ levels caused by instability of $tRNA^{Ile}$. Possibly, an improper processing was also involved, which was indicated by a strong precursor accumulation, although 5' processing was not altered. Additionally, the mature $tRNA^{Ile}$ was less aminoacylated, and the respiratory chain showed an isolated reduced activity of complex IV.

However, mutation 4296G>A, which was heteroplasmic in the patient, did not show a severe phenotype in cybrid cells. Due to the high mutation frequency in the patient and his tissue-specific disease, we rather assessed the mutation as a homoplasmic

one. The homoplasmic mutations 4290T>C and 4300A>G and the almost homoplasmic 4296G>A mutation caused symptoms in heart muscle and nerve tissues, which are highly ATP-dependent. 143B osteosarcoma cells were maintained in high glucose medium, what allows the the cells to rely on glycolysis for energy production. This difference in the cell metabolism may be another reason for the weak impact of the mutations on the cells' viability.

Altogether, the mutations caused not only five different clinical patterns, but also different molecular aberrations in the cybrid cells, although they were located in the same gene, surrounded by the same cellular environment, and the cells were maintained in the same condition. In the long term, the basic knowledge of these defined molecular differences could be taken in consideration for further development of present therapy approaches. In case of tRNA instability, one could consider a stabilizing procedure, e.g., treatment with chaperone-like molecules. In case of diminished tRNA aminoacylation, efficiency could be improved by induced upregulation of aaRS. In the best case, treatment strategies should specifically be adapted to the particular pathogenic mechanism to avoid side-effects and improve efficiency.

To fully understand the pathology of mitochondrial diseases, more knowledge of the regulatory mitochondrial network is necessary, especially about possible additional roles of mitochondrial tRNAs and also about the crosstalk between nucleus and mitochondria. Recent studies underlined this concern: e.g., tRNAs hold other functions than only amino acid transfer to the translation machinery; mitochondrial and cytosolic tRNAs can bind to cytochrome *c* and thereby regulate an apoptosis-inducing pathway (Mei et al., 2010b). tRNA mutations could potentially impact on this mechanism, which could thereby play a role in the pathology of mitochondrial diseases. Another example concerns the study of the pathomechanism of the homoplasmic 12S rRNA mutation 1555A>G (Raimundo et al., 2012). It revealed that a nuclear feedback mechanism reacts upon the downstream cascade of 12S rRNA hypermethylation, which is caused by the mitochondrial mutation. This hypermethylation induced increased ROS generation, which activated the nuclear factor E2F1 via the enzyme AMPK. This molecular mechanism enhanced apoptosis susceptibility tissue-specifically in the inner ear. The study shed light on the pathogenic mechanism of disease development, but it did not explain why other

tissues were not affected by this mechanism. Nevertheless, knowledge of this mechanism allows analyzing possible steps of the pathological cascade, which could be interrupted in homoplasmic mutated, but symptom-less tissue. It would be interesting to know if the same mechanism plays a role in pathogenesis of other homoplasmic mutations causing the same phenotype, like the known $tRNA^{Ser}$ 7472insC mutation (Toompuu et al., 1999). Furthermore, elucidation and comparison of pathogenic mechanisms of other homoplasmic diseases, like cardiomyopathy caused by mutation 4300A>G or neurological symptoms caused by mutation 4290T>C mutation in $tRNA^{Ile}$, would be interesting to gain understanding in homoplasmic disease development. Another study tried to debunk nuclear genes, which are involved in pathological mechanisms, by proteomics of cybrids containing the MERRF-causing 8344A>G mutation (Tryoen-Toth et al., 2003). They were able to show that a single mitochondrial tRNA point mutation impacted on steady-state levels of different nuclear encoded proteins, e.g., levels of nuclear encoded subunits of the respiratory chain were lower, whereas levels of pyruvate dehydrogenase subunits or a mitochondrial elongation factor were higher. This study nicely showed that mutations can affect not only mitochondrial translation, but many other proteins, which are players in other regulatory pathways. Thereby, altered protein expression can contribute to the phenotype of mitochondrial disease.

Our study serves as foundation in understanding the cells' pathology, and it could furthermore represent a first step in deciphering the molecular cascades, which are triggered by tRNA mutations. Anyhow, for this purpose, the study should in future work include the interaction of nucleus and mitochondria to understand the outcome of the disease and the tissue-specificity. According to the general definition of mitochondriopathies, the OxPhos system is affected by mutations in the mitochondrial or nuclear genome. It results in many cases in disturbances of the cells' energy supply, and most obvious, this is true for heteroplasmic mutations. Homoplasmic mitochondrial diseases also concern energetically active tissues by ATP shortage in the affected cell types, but the discussed studies imply that these mitochondrial mutations additionally have in impact on nuclear pathways (Davidson et al., 2009; Raimundo et al., 2012). A mutation-caused imbalance of the respiratory chain in energetically active tissues can reduce the available amount of ATP, but also stimulate other molecular mechanisms, like apoptosis, e.g., by increased ROS levels.

Maybe one should think the other way around than suggesting OxPhos impairments being the key mechanism of the pathogenesis. The results of our study hint to additional until now unknown regulatory functions of mitochondrial tRNAs and maybe of the respiratory chain.

The pathogenic mechanism of the heteroplasmic 4281A>G mutation was the most obvious: the altered structure of $tRNA^{Ile}$ caused a lack of aminoacylation, which drove mutant cells into an anaerobic metabolism. Consequently, symptoms developed in metabolically active muscle tissues, which depended on high ATP supply. It is not clear why the extraocular muscle is mostly affected, but this could be due to the specific physiology and properties of extraocular muscles (Yu Wai Man et al., 2005). The heteroplasmic 4284G>A mutation led to $tRNA^{Ile}$ instability, probably caused by an altered structure, which in the end affected respiratory chain complex IV activity. The reduced activity had an impact on various tissues, which possibly depended on random (or influenced) segregation of the mutation load. The homoplasmic 4290T>C mutation caused a reduced respiratory chain activity. Interactions of mitochondrial and nuclear pathways may have been responsible for the pathogenesis of tissue-specific neurological disease. Nuclear modifier genes may have caused the variable penetrance of the symptoms, so the nuclear genotype may has decided about the outbreak of disease by turning on or off a certain pathogenic mechanism. Compensatory increased mtDNA levels to overcome deficiencies in mitochondrially regulated pathways can also be a deciding factor in the question of penetrance (Moreno-Loshuertos et al., 2011). The increased mtDNA amount in 4290T>C cybrid cells could indicate such an effect. Moreover, elevated levels of other factors could be involved, like overexpression of aaRS. These enzymes can possibly have a chaperone-like effect on tRNAs, and thereby avoid an outbreak of disease (Perli et al., 2012). The heteroplasmic 4296G>A mutation also caused a reduced OxPhos activity, specifically reduced complex IV activity. The clinical pattern was tissue-specific, and due to the high mutation load we would rather assess the behavior of this mutation like a homoplasmic one. Influences of the mutation on nuclear pathways may have been involved in the outbreak of the neuronal disease in the patient. The patient did not show muscle weakness, despite a high mutation load. Therefore, the molecular mechanism must be nerve specific. The last mutation, 4300A>G, was homoplasmic and also caused a tissue-specific disease. The steady-

state levels of mutant $tRNA^{Ile}$ were decreased by processing impairments. The respiratory chain showed normal activity in mutant cybrid cells, but the cells grew slower in galactose medium. This possibly reflects increased ROS generation under respiratory stress conditions. The possibly elevated ROS may, like in case of the 1555A>G mutation in the 12S rRNA gene (Raimundo et al., 2012), trigger a pathogenic cascade including nuclear pathways.

Considering an impact of the nuclear genome by differential expression of certain genes or other epigenetic factors, and an impact of nuclear and mitochondrial polymorphisms to the disease phenotype, many unknown mechanisms in the development of mitochondriopathies are waiting to be studied. Additional knowledge of the regulatory networks of mitochondrial tRNAs, associated molecules in the tRNAs' functional cascade and the nuclear interaction is necessary to understand the pathogenesis of mitochondriopathies entirely. Understanding the molecular pathways of the pathogenic mechanisms exactly would allow the establishment of specific treatment strategies.

6. Materials & Methods

6.1 Cell Culture

The transmitochondrial 143B osteosarcoma TK^- cybrid cell lines contain the nuclear background of the human 143B osteosarcoma cell line and the mutated or wild type mitochondria of the patients. They were generated in our lab in case of the mutant cybrid cell lines 4281A>G and 4296G>A and their respective homoplasmic wild type cybrid cell lines 4281A and 4296G by a PEG based fusion of the human 143B206 *rho*^{0} cell line (King and Attardi, 1989) with the patient's platelets, followed by selection in a uridine- and pyruvate-free medium and clonal expansion (King, 1996). Homoplasmy was confirmed by PCR-RFLP and allele-specific qPCR. The 4284G>A mutant cells clones, the 4284G wild type cell clones and the 4290T>C cybrid cell clones were provided by Valeria Tiranti and Massimo Zeviani (Corona et al., 2002; Limongelli et al., 2004). The 4300A>G mutant cybrid cell clones were kindly provided by Merci M. Davidson (Davidson et al., 2009). The 143B osteosarcoma and the 143B206 *rho*^{0} cell lines served as controls. *Table 4.1* gives an overview of the clones, which were used for the experiments.

All cell lines were routinely cultured in standard DMEM medium containing 4.5 g/l glucose supplemented with 10% FCS Gold (PAA), 1 mM pyruvate and 50 µg/ ml uridine at 37 °C in an 8% CO_2 atmosphere. The wild type cell lines were maintained under the same conditions. Medium was changed every 24 – 72 hours. Medium, wash buffers and trypsine were always pre-warmed before use.

6.1.1 Passaging, Freezing and Unfreezing of Cells

For passaging, confluent cells were washed with PBS and wetted with 1x trypsine. After short incubation at 37 °C, cells were rinsed with medium and subcultured in the required dilution. For long term storage, subconfluent cells in a 75 cm^2 flask were harvested with trypsine, washed with 10 ml standard medium and stored as 1 ml aliquots in DMEM containing 4.5 g/l glucose supplemented with 20% FCS Gold, 1 mM pyruvate, 50 µg/ ml uridine and 5% DMSO in a liquid nitrogen container after slow freezing at -80 °C. A 500 µl aliquot of the cell suspension was routinely saved for mycoplasma test. The cells were pelleted and stored at -20 °C until application.

To unfreeze the cells, they were cultured in standard medium, and the medium was changed as soon as the cells were adherent.

6.1.2 Cell Counting

For counting, cells were harvested with trypsine as described, collected in 10 – 15 ml standard medium and resuspended. A small volume of 10 µl was loaded on a Neubauer hemocytometer and cells counted manually under a light microscope.

6.1.3 Growth Assays

Subconfluent cells from 25 cm^2 flasks were harvested, cell number was counted and 2x 10^5 cells were seeded in 24-well plates in standard medium. After four hours adherent cells were washed with glucose-free DMEM and cells were grown for the next 48 h in either glucose medium (DMEM containing 4.5 g/l glucose, 10% dialyzed FCS, 50 µg/ ml uridine, 1 mM pyruvate) or galactose medium (DMEM without glucose and glutamine, 10% dialyzed FCS, 50 µg/ ml uridine, 1 mM pyruvate, 2 mM glutamine, 0.9 g/l galactose). After 48 h cells were harvested with trypsine and resuspended in standard medium. Cell number was calculated in a 1:1 mixture of the cell suspension and 0.4% trypan blue by Countess Automated Cell Counter (Invitrogen). For analysis, cell number in galactose medium was calculated relative to the cell number in glucose medium for wild type and mutant cell lines (cell number in glucose = 100%).

6.2 Miscellaneous Cell Treatment

6.2.1 Mitotracker Staining

Cells were grown on cover slips in 6-well plates. The medium was changed the day before and the cells were subconfluent for the experiment. The cells were incubated in 2 ml standard medium supplemented with 500 nM Mitotracker Red 580 (Molecular Probes) at 37 °C for 30 min, washed with PBS and incubated in 300 µl 4% paraformaldehyde pH 7.4 at 37 °C for 10 min. Cells were washed three times in PBS for 5 min at room temperature, incubated in 1 ml PBS containing Hoechst 33342 (Sigma) 1:10000 for 5 min and washed again two times with H_2O. Cell were embedded in glycerol gelatin upside down on a glass slide and stored at 4 °C in the dark. Images were taken by fluorescence microscopy.

6.2.2 Electron Microscopy

Cells were seeded on coverslips in 24-well plates on the day before and grown to subconfluency. The cells were fixed in 200 µl GA solution (2.5% glutaraldehyde in 0.1% Caco buffer (cacodylic acid) pH 7.4) at 4 °C for 90 min and washed twice in 0.1 M Caco buffer at 4 °C for 15 min. Further steps were performed by our collaborator Adolf Ellinger (Medical University, Vienna), which are: dehydration by ethanol, embedding in Epon 812, cutting (80 -100 nm thich sections, UltraCut-UCT microtome (Leica)), staining with uranyl acetate and lead citrate and electron microscopy imaging at 80 kV (Tecnai 20 electron microscope, FEI).

6.3 Biochemistry: Respiratory Chain Activity

6.3.1 Polarography: Cell Respiration

The cell respiration of permeabilized cells was determined by using the OROBOROS Oxygraph-2k with an oxygen electrode. The two chambers of the device were always

washed thoroughly before and after use with alcohol and water. They were always calibrated with oxygen saturated medium before use according to the manufacturer's protocol. Wild type and mutant cells were measured in parallel in the two chambers at 37 °C. Sequential addition of substrates and inhibitors allowed stimulating or inhibiting complexes specifically. Monitoring the oxygen consumption allowed the calculation of respiration as pmol O_2/(s x ml) ("oxygen flux").

Subconfluent cells were harvested by trypsine and cells counted by use of a hematocytometer. 2x 10^6 cells in 2 ml Mitomed I were applied per chamber (Mitomed I, pH 7.1: 0.5 mM EGTA, 3 mM $MgCl_2$ (Merck), 20 mM taurine, 10 mM KH_2PO_4 (Merck), 20 mM HEPES (Sigma), 200 mM sucrose, 1g/l BSA (Sigma)). The cells were placed in the chambers, were continuously stirred at 37 °C and an aliquot was taken to count the exact cell number. The basal cell respiration was measured for 10 min. 50 µg digitonin (Fluka)/ 2x 10^6 cells was added to permeabilize the cells. In state I respiration, which represents a state of respiratory substrate starvation, the oxygen consumption decreases significantly. Complex I was stimulated by addition of 10 mM glutamate (Sigma) and 5 mM malate (Roche) and the state IV respiration monitored. Addition of 2 mM ADP (Sigma) converts state IV to state III respiration, which was monitored for 5 - 10 min. Complex II was additionally stimulated by addition of 10 mM succinate (Sigma), and ADP-stimulated, glutamate-, malate- and succinate-driven state III respiration was measured. The respiratory chain activity was interrupted at complex III by addition of 5 µM antimycin A (Sigma) and the respiration recorded. Complex IV was then stimulated by 200 µM TMPD (Aldrich) and 2 mM ascorbate (Sigma) was injected to minimize autooxidation of the substrate. The ADP-stimulated, ascorbate- and TMPD-driven state III respiration was recorded. The respiratory chain was uncoupled by 1.5 µM FCCP und the uncoupled oxygen consumption measured to evaluate the ATP synthase (complex V) function.

6.3.2 Spectrophotometry: Respiratory Chain Complex Activities

Activity measurements of the isolated respiratory chain complexes were done in isolated mitochondria by spectrophotometric assays.

6.3.2.1 Preparation of Mitochondria

Subconfluent cells were harvested from 2-4 75 cm^2 flasks with trypsine, cells were counted manually in a Neubauer hemocytometer and 1x 10^7 cell aliquots pelleted at 4 °C 500 g for 3 min. The pellets were resuspended in 1 ml chilled, hypotonic RSB buffer/ 1x 10^7 cells (RSB buffer: 10 mM Tris*Cl pH 7.6, 10 mM NaCl, 1.5 mM $CaCl_2$). After 15 min cell swelling on ice, cells were broken by aspirating them 20 times by a 1 ml syringe with a 0.4 mm needle. Cell breakage was controlled by phase contrast microscopy. The cell suspension was gently mixed with an equal volume of chilled, hypertonic MS buffer (420 mM mannitol, 140 mM sucrose, 10 mM Tris*Cl pH 7.6, 5 mM EDTA). Cell debris was pelleted two times at 4 °C 1000 g for 3 min and the supernatants transferred to fresh tubes. The mitochondria were finally pelleted at 4 °C 10000 g for 10 min, shock-frozen in liquid nitrogen and stored at -80 °C.

6.3.2.2 Analysis of Respiratory Chain Complex Activities

The frozen mitochondria pellets, derived from 1x 10^7 cells, were gently resuspended in 200 µl SETH buffer (250 mM saccharose, 10 mM Tris*Cl pH 7.4, 2 mM EDTA) and the mitochondria were broken by two freeze-thaw cycles. Samples were kept on ice during the procedure and gently resuspended before they were applied. Activity of each complex I – IV was measured separately and normalized to activity of citrate synthase activity of the same sample. We used a Hitachi U-3010 spectrophotometer.

Complex I: NADH:CoQ Oxidoreductase

Rotenone sensitive NADH oxidation was measured at 334 nm at 30 °C, with decylubiquinone as electron acceptor, complex III was inhibited by antimycin A and complex IV by KCN. Cell sample volume was 30 µl and total assay volume was 750 µl. $NADH_2$ solution was always prepared fresh.

Assay buffer containing 25 mM K-PO_4 buffer pH 7.4 (50 mM stock solution: 4 vol 50 mM K_2HPO_4 + 1 vol 50 mM KH_2PO_4), 2.8 mg/ml BSA (Sigma), 5 mM $MgCl_2$ (Merck), 0.2 mM $NADH_2$ (Roche), 2 mM KCN (Merck), 0.1 mM decylubiquinone (Sigma) and 0.004 mM antimycin A (Sigma) was incubated at 30 °C for 5 min. Background absorbance was measured during two min every 12 sec, 30 µl mitochondrial lysate was added and absorbance was measured during 6 min every 12 sec. The complex

was inhibited by 0.02 mM rotenone (Sigma) and rotenone-insensitive absorbance was measured for additional 4 min every 12 sec.

Complex I dependent Δabs/min = Δabs/min (after sample addition) - Δabs/min (before sample addition) - Δabs/min (after rotenone addition).

Complex I activity in units/l = (Δabs x total assay volume x 1000)/ (6.18 x sample volume).

Complex II: Succinate:Ubiquinone Oxidoreductase

Decylubioquinone mediated reduction of DCPIP was measured at 600 nm at 30 °C, complex I was inhibited by rotenone, complex III by antimycin A and complex IV by KCN. Cell sample volume was 10 µl and total assay volume was 750 µl. DCPIP solution was always prepared fresh.

The assay buffer containing 30 mM K-PO_4 buffer pH 7.4, 20 mM succinate (Sigma) and 3 mM KCN (Merck) was prewarmed at 30 °C for 5 min, 10 µl of the mitochondrial lysate was added and the mixture was incubated at 30 °C for 5 min. 0.004 mM antimycin A (Sigma), 0.02 mM rotenone (Sigma) and 0.13 mM DCPIP (Sigma) were added and the absorbance was measured during 2 min every 12 sec. 0.066 mM decylubiquinone (Sigma) was added and absorption was measured further 4 min every 12 sec. Complex II activity was inhibited by addition of 36 mM malonate and malonate-insensitive activity was measured every 12 sec for three min.

Complex II dependent Δabs/min = Δabs/min (after decylubiquinone addition) - Δabs/min (before decylubiquinone addition) - Δabs/min (after malonate addition).

Complex II activity in units/l = (Δabs x total assay volume x 1000)/ (19.1 x sample volume).

Complex III: Ubiquinol:Cytochrome *c* Oxidase

Antimycin A sensitive cytochrome *c* reduction was measured at 550 nm at 30 °C, with decylubiquinol as electron donor, complex I inhibition by rotenone and complex IV inhibition by KCN. Cell sample volume was 5 µl and total assay volume 750 µl.

The assay buffer containing 25 mM K-PO4 buffer pH 7.4, 2.8 mg/ml BSA (Sigma), 5 mM $MgCl_2$ (Merck), 0.01 mM rotenone (Sigma), 0.04 mM cytochrome *c* (III) (Sigma),

1 mM KCN (Merck) and 0.02 mM decylubiquinol (Sigma) was incubated at 30 °C for 5 min. After measuring absorption for 2 min every 10 sec at 550 nm, 5 µl sample was added and during the following 3 min absorption was measured every 10 sec. Complex III was inhibited by addition of 0.004 mM antimycin A (Sigma) and antimycin A-sensitive absorption was measured every 10 sec for 2 min.

Complex III dependent Δabs/min = Δabs/min (after sample addition) - Δabs/min (before sample addition) - Δabs/min (after antimycin A addition).

Complex III activity in units/l = (Δabs x total assay volume x 1000)/ (21.1 x sample volume).

Complex IV: Cytochrome *c* Oxidase

Oxidation of reduced cytochrome c (II) via complex IV was measured at 550 nm at 30 °C, while complex I was inhibited by rotenone. Cell sample volume was 10 µl and total assay volume 750 µl. K-hexacyanoferrat (III) was always prepared fresh.

85 mM HEPES-Na pH 7.2 (Sigma) and 90 mM reduced cytochrome *c* (II) (Sigma) were incubated at 30 °C for 5 min, 10 µl of the sample was added and absorption at 550 nm was measuring during eight minutes every 60 sec. For S-value determination, which indicated the cytochrome *c* (II) autooxidation, SETH buffer instead of sample was added. 0.0646 mM K-hexacyanoferrat (III) (Merck) was added and absorption measured finally over 3 min every 60 sec.

s-value = (abs [after SETH addition] – abs [after 8 min incubation])/ 21.1.

Complex IV activity in units/l = (Δabs/min x s-value x total assay volume x 1000)/ sample volume.

Citrate Synthase

Reduction of acetyl-Coenzyme A (CoA) and formation of a CoA-DTNB colorimetric complex was detected at 412 nm and 37 °C. Cell sample volume was 5 µl and total assay volume 750 µl.

A solution containing 0.1% Triton X-100 (AppliChem), 0.1 mM DTNB (Sigma) and 0.1235 mM acetyl-CoA (Sigma) was mixed with 5 µl sample and background

absorbance measured at 412 nm every 12 sec. After 2 min 0.5 mM oxaloatetic acid (Fluka) was added and absorbance measured for 2 min.

Citrate synthase dependent Δabs/min = Δabs/min (after oxaloacetic acid addition) - Δabs/min (background absorbance).

Citrate synthase activity in units/l = (Δabs x total assay volume x 1000)/ (13.6 x sample volume).

6.4 RNA and DNA Manipulations

6.4.1 Oligonucleotides

Table 6.1. *Northern Hybridization*

Name	**Specificity**	**Sequence 5'-3'**
mtIle_7r	$tRNA^{Ile}$	TGGTAGAAATAAGGGGGTTTAAG
mtLys_2r	$tRNA^{Lys}$	TGGTCACTGTAAAGAGGTGTT
mtArg_2r	$tRNA^{Arg}$	TGGTTGGTAAATATGATTATC
35SrRNA	5S rRNA	AAAGCCTACAGCACCCGGTATT

Table 6.2. *cDNA Synthesis*

Name	**Specificity**	**Sequence 5'-3'**
Primer mix 1		
mtPhe_1r	$tRNA^{Phe}$	TTATGGGGTGATGTGA
mtVal_1r	$tRNA^{Val}$	GGGCAAGTTAAGTTGAAAT
3mtLeu(UUR)1	$tRNA^{Leu(UUR)}$	CGTTAAGAAGAGGAATTGA
3mtIle3	$tRNA^{Ile}$	GAAATAAGGGGGTTTAAGC
3mtCys6	$tRNA^{Cys}$	CGGCAGGTTTGAAGC
3mtTyr8	$tRNA^{Tyr}$	CGTAACCCCTGTCTTTAGAT
mtHis_1r	$tRNA^{His}$	GGTAAATAAGGGGTCGTAA
mtSer(AGY)_1r	$tRNA^{Ser(AGY)}$	GAAAGCCATGTTGTTAGA
mtLeu(CUN)_2r	$tRNA^{Leu(CUN)}$	CGGCTTTTATTTGGAGTT

3mtGlu2	$tRNA^{Glu}$	CTATTCTCGCACGGAC
3GAPDH2	GAPDH	CCACCACCCTGTTGCTGTA
Primer mix 2		
12SrRNA_1r	12S rRNA	CCTCTAGACTAAGAGCTAATAGAA
16SrRNA_2r	16S rRNA	GGTAAGGTTGTCTGGTAG
3ND1_2	NADH dehydrogenase subunit 1	TCGTTCGGTAAGCATTAG
mtIle_5r	$tRNA^{Ile}$	GGTCTAGAGGTTCGATTCTCATA
mtSer(AGY)_1r	$tRNA^{Ser(AGY)}$	GAAAGCCATGTTGTTAGA
3ND6_2	NADH dehydrogenase subunit 6	CCCCCATAAATAGGAGAAG
3GAPDH2	GAPDH	CCACCACCCTGTTGCTGTA

Table 6.3. *PCR*

Name	**Amplicon ID**	**Sequence 5'-3'**
A1F1 A1R1	#1, A0101	GTAAAACGACGGCCAGAAATGTTTAGACGG CAGGAAACAGCTATGACGGTGTGTACGCGCT
A2F1 A3R2	#2, A0203	GTAAAACGACGGCCAGCTCACCACCTCTTG GCAGGTCAATTTCACTGGT
A4F2 A5R2	#3, A0405	TCTTACCCCGCCTGTT GGCTATCAAGAATAGGGCGAA
A6F2 A7R2	#4, A0607	GCAGAGACCAACCGAAC GAATGGGGTGGGTTTTGT
A8F2 A9R2	#5, A0809	GCTAACCGGCTTTTTGC GAAGCCTGGTAGGATAAGAATA
A10F2 A11R2	#6, A1011	CTCTTCGTCTGATCCGTCCT TTCAATCGGGAGTACTACTCG
A12F2 A13R1	#7, A1213	CCTACGAGTACACCGACTACG GTGGCCTTGGTATGTGCTTT
A14F1 A15R1	#8, A1415	CCTCTCAGCCCTCCTAATG ATTATGTGTTTTTTGGAAAGTC
A16F1 A17R1	#9, A1617	ACACCCACTCCCTCTTAG CGGGGTTGAGGGATAGGA
A18F1	#10, A1819	AGTCACAGCCCTATACTCCCT

A19R1		GGTATGGTTTTGAGTAGTCCT
A20F1 A21R1	#11, A2021	AAGCCATACTATTTATGTGCTC CGGCGCGATTGATGAAAAGG
A22F3 A23R1	#12, A2223	CAAAACTAACCCCCTAATAAAA CCCGGAGCGAGGAGAGT
A24F1 A24R1	#13, A2424	CACCCACTAGGATACCAACA AGGCTTAAGCGTTTTGAGCTG
A2F1 A2R1	A0202	GTAAAACGACGGCCAGCTCACCACCTCTTG CAGGAAACAGCTATGACTGGACAACCAGCTA
A3F2 A3R2	A0303	GCTGCATAATGAATTAACTAGA GCAGGTCAATTTCACTGGT
A5F2 A5R2	A0505	CTGTCACAAAGCGCCTTC GGCTATCAAGAATAGGGCGAA
A5F2 A6R2	A0506	CTGTCACAAAGCGCCTTC GCTATTAGAAGGATTATGGAT
A6F2 A6R2	A0606	GCAGAGACCAACCGAAC GCTATTAGAAGGATTATGGAT
A8F2 A8R2	A0808	GCTAACCGGCTTTTTGC CCTAGAAGGTTGCCTGGCT
A11F2 A12R2	A1112	CAGCGGCGTAAATCTAAC GATCAGGTTCGTCCTTTAGTGTT
A12F2 A12R2	A1212	CCTACGAGTACACCGACTACG GATCAGGTTCGTCCTTTAGTGTT
A18F1 A18R1	A1818	AGTCACAGCCCTATACTCCCT CTCTCAGCCGATGAACA
A23F1 A23R1	A2323	CTTGCCCTATTACTATCCATC CCCGGAGCGAGGAGAGT

Table 6.4. *RT-PCR*

Name	**Specificity**	**Sequence 5'-3'**
mtIle_5f mtIle_5r	$tRNA^{Ile}$ +5'+3'	GCGAATTCAATCTCCAGCA GGTCTAGAGGTTCGATTCTCATA
mtIle_5f 3mtIle3	$tRNA^{Ile}$ +5'	GCGAATTCAATCTCCAGCA GAAATAAGGGGGTTTAAGC
mtIle_6f mtIle_5r	$tRNA^{Ile}$ +3'	GCGGAGAAATATGTCTGATA GGTCTAGAGGTTCGATTCTCATA

ND4_1f mtSer(AGY)_1r	$tRNA^{His}$ +5'+3'	CCCATTCTCCTCCTATC GAAAGCCATGTTGTTAGA
ND4_1f mtHis_1r	$tRNA^{His}$ +5'	CCCATTCTCCTCCTATC GGTAAATAAGGGGTCGTAA
Cytb_1r 3ND6_2	$tRNA^{Glu}$ +5'+3'	GGGTTAGTTTTGCGTATTG CCCCCATAAATAGGAGAAG
5mtGlu3 3ND6_2	$tRNA^{Glu}$ +3'	TGTAGTCCGTGCGAGAATA CCCCCATAAATAGGAGAAG
12SrRNA-1f mtVal_1r	$tRNA^{Val}$ +5'	ACGAGCTCTAAGTGTACTGGAAA GGGCAAGTTAAGTTGAAAT
mtVal_1f 16SrRNA_2r	$tRNA^{Val}$ +3'	CAGAGTGTAGCTTAACACAAA GGTAAGGTTGTCTGGTAG
5hGAPDH2 3GAPDH2	GAPDH	CCCACTCCTCCACCTTTGAC CCACCACCCTGTTGCTGTA
5mtDNA(ND1)1 3mtDNA(ND1)1	ND1	CCCTAAAACCCGCCACATCT GAGCGATGGTGAGAGCTAAGGT
5_18SrRNA1 3_18SrRNA1	18S rRNA	CATTCGAACGTCTGCCCTATC CGTCACCCGTGGTCACCAT
TMp_mtDNA(ND1)1 (TaqMan probe)	ND1	CCATCACCCTCTACATCACCGCCC 5'FAM 3'BHQ
TMp_18SrRNA1 (TaqMan probe)	18S rRNA	ACTTTCGATGGTAGTCGCCGTGCC 5'JOE 3'BHQ
Primer mix Mycoplasma Test		
Mycopl_1f	*M. spec.* 23S rRNA	TCTGAATTTGCCGGGACCACC
Mycopl_2f	*M. pirum* 23S rRNA	GGAAAATGTTATTTTGACGGAACCT
Mycopl_3f	*M. laidlawii* 23S rRNA	GGAATCCCGTTTGAAGATAGGA
Mycopl_1r	*M. spec*. 23S rRNA	CTTTCCMTCACKGTACTRGTTCACT

Table 6.5. *Sequencing*

Amplicon ID	**Sequencing primer**	**Sequence 5'-3'**
#1, A0101	M13for	GTAAAACGACGGCCAG

#2, A0203		
#2, A0203	A2R1	CAGGAAACAGCTATGACTGGACAACCAGCTA
	A3F2	GCTGCATAATGAATTAACTAGA
	A3R2	GCAGGTCAATTTCACTGGT
#3, A0405	A4F2	TCTTACCCCGCCTGTT
	A4R2	GGGTATGTTGTTAAGAAGAGG
	A5F2	CTGTCACAAAGCGCCTTC
	A5R2	GGCTATCAAGAATAGGGCGAA
#4, A0607	A6F2	GCAGAGACCAACCGAAC
	A6R2	GCTATTAGAAGGATTATGGAT
	A7F2	CTAATTAATCCCCTGGCCC
	A7R2	GAATGGGGTGGGTTTTGT
#5, A0809	A8F2	GCTAACCGGCTTTTTGC
	A8R2	CCTAGAAGGTTGCCTGGCT
	A9F2	ACCTCGGAGCTGGTAAAAAG
#6, A1011	A10F2	CTCTTCGTCTGATCCGTCCT
	A11F2	CAGCGGCGTAAATCTAAC
	A11R2	TTCAATCGGGAGTACTACTCG
#7, A1213	A12F2	CCTACGAGTACACCGACTACG
	A12R2	GATCAGGTTCGTCCTTTAGTGTT
	A13F2	TCCCCCTCTATTGATCCC
#8, A1415	A14F1	CCTCTCAGCCCTCCTAATG
	A15F1	GTATGTCTCCATCTATTGATGA
#9, A1617	A16F1	ACACCCACTCCCTCTTAG
	A16R1	AAGTACTATTGACCCAGCGA
	A17F1	TCACTCTCACTGCCCAAG
	A17R1	CGGGGTTGAGGGATAGGA
#10, A1819	A18F1	AGTCACAGCCCTATACTCCCT
	A18R1	CTCTCAGCCGATGAACA
	A19F1	CCCAAACAACCCAGCTCT
	A19R1	GGTATGGTTTTGAGTAGTCCT
#11, A2021	A20F1	AAGCCATACTATTTATGTGCTC
	A21F1	CTCAACCCAAAAAGGCATA
#12, A2223	A22F3	CAAAACTAACCCCCTAATAAAA

	A22R1	GGTAGCTTACTGGTTGTCCTC
	A23F1	CTTGCCCTATTACTATCCATC
#13, A2424	A24F1	CACCCACTAGGATACCAACA
	A24R1	AGGCTTAAGCGTTTTGAGCTG
A0202	A2F1	GTAAAACGACGGCCAGCTCACCACCTCTTG
A0303	A3F2	GCTGCATAATGAATTAACTAGA
A0505	A5R2	GGCTATCAAGAATAGGGCGAA
A0506	A6F2	GCAGAGACCAACCGAAC
A0606	A6F2	GCAGAGACCAACCGAAC
	A6R2	GCTATTAGAAGGATTATGGAT
A0808	A8F2	GCTAACCGGCTTTTTGC
A1112	A12F2	CCTACGAGTACACCGACTACG
	A12R2	GATCAGGTTCGTCCTTTAGTGTT
A1212	A12F2	CCTACGAGTACACCGACTACG
A1818	A18F1	AGTCACAGCCCTATACTCCCT
A2323	A23R1	CCCGGAGCGAGGAGAGT

Table 6.6. *tRNA Precursors (antisense)*

Name	**Specificity**	**mtDNA Position**
pHI2	$tRNA^{Ile}$ +5'+3'	4235 – 4350
pHI3	$tRNA^{Ile}$ +3'	4263 – 4350
pHE2	$tRNA^{Glu}$ +5'+3'	14639 – 14836

Table 6.7. *tRNA Precursors (sense)*

Name	**Specificity**	**mtDNA Position**
pHI2 WT	$tRNA^{Ile}$ +5'+3'	4235 – 4350
pHI2/ 4263A>G	$tRNA^{Ile}$ +5'+3'	4235 – 4350
pHI2/ 4281A>G	$tRNA^{Ile}$ +5'+3'	4235 – 4350
pHI2/ 4284G>A	$tRNA^{Ile}$ +5'+3'	4235 – 4350
pHI2/ 4290T>C	$tRNA^{Ile}$ +5'+3'	4235 – 4350
pHI2/ 4296G>A	$tRNA^{Ile}$ +5'+3'	4235 – 4350
pHI2/ 4300A>G	$tRNA^{Ile}$ +5'+3'	4235 – 4350

6.4.2 RNA Extraction and Northern Hybridization (tRNA Steady-State Levels and Aminoacylation)

Total RNA was isolated from semiconfluent cells using the RNAtidy G reagent (Applichem A2867), according to the protocol of the manufacturer. RNA was dissolved in 1x TE pH 7.5 routinely. For aminoacylation analysis RNA was dissolved in 0.1 M NaOAc pH 4.5. tRNAs were deacylated by addition of 2 volumes 1 M Tris*Cl pH 9.0 and incubation at 37 °C for 2 h. RNAs were separated in 8% polyacrylamide 7 M urea TBE gels. Aminoacylation was analyzed in acid 8% polyacrylamide 8 M urea 0.1 M NaOAc pH 4.5 gels at 4 °C overnight (Enriquez and Attardi, 1996; Kohrer and Rajbhandary, 2008). Gels were equilibrated for 10 min in 0.5x TBE buffer before blotting. They were electroblotted to Hybond-N Nylon membranes (GE Healthcare) by the semi-dry method at 300 mA for 45 min in 0.5x TBE buffer (Trans-Blot SD Semy-Dry Electrophoretic Transfer Cell, BioRad). RNAs were cross-linked to the wet membrane at 120 mJ (Vilber Lourmat UV Crosslinker), and steady-state levels of the mature tRNA and *in vivo* aminoacylation were analyzed by Northern hybridization with radiolabeled probes.

For probe labeling 2 µM oligonucleotide complementary to the 3' end of $tRNA^{Ile}$, $tRNA^{Lys}$, $tRNA^{Arg}$ or to 5S rRNA was incubated with 25 µCi [γ-^{32}P]-ATP (3000 Ci/mmol, Perkin Elmer) and 10 units T4 polynucleotide kinase (Fermentas) in the provided kinase buffer at 37 °C for 1 h. Oligonucleotides were purified by illustra Microspin G25 columns (GE healthcare) according to the application guideline.

Pre-hybridization was carried out at 42 °C in pre-hybridization buffer (6x SSC, 10x Denhardt's solution, 0.5% SDS and 100 µg/ml salmon sperm DNA) for 60 min. Hybridization was performed overnight at 42 °C in hybridization buffer (6x SSC, 0.1% SDS and ^{32}P 5'-labeled probe). At room temperature, membranes were washed twice for 10 min in 6x SSC, 0.1% SDS, 10 min in 4x SSC, 0.1% SDS and 10 min in 2x SSC, 0.1% SDS. Radioactive signals of the wet blots in sealed bags were detected by storage phosphor autoradiography and analyzed by ImageQuant TL 7 (GE Healthcare). Membranes were stripped by incubating them three times at 80 °C in 1% SDS, 0.1x SSC, 40 mM Tris*Cl pH 7.6, rinsed with 2x SSC and reprobed.

6.4.3 DNA Extraction
(mtDNA Content, Mycoplasma Test, mtDNA Sequencing)

For analysis of mtDNA content, DNA was extracted from subconfluent cells (5-10 cm^2 vessel), which were harvested by trypsine and cell pellets stored at -20 °C. The frozen pellet was resuspended in 500 µl extraction buffer (200 mM NaCl, 20 mM Tris*Cl pH 8, 5 mM EDTA, 0.5% SDS) and proteins digested by 50 µg proteinase K at 55 °C shaking for 60 min. RNA molecules were eliminated by incubation with 50 µg RNase A at 37 °C for 10 min. The crude DNA preparation was purified by PCI extraction: 500 µl phenol/ chloroform/ isoamylalcohol was added to the preparation, phases separated by full speed centrifugation for 2 min and the upper phase transferred to a fresh tube. DNA was precipitated in presence of 500 µl isopropanol and 2 µl linear polyacrylamide as carrier at -80 °C for at least 30 min. DNA was pelleted, washed with 70% EtOH and finally resuspended in 20 µl 0.5x TE pH 8. DNA purity and concentration was determined by NanoDrop spectrophotometer (Thermo Scientific), RNA diluted to 10 ng/ µl and stored at -20 °C for real-time PCR analysis.

For mycoplasma test, an aliquot of the cell suspension, prepared for long time storage in liquid nitrogen, was centrifuged at 300 g for 5 min to pellet the cells. The pellets were treated with 100 µg/ml proteinase K in an appropriate amount (50 – 100 µl) of lysis buffer (50 mM Tris*Cl pH 8, 1 mM EDTA, 0.5% Tween-20). Lysis was performed at 55 °C and rigorous shaking for two hours was followed by 10 min incubation at 95 °C to inactivate the enzyme. The preparation was diluted 1:10 to 1:20 with 0.5 x TE and 5 µl of the supernatant was directly used for real-time PCR analysis. The same crude DNA preparation, diluted 1:20 in 0.5x TE pH 8, was applied for the purpose of sequencing the mitochondrial genome.

6.4.4 cDNA Synthesis
(tRNA Precursor Steady-State Levels)

Total RNA was extracted from cells as described. For DNase treatment in 5 µl assays, 1 µl of 0.5 µg/ µl RNA was incubated with 0.07 U/ µl DNase I (Fermentas, 1 U/ µl, RNase-free) and 1 U/ µl RiboLock RNase inhibitor (40 U/ µl, Fermentas) in 1x

DNase buffer (Fermentas) at 37 °C for 30 min. DNase was deactivated in presence of 2 mM EDTA at 90 °C for 5 min. 1 µl of 5 µM gene specific primer set 1 or 2 was annealed at 70 °C for 5 min. For analysis of steady-state levels of tRNA precursors with 5'-extensions, primer set 1 was used, and for the analysis of tRNA precursors with 3'-extensions or 5'- and 3'-extensions, primer set 2 was used. Reverse transcription was performed by 10 U/ µl RevertAid M-MuLV reverse transcriptase (200 U/ µl, Fermentas) in presence of 0.5 mM dAGCT mix (Fermentas) and 0.5 U/ µl RiboLock RNase inhibitor (40 U/ µl, Fermentas) in 1x RevertAid M-MuLV reaction buffer (Fermentas) at 42 °C for 90 min. cDNA was diluted 100-fold with 0.5x TE and reverse transcriptase was inactivated at 70 °C for 10 min. Preparations were stored at -20 °C for real-time PCR analysis.

6.4.5 Quantitative Real-Time PCR (tRNA Precursor Steady-State Levels)

The relative amount of $tRNA^{Ile}$ precursors with 5' extension, 3' extension or 5' and 3' extensions in mutant cell lines compared to wild type cells was quantified by dye-based real-time PCR and normalized to $tRNA^{His}$, $tRNA^{Val}$, $tRNA^{Glu}$ precursors or GAPDH. PCR was performed in 25 µl assays containing 5 µl cDNA preparation, 1x Real SYBR PCR mix and 0.2 µM primer mix (see *table 6.4*). We used the Stratagene Mx 3005P cycler.

5x Real SYBR PCR mix

5x PCR buffer with KCl (Fermentas)
25 mM $MgCl_2$
1 mM dATP, dGTP, dCTP
2 mM dUTP
0.15 µM ROX reference dye (Stratagene)
1.25x SYBR green (Roche)
0.0625 U/ µl *Taq* DNA polymerase (Fermentas)

Thermal Cycling

95 °C	60 sec	
95 °C 54 °C 72 °C	15 sec 30 sec 30 sec	40 cycles
95 °C 55 °C 95 °C	60 sec 30 sec 30 sec	Dissociation curve

Ct values and relative quantification were calculated by the software MxPro version 4.01 and qBase version 1.3.5.

6.4.6 Probe-Based Quantitative Real-Time PCR (mtDNA Content)

The relative amount of mtDNA in mutant cells compared to wild-type cells was analyzed by probe-based real-time PCR, using TaqMan probes specifically for ND1 and 18S rRNA. The ND1 gene copies, representing the mtDNA content, was normalized to 18 S rRNA, representing the nuclear genome content.

PCR was performed in 25 µl assays containing 5 µl DNA (10 ng/ µl), 1x Real PCR mix, 0.125 µM TaqMan probe and 0.3 µM primer mix (see *table 6.4*). We used the Stratagene Mx 3005P cycler.

5x Real PCR mix

5x PCR buffer with KCl (Fermentas)

12.5 mM $MgCl_2$

1 mM dATP, dCTP, dGTP

2 mM dUTP

0.15 µM ROX reference dye (Stratagene)

0.0625 U/ µl *Taq* DNA polymerase (Fermentas)

Thermal Cycling

95 °C	120 sec	
95 °C 60 °C	15 sec 45 sec	40 cycles

Ct values and relative quantification were calculated by the software MxPro version 4.01.

6.4.7 Quantitative Real-time PCR (Mycoplasma Test)

We routinely screened out mycoplasma contaminations of the cell lines when they were harvested for long time storage in liquid nitrogen. A SYBR based real-time PCR with mycoplasma specific primers was applied (Ishikawa et al., 2006), in which a positive control, containing mycoplasma DNA, and a negative control, devoid of mycoplasma DNA, was included.

PCR was performed in 25 µl assays containing 5 µl crude DNA preparation, 1x Real SYBR PCR mix and 0.2 µM primer mix (see *table 6.4*). We used the Stratagene Mx 3005P cycler.

5x Real SYBR PCR mix

5x PCR buffer with KCl (Fermentas)

25 mM $MgCl_2$

1 mM dATP, dGTP, dCTP

2 mM dUTP

0.15 µM ROX reference dye (Stratagene)

1.25x SYBR green (Roche)

0.0625 U/ µl *Taq* DNA polymerase (Fermentas)

Thermal Cycling

95 °C	60 sec	
95 °C 65 °C	15 sec 45 sec	40 cycles
95 °C 55 °C 95 °C	60 sec 30 sec 30 sec	Dissociation curve

Ct values and relative quantification were calculated by the software MxPro version 4.01.

6.4.8 PCR (mtDNA Sequencing)

For the purpose of sequencing the mitochondrial genome, 13 overlapping mtDNA sequences (#1 - #13, *table 6.3*), covering the whole genome, were amplified from a crude DNA preparation. MtDNA regions, which were not clearly readable, were analyzed by 10 alternative amplicons (*table 6.3*).

PCR was performed in 25 µl assays containing 1 µl crude DNA preparation, 1.5 mM $MgCl_2$, 0.2 mM dAGCT mix, 0.0125 U/ µl Phusion DNA polymerase or hot start Phusion polymerase (2 U/ µl, Finnzymes) and 0.2 µM primer mix (*see table 6.3*) in 1x Phusion HF buffer (Finnzymes). We used the Mastercycler ep (Eppendorf).

Thermal Cycling

95 °C	120 sec	
95 °C 58 °C 72 °C	15 sec 30 sec 40 sec	35 cycles
72 °C	180 sec	

PCR products were controlled in 1% agarose gels with 1x Takara loading buffer, the size marker GeneRuler 100 bp Plus DNA ladder (Fermentas). Nucleic acids were stained with Midori Green. PCR products were purified with the GeneJET PCR Purification Kit (Fermentas), eluted in 50 µl elution buffer and DNA concentration determined by NanoDrop spectrophotometer.

For sequencing, amplicons and sequencing primers (*table 6.5*) were sent to 4base lab GmbH (Reutlingen, Germany). Sequences were aligned to the Revised Cambridge Reference Sequence (Andrews et al., 1999) and SNPs verified by comparison to the mtSNP database (http://mtsnp.tmig.or.jp/mtsnp/search_mtSNP_e.html) and the Mitomap SNP database (http://mitomap.org/MITOMAP).

6.4.9 RNase Protection Assay (tRNA Steady-State Levels)

RNase protection assay was applied to verify Northern Blot and quantitative real-time analysis of mature tRNA and tRNA precursor steady-state levels. Three different antisense probes were used for RNase protection assay: two sequences complementary to $tRNA^{Ile}$ precursor (pHI2, pHI3, *table 6.6*) and one probe complementary to $tRNA^{Glu}$ precursor (pHE2, *table 6.6*). For antisense probe synthesis, pGEM-1 plasmid (Promega), containing the tRNA precursor sequences, were cloned in *E.coli* DH5 cells and selected by ampicilin resistence. Plasmids were prepared by the Plasmid Plus Kit Mini (Qiagen) according to the manufacturer's protocol and DNA concentration determined by NanoDrop Spectrophotometer. 10 µg plasmid was linearized by 10 µl FastDigest restriction enzyme (pHI2 and pHE2: *Eco*RI; pHI3: *Pvu*II, Fermentas) according to the manufacturer's protocol, PCI (phenol/ chloroform/ isoamylalcohol) extracted, precipitated by 1 volume isopropanol in the presence of 100 mM NH_4OAc and 2 µl linear polyacrylamide as carrier. DNA was dissolved in water and the concentration determined by NanoDrop spectrophotometer. Digestion was controlled by running an aliquot of undigested and digested plasmid in a 1% agarose gel. Nucleic acids were stained with Midori Green. Antisense probes for RNA protection assay was *in vitro* transcribed and radiolabeled from SP6 promoter of these templates as follows:

In vitro Transcription of Antisense Probe

0.5 µl digested plasmid (phI2 x *Eco*RI, phI3 x *Pvu*II or phE2 x *Eco*RI)

0.25 µl H_2O

1 µl 5x transcription buffer (Promega)

0.5 µl 5 mM AGC mix

0.25 µl RiboLock RNase inhibitor (40 U/ µl, Fermentas)

0.5 µl SP6 RNA polymerase (20 U/ µl, Promega)

2 µl [α-^{32}P]-UTP (800 Ci/ mmol, Perkin Elmer)

The *in vitro* transcription was incubated at 39 °C for 90 min and stopped by addition of 50 µl guanidium mix (4 M guanidium thiocyanate, 1 M NH_4OAc, 10 mM EDTA). The nucleic acids were precipitated overnight by 2.5 volumes 100% ethanol in presence of 2 µl LPA as carrier, washed with 70% ethanol and the DNA pellet dissolved in F2 loading buffer (85% formamide, 5% glycerol, 220 mM sucrose, 10 mM EDTA, 0.02% bromphenolblue, 0.02% xylene cyanol).

The probes were purified by denaturing polyacrylamide gel electrophoresis (7 M urea, 8% polyacrylamide/ bisacrylamide [19:1]), the radioactive bands cut and eluted in 200-300 µl elution buffer (0.5 M NH_4OAc, 1 mM EDTA, 0.1% SDS) for 3 h at 45 °C 600 rpm or overnight. 1 µl was transferred to 3 ml scintillation liquid and counts/ µl measured by scintillation counter.

Total RNA of the 22 cell lines was extracted by RNAtidy G according to the standard protocol and diluted to 0.5 µg/ µl 1x TE pH 7.5. 2 µl of the RNA sample (or water in case of the 2 control assays) was mixed with 8 µl DNase digestion mix and incubated at 37 °C for 15 min.

Master mix DNase Digestion (26x)

163.8 µl H_2O

20.8 µl 10x DNase buffer (+ $MgCl_2$, Fermentas)

13 µl *Saccharomyces cerevisiae* tRNA (10 µg/ µl)

5.2 µl RiboLock RNase inhibitor (40 U/ µl, Fermentas)

5.2 µl DNase I RNase-free (1 U/ µl, Fermentas)

DNA digestion was stopped by addition of a Gua-probe mix, which contained 50 µl guanidium mix (4 M guanidium thiocyanate, 1 M NH_4OAc, 10 mM EDTA), 2 µl LPA

and an aliquot of the probe (10000 counts). Nucleic acids were precipitated by addition of 2.5 volumes 100% ethanol, washed with 70% ethanol and pellets dissolved in 10 µl hybridization buffer (80% formamide, 40 mM PIPES pH 6.4, 1 mM EDTA, 400 mM NaCl). The denatured samples (5 min at 90 °C) were hybridized overnight at 45 °C.

For RNase digestion, 100 µl (control 2: 110 µl) RNase digestion buffer (600 mM NaCl, 10 mM Tris*Cl pH 7.4, 5 mM EDTA) was added. 10 µl RNase mix was applied to the samples except for control 2 (final volume 120 µl) and single-stranded RNA was digested at 30 °C for 90 min.

RNase Master mix

300 µl RNase digestion buffer

1 µl RNase A (10 mg/ ml, Sigma)

2 µl T1 RNase (366 U/ ml)

RNases were degraded by 6 µl 10% SDS and 4 µl proteinase K (10 mg/ ml, Roche) at 37 °C for 30 min. RNA was isolated by 100 µl PCI, precipitated by 300 µl 100% ethanol, washed with 70% ethanol and the air-dried pellets finally dissolved in 8 µl F2 loading buffer.

Denatured RNAs (5 min at 90 °C) were separated in an 8% polyacrylamide 7 M urea gel. Gels were transferred to Whatman paper, covered by plastic wrap and dried at 80 °C for 45 min in a vacuum dryer. Radioactive signals were detected by storage phosphor autoradiography and analyzed by ImageQuant TL 7 (GE Healthcare).

6.5 tRNA Maturation and Function

6.5.1 5' Processing

6.5.1.1 Precursor tRNA^{Ile} Substrates

For (mt)tRNA^{Ile} wild type and mutant precursors, nucleotides 4235 – 4350 of the human mitochondrial genome were cloned into the *Eco*RI/*Xba*I sites of pGEM-1

(Promega). After *Sal*I digestion for linearization of the plasmid, labeled RNA substrates were transcribed from the T7 promoter with T7 RNA polymerase (Fermentas), 500 µM ATP, CTP, UTP, 100 µM GTP, 10 µCi [α^{32}P]-GTP (800 Ci/ mmol) and 10 units RiboLock RNase inhibitor (Fermentas) in 1x *in vitro* transcription buffer (Fermentas). Wild type and mutant transcripts of 141 nucleotides in length (*table 6.7*) were purified by denaturing polyacrylamide gel electrophoresis as described for RNase protection assay probes and dissolved in 1 mM EDTA.

6.5.1.2 Mitochondrial RNase P

Mitochondrial RNase P was reconstituted from purified recombinant proteins MRPP1, MRPP2 and MRPP3 essentially as previously described (Holzmann et al., 2008).

6.5.1.3 Enzyme Assays

Processing assays were carried out in parallel for wild type and mutant substrates in 12 µl reaction mixtures containing 30 mM Tris*Cl pH 7.8, 30 mM NaCl, 4.5 mM $MgCl_2$, 200 µg/ml BSA, 30000 cpm of RNA substrate (approximately 30 nM final concentration) and 25 nM mtRNase P. Enzyme reactions were incubated at 21°C. After 4, 8, 12 or 16 min aliquots were withdrawn and stopped by addition to an equal volume of F2 loading buffer. Reaction products were resolved by denaturing polyacrylamide gel electrophoresis as described and detected by phosphor storage autoradiography. Image quant TL (GE Healthcare) was used for relative quantification of reaction products.

6.5.2 tRNA Stability and Resynthesis

For tRNA stability measurements, cells were seeded in 6-wells the day before and grown in standard medium. Fresh medium containing 250 ng/ µl ethidium bromide was applied at time-point zero to block mitochondrial transcription. Cells were harvested with 300 µl RNAtidy G (Applichem) at time-point zero and at different time-point between 3 and 24 h. For tRNA resynthesis measurements, cells were seeded in 6 cm plates at time-point zero and treated with 250 ng/ µl ethidium bromide. After 48 h cells were split in 6-wells in standard medium without ethidium bromide and cultured for additional 6 days. Cells were harvested at time-point zero, after 48 h

ethidium bromide treatment and then every 24 or 48 h after ethidium bromide release and stored at -20 °C.

Isolation of total RNA was performed in parallel for all samples according to the standard procedure and finally dissolved in 1x TE pH 7.5. Concentration was determined by NanoDrop spectrophotometer and adjusted to 500 ng/ µl. tRNA levels in 2.5 ng total RNA were analyzed by Northern hybridization as described in *chapter 6.4.2*. The tRNA amount at different time-points was normalized to 5S rRNA and relatively quantified to time-point zero.

6.5.3 Aminoacylation Assay ("in Organello")

In vivo aminoacylation was analyzed by Northern hybridization under acidic conditions as described in *RNA extraction and Northern hybridization*.

For *in organello* aminoacylation, subconfluent cells from eight 10 cm dishes were harvested with trypsine, resuspended in medium, counted manually in a Neubauer hemocytometer, washed twice in chilled PBS and resuspended in 1 ml cold RSB buffer/ 1x 10^7 cells (RSB buffer: 10 mM Tris*Cl pH 7.6, 10 mM NaCl, 1.5 mM $CaCl_2$). After 15 min cell swelling on ice, the cells were broken by aspirating them 20 times by a 1 ml syringe with a 0.4 mm needle. Cell breakage was controlled by phase contrast microscope. The cell suspension was gently mixed with an equal volume of chilled, hypertonic MS buffer (420 mM mannitol, 140 mM sucrose, 10 mM Tris*Cl pH 7.6, 5 mM EDTA). Cell debris was pelleted two times at 4 °C 1000 g for 3 min and the supernatants, containing the mitochondria, transferred to fresh tubes. To maximize the yield of mitochondria, collected cell debris was resuspended in 1:1 RSB/ MS buffer, centrifuged at 4 °C 1000 g for 3 min and supernatant transferred to the crude mitochondria solution. The mitochondria were finally pelleted at 4 °C 10000 g for 10 min and resuspended in 1 ml homogenization buffer (320 mM sucrose, 1 mM EDTA, 10 mM Tris*Cl pH 7.4). An aliquot was used for determination of protein concentration by Bradford assay. The mitochondria were pelleted at 15000 g 4 °C for 10 min and kept on ice.

Mitochondria were resuspended in 0.5 ml aminoacylation buffer/ 1 mg protein (10 mM Tris*Cl pH 7.4, 25 mM sucrose, 75 mM sorbitol, 100 mM KCl, 10 mM K_2HPO_4,

0.05 mM EDTA, 5 mM MgCl2, 1 mg/ml BSA, 10 mM glutamate, 2.5 mM malate, 10 µM amino acids (except isoleucine), 1 mM ADP, 10 µM L-[^{14}C]-isoleucine (0.05 mCi/ml, 0.307 Ci/mmol, Perkin Elmer)) and incubated by rotation at 37 °C for 15 min. Mitochondria were pelleted at 15000 g 4 °C for 3 min, resuspended in 500 µl RNAtidy G and total mitochondrial RNA isolated under acidic conditions as described above. RNA was finally dissolved in 0.1 M NaOAc, 1 mM EDTA pH 4.5, at which the amount of required buffer was estimated by formerly determined total protein content (20 µl buffer/ 1 mg protein). 10 µg total RNA was electrophoresed at 4 °C under acidic conditions through a 8% polyacrylamide 8 M urea 0.1 M NaOAc pH 4.5 gel overnight. Gels were electroblotted to Hybond-N Nylon membranes (GE Healthcare) with the semi-dry method at 300 mA for 60 min in 0.1 M NaOAc pH 4.5 buffer. RNAs were cross-linked to the membrane at 120 mJ, membranes air-dried at 60 °C and exposed for autoradiography as described above in *RNA extraction and Northern hybridization*.

6.6 Mitochondrial Proteins

6.6.1 Metabolic Labeling of Mitochondrial Proteins

Cells were seeded in 6-wells and were subconfluent during the procedure. They were incubated twice for 10 min in methionine- and cysteine-free DMEM high glucose (HyClone) supplemented with 2 mM glutamine, 50 µg/ ml uridine, 1 mM pyruvate and 10 µM non-essential amino acids (Sigma Aldrich) without FCS. For further 10 min, the cells were incubated in 0.7 ml of the same medium but supplemented with 10% dialyzed FCS and 100 µg/ ml emetine hydrochloride to inhibit cytosolic translation. 200 µl of the medium was discarded and 10 µl labeled amino acids (73% [^{35}S]-Met, 22% [^{35}S]-Cys, 11 mCi/ ml, 1175 Ci/ mmol, 9.404 µM, Perkin-Elmer) applied per well. During 30 min incubation at 37 °C, the plates were gently moved every 5 min to cover the whole surface with medium. Cell were washed with cold standard medium, washed with PBS, harvested with trypsine, rinsed with cold PBS and transferred to protein low binding tubes (Eppendorf). Cells were pelleted at 300 g 4 °C for 4 min,

washed three times with cold PBS, finally resuspended in 30 µl cold PBS with protease inhibitor (Sigma Aldrich), frozen in liquid nitrogen and stored at -80 °C.

Protein concentration of the cell suspension was determined photometrically by Bradford assay (BioRad) and cells lysed in 1 volume 2x dissociation buffer (20% glycerol, 1.5% SDS, 250 mM Tris*Cl pH 6.8, 0.01% bromphenolblue, 100 mM DTT) and 0.5 µl Benzonase nuclease (25 U/ µl, Novagen) for 1 h. Without previous boiling, protein (50 µg) was separated in 15% SDS polyacrylamide gels at 25 mA for 5-6 h to avoid heating. Spectra multicolor low range (Fermentas) was used as marker. The gel was incubated in fixing solution (3% glycerol, 10% acetic acid, 30% methanol) overnight, dried at 70 °C for 5 h in vacuum and signals identified by storage phosphor autoradiography using a low energy screen. To control the protein load, the gel was rehydrated in fixing solution for 1 h, washed with water, total protein stained with 0.1% Coomassie Brilliant Blue R-250 solution (50% ,ethanol, 10% acetic acid) for 45 min, destained overnight (12% ethanol, 7% acetic acid) and scanned by an image scanner.

6.6.2 Western Blotting

Table 6.8. *Primary Antibodies*

Specificity	**Host type**	**applied Dilution**	**Supplier**
NDUFB8; complex I β subcomplex SU 8	Rabbit	1:2000 75 pg/µl	Sigma
Complex II 70 kDa SU	Mouse	1:5000 0.1 ng/ µl	Molecular Probes
Complex III core I SU	Mouse	1:5000 0.1 ng/ µl	Molecular Probes
Complex IV SU I	Mouse	1:500 1 ng/ µl	Molecular Probes
Complex IV SU II	Mouse	1:500 1 ng/ µl	Molecular Probes
Complex IV SU IV	Mouse	1:100 2.5 ng/ µl	Molecular Probes
Complex IV SU V	Mouse	1:500 1 ng/ µl	Molecular Probes
Complex V SU a	Mouse	1:1000 0.5 ng/ µl	Molecular Probes
Porin 31HL, voltage-dependent anion channel 1 (VDAC)	Mouse	1:5000 0.2 ng/ µl	Calbiochem
GAPDH	Mouse	1:2000 0.5 ng/ µl	Ambion

Table 6.9. *Secondary Antibodies*

Specificity	**applied dilution**	**Supplier**
HRP-conjugated anti-mouse	1:20000 in 0.3% Tween/ PBS	DAKO P0260
HRP-conjugated anti-rabbit	1:20000 in 0.3% Tween/ PBS	DAKO P0448

Subconfluent cells from 10 cm plates were harvested with trypsine, washed with PBS and split in two pellets. Cell pellets were lysed in 50 µl hunt buffer (20 mM Tris*Cl pH 8, 100 mM NaCl, 1 mM EDTA, 0.5% Nonidet P40) and 0.3 µl protease inhibitor for 30 min on ice. Cell debris was pelleted at full speed 4 °C for 10 min and protein solution transferred to fresh tubes. Protein concentration was determined photometrically by Bradford assay (BioRad). 50 µg cell lysates were resolved in 10% or 15% polyacrylamid 6 M urea SDS gels without previous boiling of the samples. PageRuler plus prestained protein ladder (Fermentas) served as size marker. The proteins were transferred to a Hybond-P PVDF membrane (Amersham GE Healthcare) by the semi-dry method (Trans-Blot SD Semi-Dry Transfer Cell, BioRad) at 12 V for 45 min in Tris-glycine blotting buffer (48 mM Tris, 39 mM glycine, 0.01% SDS, 10% methanol). Membranes were washed with 0.3% PBST and non-specific sites were blocked overnight in blocking solution (2% nonfat milk, 0.3% Tween, 1x PBS). The membrane was exposed to the primary antibody in blocking solution for 90 min, washed three times with 0.3% Tween/ PBS for 10 min, exposed to the HRP (horseradish peroxidase)-labeled secondary antibody in 0.3% Tween/ PBS for 120 min and washed again three times in 0.3% Tween/ PBS for 10 min. The membrane was exposed to ECL detection solution (Amersham GE Healthcare) for 5 min and signals detected by the VDS-CL imaging system. The membranes were washed in 0.3% Tween/ PBS and, without stripping, re-used for detection with different primary antibodies against several proteins of different sizes.

7. Literature

Allen, J.F. (2003). Why chloroplasts and mitochondria contain genomes. Comparative and functional genomics *4*, 31-36.

Anderson, S., Bankier, A.T., Barrell, B.G., de Bruijn, M.H., Coulson, A.R., Drouin, J., Eperon, I.C., Nierlich, D.P., Roe, B.A., Sanger, F.*, et al.* (1981). Sequence and organization of the human mitochondrial genome. Nature *290*, 457-465.

Andrews, R.M., Kubacka, I., Chinnery, P.F., Lightowlers, R.N., Turnbull, D.M., and Howell, N. (1999). Reanalysis and revision of the Cambridge reference sequence for human mitochondrial DNA. Nature genetics *23*, 147.

Antonicka, H., Sasarman, F., Kennaway, N.G., and Shoubridge, E.A. (2006). The molecular basis for tissue specificity of the oxidative phosphorylation deficiencies in patients with mutations in the mitochondrial translation factor EFG1. Human molecular genetics *15*, 1835-1846.

Barat, C., Lullien, V., Schatz, O., Keith, G., Nugeyre, M.T., Gruninger-Leitch, F., Barre-Sinoussi, F., LeGrice, S.F., and Darlix, J.L. (1989). HIV-1 reverse transcriptase specifically interacts with the anticodon domain of its cognate primer tRNA. The EMBO journal *8*, 3279-3285.

Battersby, B.J., Loredo-Osti, J.C., and Shoubridge, E.A. (2003). Nuclear genetic control of mitochondrial DNA segregation. Nature genetics *33*, 183-186.

Berardo, A., Coku, J., Kurt, B., DiMauro, S., and Hirano, M. (2010). A novel mutation in the tRNAIle gene (MTTI) affecting the variable loop in a patient with chronic progressive external ophthalmoplegia (CPEO). Neuromuscular disorders : NMD *20*, 204-206.

Bogenhagen, D., and Clayton, D.A. (1977). Mouse L cell mitochondrial DNA molecules are selected randomly for replication throughout the cell cycle. Cell *11*, 719-727.

Borthwick, G.M., Taylor, R.W., Walls, T.J., Tonska, K., Taylor, G.A., Shaw, P.J., Ince, P.G., and Turnbull, D.M. (2006). Motor neuron disease in a patient with a mitochondrial tRNAIle mutation. Annals of neurology *59*, 570-574.

Brandon, M.C., Lott, M.T., Nguyen, K.C., Spolim, S., Navathe, S.B., Baldi, P., and Wallace, D.C. (2005). MITOMAP: a human mitochondrial genome database--2004 update. Nucleic acids research *33*, D611-613.

Brandt, U. (2006). Energy converting NADH:quinone oxidoreductase (complex I). Annual review of biochemistry *75*, 69-92.

Brzezniak, L.K., Bijata, M., Szczesny, R.J., and Stepien, P.P. (2011). Involvement of human ELAC2 gene product in 3' end processing of mitochondrial tRNAs. RNA biology *8*, 616-626.

Calvo, S., Jain, M., Xie, X., Sheth, S.A., Chang, B., Goldberger, O.A., Spinazzola, A., Zeviani, M., Carr, S.A., and Mootha, V.K. (2006). Systematic identification of human mitochondrial disease genes through integrative genomics. Nature genetics *38*, 576-582.

Campos, Y., Gamez, J., Garcia, A., Andreu, A.L., Rubio, J.C., Martin, M.A., del Hoyo, P., Navarro, C., Cervera, C., Garesse, R.*, et al.* (2001). A new mtDNA mutation in the tRNA(Leu(UUR)) gene associated with ocular myopathy. Neuromuscular disorders : NMD *11*, 477-480.

Campos, Y., Garcia, A., Lopez, A., Jimenez, S., Rubio, J.C., Del Hoyo, P., Bustos, F., Martin, M.A., Cabello, A., Ricoy, J.R.*, et al.* (2002). Cosegregation of the mitochondrial DNA A1555G and G4309A mutations results in deafness and mitochondrial myopathy. Muscle & nerve *25*, 185-188.

Cann, R.L., Stoneking, M., and Wilson, A.C. (1987). Mitochondrial DNA and human evolution. Nature *325*, 31-36.
Casali, C., d'Amati, G., Bernucci, P., DeBiase, L., Autore, C., Santorelli, F.M., Coviello, D., and Gallo, P. (1999). Maternally inherited cardiomyopathy: clinical and molecular characterization of a large kindred harboring the A4300G point mutation in mitochondrial deoxyribonucleic acid. Journal of the American College of Cardiology *33*, 1584-1589.
Casali, C., Santorelli, F.M., G, D.A., Bernucci, P., DeBiase, L., and DiMauro, S. (1995). A novel mtDNA point mutation in maternally inherited cardiomyopathy. Biochemical and biophysical research communications *213*, 588-593.
Chamkha, I., Mkaouar-Rebai, E., Aloulou, H., Chabchoub, I., Kifagi, C., Fendri-Kriaa, N., Kammoun, T., Hachicha, M., and Fakhfakh, F. (2011). A novel m.3395A>G missense mutation in the mitochondrial ND1 gene associated with the new tRNA(Ile) m.4316A>G mutation in a patient with hypertrophic cardiomyopathy and profound hearing loss. Biochemical and biophysical research communications *404*, 504-510.
Chandra, D., and Singh, K.K. (2011). Genetic insights into OXPHOS defect and its role in cancer. Biochimica et biophysica acta *1807*, 620-625.
Chinnery, P.F., Johnson, M.A., Taylor, R.W., Durward, W.F., and Turnbull, D.M. (1997). A novel mitochondrial tRNA isoleucine gene mutation causing chronic progressive external ophthalmoplegia. Neurology *49*, 1166-1168.
Chinnery, P.F., and Turnbull, D.M. (2001). Epidemiology and treatment of mitochondrial disorders. American journal of medical genetics *106*, 94-101.
Christian, B.E., and Spremulli, L.L. (2011). Mechanism of protein biosynthesis in mammalian mitochondria. Biochimica et biophysica acta.
Clason, T., Ruiz, T., Schagger, H., Peng, G., Zickermann, V., Brandt, U., Michel, H., and Radermacher, M. (2010). The structure of eukaryotic and prokaryotic complex I. Journal of structural biology *169*, 81-88.
Clayton, D.A. (1982). Replication of animal mitochondrial DNA. Cell *28*, 693-705.
Cock, H.R., Tabrizi, S.J., Cooper, J.M., and Schapira, A.H. (1998). The influence of nuclear background on the biochemical expression of 3460 Leber's hereditary optic neuropathy. Annals of neurology *44*, 187-193.
Corona, P., Lamantea, E., Greco, M., Carrara, F., Agostino, A., Guidetti, D., Dotti, M.T., Mariotti, C., and Zeviani, M. (2002). Novel heteroplasmic mtDNA mutation in a family with heterogeneous clinical presentations. Annals of neurology *51*, 118-122.
Cox, R., Platt, J., Chen, L.C., Tang, S., Wong, L.J., and Enns, G.M. (2012). Leigh syndrome caused by a novel m.4296G>A mutation in mitochondrial tRNA isoleucine. Mitochondrion *12*, 258-261.
Crimi, M., Del Bo, R., Galbiati, S., Sciacco, M., Bordoni, A., Bresolin, N., and Comi, G.P. (2003). Mitochondrial A12308G polymorphism affects clinical features in patients with single mtDNA macrodeletion. European journal of human genetics : EJHG *11*, 896-898.
Crimi, M., Galbiati, S., Sciacco, M., Bordoni, A., Natali, M.G., Raimondi, M., Bresolin, N., and Comi, G.P. (2004). Mitochondrial-DNA nucleotides G4298A and T10010C as pathogenic mutations: the confirmation in two new cases. Mitochondrion *3*, 279-283.
Davidson, M.M., Walker, W.F., Hernandez-Rosa, E., and Nesti, C. (2009). Evidence for nuclear modifier gene in mitochondrial cardiomyopathy. Journal of Molecular & Cellular Cardiology *46*, 936-942.
Degoul, F., Brule, H., Cepanec, C., Helm, M., Marsac, C., Leroux, J., Giege, R., and Florentz, C. (1998). Isoleucylation properties of native human mitochondrial tRNAIle and tRNAIle transcripts. Implications for cardiomyopathy-related point mutations (4269, 4317) in the tRNAIle gene. Human molecular genetics *7*, 347-354.
DeLuca, S.Z., and O'Farrell, P.H. (2012). Barriers to male transmission of mitochondrial DNA in sperm development. Developmental cell *22*, 660-668.

Devasagayam, T.P., Tilak, J.C., Boloor, K.K., Sane, K.S., Ghaskadbi, S.S., and Lele, R.D. (2004). Free radicals and antioxidants in human health: current status and future prospects. The Journal of the Association of Physicians of India *52*, 794-804.

Diaz, F., Kotarsky, H., Fellman, V., and Moraes, C.T. (2011). Mitochondrial disorders caused by mutations in respiratory chain assembly factors. Seminars in fetal & neonatal medicine *16*, 197-204.

Dimauro, S., and Davidzon, G. (2005). Mitochondrial DNA and disease. Annals of medicine *37*, 222-232.

DiMauro, S., and Schon, E.A. (2003). Mitochondrial respiratory-chain diseases. The New England journal of medicine *348*, 2656-2668.

Dittmar, K.A., Goodenbour, J.M., and Pan, T. (2006). Tissue-specific differences in human transfer RNA expression. PLoS genetics *2*, e221.

Druzhyna, N.M., Wilson, G.L., and LeDoux, S.P. (2008). Mitochondrial DNA repair in aging and disease. Mechanisms of ageing and development *129*, 383-390.

Duvezin-Caubet, S., Jagasia, R., Wagener, J., Hofmann, S., Trifunovic, A., Hansson, A., Chomyn, A., Bauer, M.F., Attardi, G., Larsson, N.G*., et al.* (2006). Proteolytic processing of OPA1 links mitochondrial dysfunction to alterations in mitochondrial morphology. The Journal of biological chemistry *281*, 37972-37979.

Edgar, D., and Trifunovic, A. (2009). The mtDNA mutator mouse: Dissecting mitochondrial involvement in aging. Aging *1*, 1028-1032.

Ekstrand, M.I., Falkenberg, M., Rantanen, A., Park, C.B., Gaspari, M., Hultenby, K., Rustin, P., Gustafsson, C.M., and Larsson, N.G. (2004). Mitochondrial transcription factor A regulates mtDNA copy number in mammals. Human molecular genetics *13*, 935-944.

El Meziane, A., Lehtinen, S.K., Hance, N., Nijtmans, L.G., Dunbar, D., Holt, I.J., and Jacobs, H.T. (1998). A tRNA suppressor mutation in human mitochondria. Nature genetics *18*, 350-353.

Elliott, H.R., Samuels, D.C., Eden, J.A., Relton, C.L., and Chinnery, P.F. (2008). Pathogenic mitochondrial DNA mutations are common in the general population. American journal of human genetics *83*, 254-260.

Elston, T., Wang, H., and Oster, G. (1998). Energy transduction in ATP synthase. Nature *391*, 510-513.

Emmanuele, V., Sotiriou, E., Shirazi, M., Tanji, K., Haller, R.G., Heinicke, K., Bosch, P.E., Hirano, M., and DiMauro, S. (2011). Recurrent myoglobinuria in a sporadic patient with a novel mitochondrial DNA tRNA(Ile) mutation. Journal of the neurological sciences *303*, 39-42.

Engel, W.K. (1963). Adenosine Triphosphatase of Sarcoplasmic Reticulum Triads and Sarcolemma Identified Histochemically. Nature *200*, 588-589.

Enriquez, J.A., and Attardi, G. (1996). Analysis of aminoacylation of human mitochondrial tRNAs. Methods in enzymology *264*, 183-196.

Enriquez, J.A., Chomyn, A., and Attardi, G. (1995). MtDNA mutation in MERRF syndrome causes defective aminoacylation of tRNA(Lys) and premature translation termination. Nature genetics *10*, 47-55.

Esteves, A.R., Lu, J., Rodova, M., Onyango, I., Lezi, E., Dubinsky, R., Lyons, K.E., Pahwa, R., Burns, J.M., Cardoso, S.M*., et al.* (2010). Mitochondrial respiration and respiration-associated proteins in cell lines created through Parkinson's subject mitochondrial transfer. Journal of neurochemistry *113*, 674-682.

Falkenberg, M., and Larsson, N.G. (2009). Structure casts light on mtDNA replication. Cell *139*, 231-233.

Fan, W., Waymire, K.G., Narula, N., Li, P., Rocher, C., Coskun, P.E., Vannan, M.A., Narula, J., Macgregor, G.R., and Wallace, D.C. (2008). A mouse model of mitochondrial disease reveals germline selection against severe mtDNA mutations. Science *319*, 958-962.

Fernandez-Silva, P., Enriquez, J.A., and Montoya, J. (2003). Replication and transcription of mammalian mitochondrial DNA. Experimental physiology *88*, 41-56.

Fernandez-Vizarra, E., Tiranti, V., and Zeviani, M. (2009). Assembly of the oxidative phosphorylation system in humans: what we have learned by studying its defects. Biochimica et biophysica acta *1793*, 200-211.

Finnila, S., Hassinen, I.E., and Majamaa, K. (2001). Phylogenetic analysis of mitochondrial DNA in patients with an occipital stroke. Evaluation of mutations by using sequence data on the entire coding region. Mutation research *458*, 31-39.
Florentz, C., Sohm, B., Tryoen-Toth, P., Putz, J., and Sissler, M. (2003). Human mitochondrial tRNAs in health and disease. Cellular and molecular life sciences : CMLS *60*, 1356-1375.
Fontanesi, F., Soto, I.C., Horn, D., and Barrientos, A. (2006). Assembly of mitochondrial cytochrome c-oxidase, a complicated and highly regulated cellular process. American journal of physiology Cell physiology *291*, C1129-1147.
Franceschina, L., Salani, S., Bordoni, A., Sciacco, M., Napoli, L., Comi, G.P., Prelle, A., Fortunato, F., Hadjigeorgiou, G.M., Farina, E*., et al.* (1998). A novel mitochondrial tRNA(Ile) point mutation in chronic progressive external ophthalmoplegia. Journal of neurology *245*, 755-758.
Gaspari, M., Larsson, N.G., and Gustafsson, C.M. (2004). The transcription machinery in mammalian mitochondria. Biochimica et biophysica acta *1659*, 148-152.
Giles, R.E., Blanc, H., Cann, H.M., and Wallace, D.C. (1980). Maternal inheritance of human mitochondrial DNA. Proceedings of the National Academy of Sciences of the United States of America *77*, 6715-6719.
Glatz, C., D'Aco, K., Smith, S., and Sondheimer, N. (2011). Mutation in the mitochondrial tRNA(Val) causes mitochondrial encephalopathy, lactic acidosis and stroke-like episodes. Mitochondrion *11*, 615-619.
Gnaiger, E., Lassnig, B., Kuznetsov, A., Rieger, G., and Margreiter, R. (1998). Mitochondrial oxygen affinity, respiratory flux control and excess capacity of cytochrome c oxidase. The Journal of experimental biology *201*, 1129-1139.
Gobert, A., Gutmann, B., Taschner, A., Gossringer, M., Holzmann, J., Hartmann, R.K., Rossmanith, W., and Giege, P. (2010). A single Arabidopsis organellar protein has RNase P activity. Nature structural & molecular biology *17*, 740-744.
Grasso, M., Diegoli, M., Brega, A., Campana, C., Tavazzi, L., and Arbustini, E. (2001). The mitochondrial DNA mutation T12297C affects a highly conserved nucleotide of tRNA(Leu(CUN)) and is associated with dilated cardiomyopathy. European journal of human genetics : EJHG *9*, 311-315.
Gray, M.W., Burger, G., and Lang, B.F. (1999). Mitochondrial evolution. Science *283*, 1476-1481.
Gutierrez Cortes, N., Pertuiset, C., Dumon, E., Borlin, M., Hebert-Chatelain, E., Pierron, D., Feldmann, D., Jonard, L., Marlin, S., Letellier, T*., et al.* (2012). Novel mitochondrial DNA mutations responsible for maternally inherited nonsyndromic hearing loss. Human mutation *33*, 681-689.
Hahn, A., Schanzer, A., Neubauer, B.A., Gizewski, E., Ahting, U., and Rolinski, B. (2011). MERRF-like phenotype associated with a rare mitochondrial trnaile mutation (m.4284 G>A). Neuropediatrics *42*, 148-151.
Hamanaka, R.B., and Chandel, N.S. (2010). Mitochondrial reactive oxygen species regulate cellular signaling and dictate biological outcomes. Trends in biochemical sciences *35*, 505-513.
Hao, H., and Moraes, C.T. (1997). A disease-associated G5703A mutation in human mitochondrial DNA causes a conformational change and a marked decrease in steady-state levels of mitochondrial tRNA(Asn). Molecular and cellular biology *17*, 6831-6837.
He, J., Mao, C.C., Reyes, A., Sembongi, H., Di Re, M., Granycome, C., Clippingdale, A.B., Fearnley, I.M., Harbour, M., Robinson, A.J*., et al.* (2007). The AAA+ protein ATAD3 has displacement loop binding properties and is involved in mitochondrial nucleoid organization. The Journal of cell biology *176*, 141-146.
Helm, M. (2006). Post-transcriptional nucleotide modification and alternative folding of RNA. Nucleic acids research *34*, 721-733.
Helm, M., Brule, H., Friede, D., Giege, R., Putz, D., and Florentz, C. (2000). Search for characteristic structural features of mammalian mitochondrial tRNAs. RNA *6*, 1356-1379.
Hino, N., Suzuki, T., Yasukawa, T., Seio, K., Watanabe, K., and Ueda, T. (2004). The pathogenic A4269G mutation in human mitochondrial tRNA(Ile) alters the T-stem structure and decreases the binding affinity for elongation factor Tu. Genes to cells : devoted to molecular & cellular mechanisms *9*, 243-252.

Holt, I.J., Harding, A.E., and Morgan-Hughes, J.A. (1988). Deletions of muscle mitochondrial DNA in patients with mitochondrial myopathies. Nature *331*, 717-719.
Holt, I.J., Lorimer, H.E., and Jacobs, H.T. (2000). Coupled leading- and lagging-strand synthesis of mammalian mitochondrial DNA. Cell *100*, 515-524.
Holzmann, J., Frank, P., Loffler, E., Bennett, K.L., Gerner, C., and Rossmanith, W. (2008). RNase P without RNA: identification and functional reconstitution of the human mitochondrial tRNA processing enzyme. Cell *135*, 462-474.
Hudson, G., and Chinnery, P.F. (2006). Mitochondrial DNA polymerase-gamma and human disease. Human molecular genetics *15 Spec No 2*, R244-252.
Huttemann, M., Klewer, S., Lee, I., Pecinova, A., Pecina, P., Liu, J., Lee, M., Doan, J.W., Larson, D., Slack, E*., et al.* (2012). Mice deleted for heart-type cytochrome c oxidase subunit 7a1 develop dilated cardiomyopathy. Mitochondrion *12*, 294-304.
Ienco, E.C., Simoncini, C., Orsucci, D., Petrucci, L., Filosto, M., Mancuso, M., and Siciliano, G. (2011). May "mitochondrial eve" and mitochondrial haplogroups play a role in neurodegeneration and Alzheimer's disease? International journal of Alzheimer's disease *2011*, 709061.
Ishikawa, Y., Kozakai, T., Morita, H., Saida, K., Oka, S., and Masuo, Y. (2006). Rapid detection of mycoplasma contamination in cell cultures using SYBR Green-based real-time polymerase chain reaction. In vitro cellular & developmental biology Animal *42*, 63-69.
Iwata, S., Lee, J.W., Okada, K., Lee, J.K., Iwata, M., Rasmussen, B., Link, T.A., Ramaswamy, S., and Jap, B.K. (1998). Complete structure of the 11-subunit bovine mitochondrial cytochrome bc1 complex. Science *281*, 64-71.
Janssen, G.M., Maassen, J.A., and van Den Ouweland, J.M. (1999). The diabetes-associated 3243 mutation in the mitochondrial tRNA(Leu(UUR)) gene causes severe mitochondrial dysfunction without a strong decrease in protein synthesis rate. The Journal of biological chemistry *274*, 29744-29748.
Jenuth, J.P., Peterson, A.C., Fu, K., and Shoubridge, E.A. (1996). Random genetic drift in the female germline explains the rapid segregation of mammalian mitochondrial DNA. Nature genetics *14*, 146-151.
Jenuth, J.P., Peterson, A.C., and Shoubridge, E.A. (1997). Tissue-specific selection for different mtDNA genotypes in heteroplasmic mice. Nature genetics *16*, 93-95.
Jones, C.N., Jones, C.I., Graham, W.D., Agris, P.F., and Spremulli, L.L. (2008). A disease-causing point mutation in human mitochondrial tRNAMet rsults in tRNA misfolding leading to defects in translational initiation and elongation. The Journal of biological chemistry *283*, 34445-34456.
Kaipparettu, B.A., Ma, Y., and Wong, L.J. (2010). Functional effects of cancer mitochondria on energy metabolism and tumorigenesis: utility of transmitochondrial cybrids. Annals of the New York Academy of Sciences *1201*, 137-146.
Kasahara, A., Ishikawa, K., Yamaoka, M., Ito, M., Watanabe, N., Akimoto, M., Sato, A., Nakada, K., Endo, H., Suda, Y*., et al.* (2006). Generation of trans-mitochondrial mice carrying homoplasmic mtDNAs with a missense mutation in a structural gene using ES cells. Human molecular genetics *15*, 871-881.
Kawarai, T., Kawakami, H., Kozuka, K., Izumi, Y., Matsuyama, Z., Watanabe, C., Kohriyama, T., and Nakamura, S. (1997). A new mitochondrial DNA mutation associated with mitochondrial myopathy: tRNA(Leu)(UUR) 3254C-to-G. Neurology *49*, 598-600.
Kelley, S.O., Steinberg, S.V., and Schimmel, P. (2000). Functional defects of pathogenic human mitochondrial tRNAs related to structural fragility. Nature structural biology *7*, 862-865.
Khrapko, K., Kraytsberg, Y., de Grey, A.D., Vijg, J., and Schon, E.A. (2006). Does premature aging of the mtDNA mutator mouse prove that mtDNA mutations are involved in natural aging? Aging cell *5*, 279-282.
King, M.P. (1996). Use of ethidium bromide to manipulate ratio of mutated and wild-type mitochondrial DNA in cultured cells. Methods in enzymology *264*, 339-344.
King, M.P., and Attardi, G. (1989). Human cells lacking mtDNA: repopulation with exogenous mitochondria by complementation. Science *246*, 500-503.

Kirino, Y., Goto, Y., Campos, Y., Arenas, J., and Suzuki, T. (2005). Specific correlation between the wobble modification deficiency in mutant tRNAs and the clinical features of a human mitochondrial disease. Proceedings of the National Academy of Sciences of the United States of America *102*, 7127-7132.

Koga, Y., Povalko, N., Nishioka, J., Katayama, K., Shuichi, Y., and Matsuishi, T. (2011). Molecular pathology of MELAS and l-arginine effects. Biochimica et biophysica acta.

Kohrer, C., and Rajbhandary, U.L. (2008). The many applications of acid urea polyacrylamide gel electrophoresis to studies of tRNAs and aminoacyl-tRNA synthetases. Methods *44*, 129-138.

Kornblum, C., Zsurka, G., Wiesner, R.J., Schroder, R., and Kunz, W.S. (2008). Concerted action of two novel tRNA mtDNA point mutations in chronic progressive external ophthalmoplegia. Bioscience reports *28*, 89-96.

Kruse, B., Narasimhan, N., and Attardi, G. (1989). Termination of transcription in human mitochondria: identification and purification of a DNA binding protein factor that promotes termination. Cell *58*, 391-397.

Kujoth, G.C., Hiona, A., Pugh, T.D., Someya, S., Panzer, K., Wohlgemuth, S.E., Hofer, T., Seo, A.Y., Sullivan, R., Jobling, W.A*., et al.* (2005). Mitochondrial DNA mutations, oxidative stress, and apoptosis in mammalian aging. Science *309*, 481-484.

Kukat, C., Wurm, C.A., Spahr, H., Falkenberg, M., Larsson, N.G., and Jakobs, S. (2011). Super-resolution microscopy reveals that mammalian mitochondrial nucleoids have a uniform size and frequently contain a single copy of mtDNA. Proceedings of the National Academy of Sciences of the United States of America *108*, 13534-13539.

Larsson, N.G. (2010). Somatic mitochondrial DNA mutations in mammalian aging. Annual review of biochemistry *79*, 683-706.

Larsson, N.G., and Clayton, D.A. (1995). Molecular genetic aspects of human mitochondrial disorders. Annual review of genetics *29*, 151-178.

Ledoux, S., Olejniczak, M., and Uhlenbeck, O.C. (2009). A sequence element that tunes Escherichia coli tRNA(Ala)(GGC) to ensure accurate decoding. Nature structural & molecular biology *16*, 359-364.

Lee, J.W., Beebe, K., Nangle, L.A., Jang, J., Longo-Guess, C.M., Cook, S.A., Davisson, M.T., Sundberg, J.P., Schimmel, P., and Ackerman, S.L. (2006). Editing-defective tRNA synthetase causes protein misfolding and neurodegeneration. Nature *443*, 50-55.

Lee, Y.J., Jeong, S.Y., Karbowski, M., Smith, C.L., and Youle, R.J. (2004). Roles of the mammalian mitochondrial fission and fusion mediators Fis1, Drp1, and Opa1 in apoptosis. Molecular biology of the cell *15*, 5001-5011.

Levinger, L., Giegé, R., and Florentz, C. (2003). Pathology-related substitutions in human mitochondrial $tRNA^{Ile}$ reduce precursor 3' end processing efficiency *in vitro*. Nucleic acids research *31*, 1904-1912.

Li, R., and Guan, M.X. (2010). Human mitochondrial leucyl-tRNA synthetase corrects mitochondrial dysfunctions due to the tRNALeu(UUR) A3243G mutation, associated with mitochondrial encephalomyopathy, lactic acidosis, and stroke-like symptoms and diabetes. Molecular and cellular biology *30*, 2147-2154.

Limongelli, A., Schaefer, J., Jackson, S., Invernizzi, F., Kirino, Y., Suzuki, T., Reichmann, H., and Zeviani, M. (2004). Variable penetrance of a familial progressive necrotising encephalopathy due to a novel tRNA(Ile) homoplasmic mutation in the mitochondrial genome. Journal of medical genetics *41*, 342-349.

Litonin, D., Sologub, M., Shi, Y., Savkina, M., Anikin, M., Falkenberg, M., Gustafsson, C.M., and Temiakov, D. (2010). Human mitochondrial transcription revisited: only TFAM and TFB2M are required for transcription of the mitochondrial genes in vitro. The Journal of biological chemistry *285*, 18129-18133.

Loveland, B., Wang, C.R., Yonekawa, H., Hermel, E., and Lindahl, K.F. (1990). Maternally transmitted histocompatibility antigen of mice: a hydrophobic peptide of a mitochondrially encoded protein. Cell *60*, 971-980.

Manam, S., and Van Tuyle, G.C. (1987). Separation and characterization of 5'- and 3'-tRNA processing nucleases from rat liver mitochondria. The Journal of biological chemistry *262*, 10272-10279.
Mao, P., and Reddy, P.H. (2011). Aging and amyloid beta-induced oxidative DNA damage and mitochondrial dysfunction in Alzheimer's disease: implications for early intervention and therapeutics. Biochimica et biophysica acta *1812*, 1359-1370.
Marchington, D.R., Barlow, D., and Poulton, J. (1999). Transmitochondrial mice carrying resistance to chloramphenicol on mitochondrial DNA: developing the first mouse model of mitochondrial DNA disease. Nature medicine *5*, 957-960.
Masucci, J.P., Davidson, M., Koga, Y., Schon, E.A., and King, M.P. (1995). In vitro analysis of mutations causing myoclonus epilepsy with ragged-red fibers in the mitochondrial tRNA(Lys)gene: two genotypes produce similar phenotypes. Molecular and cellular biology *15*, 2872-2881.
McFarland, R., Elson, J.L., Taylor, R.W., Howell, N., and Turnbull, D.M. (2004). Assigning pathogenicity to mitochondrial tRNA mutations: when "definitely maybe" is not good enough. Trends in genetics : TIG *20*, 591-596.
McFarland, R., Taylor, R.W., and Turnbull, D.M. (2007). Mitochondrial disease--its impact, etiology, and pathology. Current topics in developmental biology *77*, 113-155.
Mei, Y., Stonestrom, A., Hou, Y.M., and Yang, X. (2010a). Apoptotic regulation and tRNA. Protein & cell *1*, 795-801.
Mei, Y., Yong, J., Liu, H., Shi, Y., Meinkoth, J., Dreyfuss, G., and Yang, X. (2010b). tRNA binds to cytochrome c and inhibits caspase activation. Molecular cell *37*, 668-678.
Merante, F., Myint, T., Tein, I., Benson, L., and Robinson, B.H. (1996). An additional mitochondrial tRNA(Ile) point mutation (A-to-G at nucleotide 4295) causing hypertrophic cardiomyopathy. Human mutation *8*, 216-222.
Messmer, M., Gaudry, A., Sissler, M., and Florentz, C. (2009). Pathology-related mutation A7526G (A9G) helps in the understanding of the 3D structural core of human mitochondrial tRNA(Asp). RNA *15*, 1462-1468.
Metodiev, M.D., Lesko, N., Park, C.B., Camara, Y., Shi, Y., Wibom, R., Hultenby, K., Gustafsson, C.M., and Larsson, N.G. (2009). Methylation of 12S rRNA is necessary for in vivo stability of the small subunit of the mammalian mitochondrial ribosome. Cell metabolism *9*, 386-397.
Mishmar, D., Ruiz-Pesini, E., Brandon, M., and Wallace, D.C. (2004). Mitochondrial DNA-like sequences in the nucleus (NUMTs): insights into our African origins and the mechanism of foreign DNA integration. Human mutation *23*, 125-133.
Mitchell, P. (1961). Coupling of phosphorylation to electron and hydrogen transfer by a chemi-osmotic type of mechanism. Nature *191*, 144-148.
Montanari, A., De Luca, C., Di Micco, P., Morea, V., Frontali, L., and Francisci, S. (2011). Structural and functional role of bases 32 and 33 in the anticodon loop of yeast mitochondrial tRNAIle. RNA *17*, 1983-1996.
Montoya, J., Christianson, T., Levens, D., Rabinowitz, M., and Attardi, G. (1982). Identification of initiation sites for heavy-strand and light-strand transcription in human mitochondrial DNA. Proceedings of the National Academy of Sciences of the United States of America *79*, 7195-7199.
Moraes, C.T., Ciacci, F., Bonilla, E., Jansen, C., Hirano, M., Rao, N., Lovelace, R.E., Rowland, L.P., Schon, E.A., and DiMauro, S. (1993). Two novel pathogenic mitochondrial DNA mutations affecting organelle number and protein synthesis. Is the tRNA(Leu(UUR)) gene an etiologic hot spot? The Journal of clinical investigation *92*, 2906-2915.
Moraes, C.T., Dey, R., and Barrientos, A. (2001). Transmitochondrial technology in animal cells. Methods in cell biology *65*, 397-412.
Morais, V.A., and De Strooper, B. (2010). Mitochondria dysfunction and neurodegenerative disorders: cause or consequence. Journal of Alzheimer's disease : JAD *20 Suppl 2*, S255-263.
Moreno-Loshuertos, R., Ferrin, G., Acin-Perez, R., Gallardo, M.E., Viscomi, C., Perez-Martos, A., Zeviani, M., Fernandez-Silva, P., and Enriquez, J.A. (2011). Evolution meets disease: penetrance and functional epistasis of mitochondrial tRNA mutations. PLoS genetics *7*, e1001379.

Morse, M.C., Bleau, G., Dabhi, V.M., Hetu, F., Drobetsky, E.A., Lindahl, K.F., and Perreault, C. (1996). The COI mitochondrial gene encodes a minor histocompatibility antigen presented by H2-M3. J Immunol *156*, 3301-3307.

Motorin, Y., and Helm, M. (2010). tRNA stabilization by modified nucleotides. Biochemistry *49*, 4934-4944.

Munnich, A., and Rustin, P. (2001). Clinical spectrum and diagnosis of mitochondrial disorders. American journal of medical genetics *106*, 4-17.

Murakami, H., Ohta, A., and Suga, H. (2009). Bases in the anticodon loop of tRNA(Ala)(GGC) prevent misreading. Nature structural & molecular biology *16*, 353-358.

Nagaike, T., Suzuki, T., Tomari, Y., Takemoto-Hori, C., Negayama, F., Watanabe, K., and Ueda, T. (2001). Identification and characterization of mammalian mitochondrial tRNA nucleotidyltransferases. The Journal of biological chemistry *276*, 40041-40049.

Nagao, A., Suzuki, T., Katoh, T., and Sakaguchi, Y. (2009). Biogenesis of glutaminyl-mt tRNAGln in human mitochondria. Proceedings of the National Academy of Sciences of the United States of America *106*, 16209-16214.

Nakada, K., and Hayashi, J. (2011). Transmitochondrial mice as models for mitochondrial DNA-based diseases. Experimental animals / Japanese Association for Laboratory Animal Science *60*, 421-431.

Nakada, K., Inoue, K., Ono, T., Isobe, K., Ogura, A., Goto, Y.I., Nonaka, I., and Hayashi, J.I. (2001). Inter-mitochondrial complementation: Mitochondria-specific system preventing mice from expression of disease phenotypes by mutant mtDNA. Nature medicine *7*, 934-940.

Noji, H., and Yoshida, M. (2001). The rotary machine in the cell, ATP synthase. The Journal of biological chemistry *276*, 1665-1668.

Ohtsuki, T., Kawai, G., and Watanabe, K. (2002). The minimal tRNA: unique structure of Ascaris suum mitochondrial tRNA(Ser)(UCU) having a short T arm and lacking the entire D arm. FEBS letters *514*, 37-43.

Ojala, D., Montoya, J., and Attardi, G. (1981). tRNA punctuation model of RNA processing in human mitochondria. Nature *290*, 470-474.

Olejniczak, M., Dale, T., Fahlman, R.P., and Uhlenbeck, O.C. (2005). Idiosyncratic tuning of tRNAs to achieve uniform ribosome binding. Nature structural & molecular biology *12*, 788-793.

Ono, T., Isobe, K., Nakada, K., and Hayashi, J.I. (2001). Human cells are protected from mitochondrial dysfunction by complementation of DNA products in fused mitochondria. Nature genetics *28*, 272-275.

Onyango, I., Khan, S., Miller, B., Swerdlow, R., Trimmer, P., and Bennett, P., Jr. (2006). Mitochondrial genomic contribution to mitochondrial dysfunction in Alzheimer's disease. Journal of Alzheimer's disease : JAD *9*, 183-193.

Park, C.B., and Larsson, N.G. (2011). Mitochondrial DNA mutations in disease and aging. The Journal of cell biology *193*, 809-818.

Patchett, D.C., and Grover, M.L. (2011). Mitochondrial myopathy presenting as rhabdomyolysis. The Journal of the American Osteopathic Association *111*, 404-405.

Perli, E., Giordano, C., Tuppen, H.A., Montopoli, M., Montanari, A., Orlandi, M., Pisano, A., Catanzaro, D., Caparrotta, L., Musumeci, B.*, et al.* (2012). Isoleucyl-tRNA synthetase levels modulate the penetrance of a homoplasmic m.4277T>C mitochondrial tRNA(Ile) mutation causing hypertrophic cardiomyopathy. Human molecular genetics *21*, 85-100.

Pesole, G., Gissi, C., De Chirico, A., and Saccone, C. (1999). Nucleotide substitution rate of mammalian mitochondrial genomes. Journal of molecular evolution *48*, 427-434.

Pierron, D., Letellier, T., and Grossman, L.I. (2012). Mitogroup: continent-specific clusters of mitochondrial OXPHOS complexes based on nuclear non-synonymous polymorphisms. Mitochondrion *12*, 237-241.

Pinos, T., Marotta, M., Gallardo, E., Illa, I., Diaz-Manera, J., Gonzalez-Vioque, E., Garcia-Arumi, E., Andreu, A.L., and Marti, R. (2011). A novel mutation in the mitochondrial tRNA(Ala) gene (m.5636T>C) in a patient with progressive external ophthalmoplegia. Mitochondrion *11*, 228-233.

Porcelli, A.M., Ghelli, A., Ceccarelli, C., Lang, M., Cenacchi, G., Capristo, M., Pennisi, L.F., Morra, I., Ciccarelli, E., Melcarne, A.*, et al.* (2010). The genetic and metabolic signature of oncocytic transformation implicates HIF1alpha destabilization. Human molecular genetics *19*, 1019-1032.
Prezant, T.R., Agapian, J.V., Bohlman, M.C., Bu, X., Oztas, S., Qiu, W.Q., Arnos, K.S., Cortopassi, G.A., Jaber, L., Rotter, J.I.*, et al.* (1993). Mitochondrial ribosomal RNA mutation associated with both antibiotic-induced and non-syndromic deafness. Nature genetics *4*, 289-294.
Pulkes, T., Sweeney, M.G., and Hanna, M.G. (2000). Increased risk of stroke in patients with the A12308G polymorphism in mitochondria. Lancet *356*, 2068-2069.
Putz, J., Dupuis, B., Sissler, M., and Florentz, C. (2007). Mamit-tRNA, a database of mammalian mitochondrial tRNA primary and secondary structures. RNA *13*, 1184-1190.
Raimundo, N., Song, L., Shutt, T.E., McKay, S.E., Cotney, J., Guan, M.X., Gilliland, T.C., Hohuan, D., Santos-Sacchi, J., and Shadel, G.S. (2012). Mitochondrial stress engages E2F1 apoptotic signaling to cause deafness. Cell *148*, 716-726.
Reichert, A.S., Thurlow, D.L., and Morl, M. (2001). A eubacterial origin for the human tRNA nucleotidyltransferase? Biological chemistry *382*, 1431-1438.
Rhee, S.G. (1999). Redox signaling: hydrogen peroxide as intracellular messenger. Experimental & molecular medicine *31*, 53-59.
Rossmanith, W. (2011a). Localization of human RNase Z isoforms: dual nuclear/mitochondrial targeting of the ELAC2 gene product by alternative translation initiation. PloS one *6*, e19152.
Rossmanith, W. (2011b). Of P and Z: Mitochondrial tRNA processing enzymes. Biochimica et biophysica acta.
Rossmanith, W., Freilinger, M., Roka, J., Raffelsberger, T., Moser-Thier, K., Prayer, D., Bernert, G., and Bittner, R.E. (2008). Isolated cytochrome *c* oxidase deficiency as a cause of MELAS. Journal of medical genetics *45*, 117-121.
Rotig, A. (2011). Human diseases with impaired mitochondrial protein synthesis. Biochimica et biophysica acta *1807*, 1198-1205.
Rubio, M.A., Rinehart, J.J., Krett, B., Duvezin-Caubet, S., Reichert, A.S., Soll, D., and Alfonzo, J.D. (2008). Mammalian mitochondria have the innate ability to import tRNAs by a mechanism distinct from protein import. Proceedings of the National Academy of Sciences of the United States of America *105*, 9186-9191.
Rustin, P., Chretien, D., Bourgeron, T., Gerard, B., Rötig, A., Saudubray, J.M., and Munnich, A. (1994). Biochemical and molecular investigations in respiratory chain deficiencies. Clin Chim Acta *228*, 35-51.
Ruzzenente, B., Metodiev, M.D., Wredenberg, A., Bratic, A., Park, C.B., Camara, Y., Milenkovic, D., Zickermann, V., Wibom, R., Hultenby, K.*, et al.* (2012). LRPPRC is necessary for polyadenylation and coordination of translation of mitochondrial mRNAs. The EMBO journal *31*, 443-456.
Ryckelynck, M., Giege, R., and Frugier, M. (2005). tRNAs and tRNA mimics as cornerstones of aminoacyl-tRNA synthetase regulations. Biochimie *87*, 835-845.
Sampath, P., Mazumder, B., Seshadri, V., Gerber, C.A., Chavatte, L., Kinter, M., Ting, S.M., Dignam, J.D., Kim, S., Driscoll, D.M.*, et al.* (2004). Noncanonical function of glutamyl-prolyl-tRNA synthetase: gene-specific silencing of translation. Cell *119*, 195-208.
Santorelli, F.M., Mak, S.C., Vazquez-Acevedo, M., Gonzalez-Astiazaran, A., Ridaura-Sanz, C., Gonzalez-Halphen, D., and DiMauro, S. (1995). A novel mitochondrial DNA point mutation associated with mitochondrial encephalocardiomyopathy. Biochemical and biophysical research communications *216*, 835-840.
Schaller, A., Desetty, R., Hahn, D., Jackson, C.B., Nuoffer, J.M., Gallati, S., and Levinger, L. (2011). Impairment of mitochondrial tRNAIle processing by a novel mutation associated with chronic progressive external ophthalmoplegia. Mitochondrion *11*, 488-496.
Schimmel, P., and Guo, M. (2009). A tipping point for mistranslation and disease. Nature structural & molecular biology *16*, 348-349.
Schneider, A. (2011). Mitochondrial tRNA import and its consequences for mitochondrial translation. Annual review of biochemistry *80*, 1033-1053.

Schon, E.A., and DiMauro, S. (2007). Mitochondrial mutations: genotype to phenotype. Novartis Foundation symposium *287*, 214-225; discussion 226-233.
Schwartz, M., and Vissing, J. (2002). Paternal inheritance of mitochondrial DNA. The New England journal of medicine *347*, 576-580.
Shadel, G.S., and Clayton, D.A. (1997). Mitochondrial DNA maintenance in vertebrates. Annual review of biochemistry *66*, 409-435.
Silvestri, G., Servidei, S., Rana, M., Ricci, E., Spinazzola, A., Paris, E., and Tonali, P. (1996). A novel mitochondrial DNA point mutation in the tRNA(Ile) gene is associated with progressive external ophtalmoplegia. Biochemical and biophysical research communications *220*, 623-627.
Sissler, M., Lorber, B., Messmer, M., Schaller, A., Putz, J., and Florentz, C. (2008). Handling mammalian mitochondrial tRNAs and aminoacyl-tRNA synthetases for functional and structural characterization. Methods *44*, 176-189.
Sligh, J.E., Levy, S.E., Waymire, K.G., Allard, P., Dillehay, D.L., Nusinowitz, S., Heckenlively, J.R., MacGregor, G.R., and Wallace, D.C. (2000). Maternal germ-line transmission of mutant mtDNAs from embryonic stem cell-derived chimeric mice. Proceedings of the National Academy of Sciences of the United States of America *97*, 14461-14466.
Smeitink, J., van den Heuvel, L., and DiMauro, S. (2001). The genetics and pathology of oxidative phosphorylation. Nature reviews Genetics *2*, 342-352.
Smits, B.W., Hol, F.A., van den Heuvel, L.P., Drost, G., Rodenburg, R.J., Ter Laak, H.J., and van Engelen, B.G. (2007). Chronic progressive external ophthalmoplegia caused by an m.4267A > G mutation in the mitochondrial tRNAIle. Journal of neurology *254*, 1614-1615.
Souilem, S., Chebel, S., Mancuso, M., Petrozzi, L., Siciliano, G., FrihAyed, M., Hentati, F., and Amouri, R. (2011). A novel mitochondrial tRNA(Ile) point mutation associated with chronic progressive external ophthalmoplegia and hyperCKemia. Journal of the neurological sciences *300*, 187-190.
Spinazzola, A., and Zeviani, M. (2009). Disorders from perturbations of nuclear-mitochondrial intergenomic cross-talk. Journal of internal medicine *265*, 174-192.
Stark, B.C., Kole, R., Bowman, E.J., and Altman, S. (1978). Ribonuclease P: an enzyme with an essential RNA component. Proceedings of the National Academy of Sciences of the United States of America *75*, 3717-3721.
Stewart, J.B., Freyer, C., Elson, J.L., and Larsson, N.G. (2008a). Purifying selection of mtDNA and its implications for understanding evolution and mitochondrial disease. Nature reviews Genetics *9*, 657-662.
Stewart, J.B., Freyer, C., Elson, J.L., Wredenberg, A., Cansu, Z., Trifunovic, A., and Larsson, N.G. (2008b). Strong purifying selection in transmission of mammalian mitochondrial DNA. PLoS biology *6*, e10.
Sutovsky, P., Moreno, R.D., Ramalho-Santos, J., Dominko, T., Simerly, C., and Schatten, G. (1999). Ubiquitin tag for sperm mitochondria. Nature *402*, 371-372.
Suzuki, T., Nagao, A., and Suzuki, T. (2011). Human mitochondrial tRNAs: biogenesis, function, structural aspects, and diseases. Annual review of genetics *45*, 299-329.
Tanaka, M., Ino, H., Ohno, K., Hattori, K., Sato, W., Ozawa, T., Tanaka, T., and Itoyama, S. (1990). Mitochondrial mutation in fatal infantile cardiomyopathy. Lancet *336*, 1452.
Taniike, M., Fukushima, H., Yanagihara, I., Tsukamoto, H., Tanaka, J., Fujimura, H., Nagai, T., Sano, T., Yamaoka, K., Inui, K*., et al.* (1992). Mitochondrial tRNA(Ile) mutation in fatal cardiomyopathy. Biochemical and biophysical research communications *186*, 47-53.
Taylor, R.W., Chinnery, P.F., Bates, M.J., Jackson, M.J., Johnson, M.A., Andrews, R.M., and Turnbull, D.M. (1998). A novel mitochondrial DNA point mutation in the tRNA(Ile) gene: studies in a patient presenting with chronic progressive external ophthalmoplegia and multiple sclerosis. Biochemical and biophysical research communications *243*, 47-51.
Taylor, R.W., Giordano, C., Davidson, M.M., d'Amati, G., Bain, H., Hayes, C.M., Leonard, H., Barron, M.J., Casali, C., Santorelli, F.M*., et al.* (2003). A homoplasmic mitochondrial transfer ribonucleic acid mutation as a cause of maternally inherited hypertrophic cardiomyopathy. Journal of the American College of Cardiology *41*, 1786-1796.

Taylor, R.W., Schaefer, A.M., McFarland, R., Maddison, P., and Turnbull, D.M. (2002). A novel mitochondrial DNA tRNA(Ile) (A4267G) mutation in a sporadic patient with mitochondrial myopathy. Neuromuscular disorders : NMD *12*, 659-664.
Taylor, R.W., and Turnbull, D.M. (2005). Mitochondrial DNA mutations in human disease. Nature reviews Genetics *6*, 389-402.
Temperley, R., Richter, R., Dennerlein, S., Lightowlers, R.N., and Chrzanowska-Lightowlers, Z.M. (2010). Hungry codons promote frameshifting in human mitochondrial ribosomes. Science *327*, 301.
Tolkunova, E., Park, H., Xia, J., King, M.P., and Davidson, E. (2000). The human lysyl-tRNA synthetase gene encodes both the cytoplasmic and mitochondrial enzymes by means of an unusual alternative splicing of the primary transcript. The Journal of biological chemistry *275*, 35063-35069.
Toompuu, M., Levinger, L.L., Nadal, A., Gomez, J., and Jacobs, H.T. (2004). The 7472insC mtDNA mutation impairs 5' and 3' processing of tRNA(Ser(UCN)). Biochemical and biophysical research communications *322*, 803-813.
Toompuu, M., Tiranti, V., Zeviani, M., and Jacobs, H.T. (1999). Molecular phenotype of the np 7472 deafness-associated mitochondrial mutation in osteosarcoma cell cybrids. Human molecular genetics *8*, 2275-2283.
Toompuu, M., Yasukawa, T., Suzuki, T., Hakkinen, T., Spelbrink, J.N., Watanabe, K., and Jacobs, H.T. (2002). The 7472insC mitochondrial DNA mutation impairs the synthesis and extent of aminoacylation of tRNASer(UCN) but not its structure or rate of turnover. The Journal of biological chemistry *277*, 22240-22250.
Trifunovic, A., Wredenberg, A., Falkenberg, M., Spelbrink, J.N., Rovio, A.T., Bruder, C.E., Bohlooly, Y.M., Gidlof, S., Oldfors, A., Wibom, R*., et al.* (2004). Premature ageing in mice expressing defective mitochondrial DNA polymerase. Nature *429*, 417-423.
Tryoen-Toth, P., Richert, S., Sohm, B., Mine, M., Marsac, C., Van Dorsselaer, A., Leize, E., and Florentz, C. (2003). Proteomic consequences of a human mitochondrial tRNA mutation beyond the frame of mitochondrial translation. The Journal of biological chemistry *278*, 24314-24323.
Tsukihara, T., Aoyama, H., Yamashita, E., Tomizaki, T., Yamaguchi, H., Shinzawa-Itoh, K., Nakashima, R., Yaono, R., and Yoshikawa, S. (1995). Structures of metal sites of oxidized bovine heart cytochrome c oxidase at 2.8 A. Science *269*, 1069-1074.
Valente, L., Piga, D., Lamantea, E., Carrara, F., Uziel, G., Cudia, P., Zani, A., Farina, L., Morandi, L., Mora, M*., et al.* (2009). Identification of novel mutations in five patients with mitochondrial encephalomyopathy. Biochimica et biophysica acta *1787*, 491-501.
van der Giezen, M., and Tovar, J. (2005). Degenerate mitochondria. EMBO reports *6*, 525-530.
van Oven, M., and Kayser, M. (2009). Updated comprehensive phylogenetic tree of global human mitochondrial DNA variation. Human mutation *30*, E386-394.
Vilardo, E., Nachbagauer, C., Buzet, A., Taschner, A., Holzmann, J., and Rossmanith, W. (2012). A subcomplex of human mitochondrial RNase P is a bifunctional methyltransferase - extensive moonlighting in mitochondrial tRNA biogenesis. Nucleic acids research.
Vithayathil, S.A., Ma, Y., and Kaipparettu, B.A. (2012). Transmitochondrial cybrids: tools for functional studies of mutant mitochondria. Methods Mol Biol *837*, 219-230.
von Heijne, G. (1986). Why mitochondria need a genome. FEBS letters *198*, 1-4.
Wallace, D.C. (1999). Mitochondrial diseases in man and mouse. Science *283*, 1482-1488.
Wallace, D.C. (2005). A mitochondrial paradigm of metabolic and degenerative diseases, aging, and cancer: a dawn for evolutionary medicine. Annual review of genetics *39*, 359-407.
Wallace, D.C., Singh, G., Lott, M.T., Hodge, J.A., Schurr, T.G., Lezza, A.M., Elsas, L.J., 2nd, and Nikoskelainen, E.K. (1988). Mitochondrial DNA mutation associated with Leber's hereditary optic neuropathy. Science *242*, 1427-1430.
Wang, S., Li, R., Fettermann, A., Li, Z., Qian, Y., Liu, Y., Wang, X., Zhou, A., Mo, J.Q., Yang, L*., et al.* (2011). Maternally inherited essential hypertension is associated with the novel 4263A>G mutation in the mitochondrial tRNAIle gene in a large Han Chinese family. Circulation research *108*, 862-870.
Weisblum, B. (1999). Back to Camelot: defining the specific role of tRNA in protein synthesis. Trends in biochemical sciences *24*, 247-250.

Wek, R.C., Jackson, B.M., and Hinnebusch, A.G. (1989). Juxtaposition of domains homologous to protein kinases and histidyl-tRNA synthetases in GCN2 protein suggests a mechanism for coupling GCN4 expression to amino acid availability. Proceedings of the National Academy of Sciences of the United States of America *86*, 4579-4583.

Wilson, F.H., Hariri, A., Farhi, A., Zhao, H., Petersen, K.F., Toka, H.R., Nelson-Williams, C., Raja, K.M., Kashgarian, M., Shulman, G.I.*, et al.* (2004). A cluster of metabolic defects caused by mutation in a mitochondrial tRNA. Science *306*, 1190-1194.

Wittenhagen, L.M., and Kelley, S.O. (2003). Impact of disease-related mitochondrial mutations on tRNA structure and function. Trends in biochemical sciences *28*, 605-611.

Wolstenholme, D.R., Macfarlane, J.L., Okimoto, R., Clary, D.O., and Wahleithner, J.A. (1987). Bizarre tRNAs inferred from DNA sequences of mitochondrial genomes of nematode worms. Proceedings of the National Academy of Sciences of the United States of America *84*, 1324-1328.

Yadavalli, S.S., and Ibba, M. (2012). Quality control in aminoacyl-tRNA synthesis its role in translational fidelity. Advances in protein chemistry and structural biology *86*, 1-43.

Yang, S.Y., He, X.Y., and Miller, D. (2011). Hydroxysteroid (17beta) dehydrogenase X in human health and disease. Molecular and cellular endocrinology *343*, 1-6.

Yankovskaya, V., Horsefield, R., Tornroth, S., Luna-Chavez, C., Miyoshi, H., Leger, C., Byrne, B., Cecchini, G., and Iwata, S. (2003). Architecture of succinate dehydrogenase and reactive oxygen species generation. Science *299*, 700-704.

Yarham, J.W., Al-Dosary, M., Blakely, E.L., Alston, C.L., Taylor, R.W., Elson, J.L., and McFarland, R. (2011). A comparative analysis approach to determining the pathogenicity of mitochondrial tRNA mutations. Human mutation *32*, 1319-1325.

Yasukawa, T., Kirino, Y., Ishii, N., Holt, I.J., Jacobs, H.T., Makifuchi, T., Fukuhara, N., Ohta, S., Suzuki, T., and Watanabe, K. (2005). Wobble modification deficiency in mutant tRNAs in patients with mitochondrial diseases. FEBS letters *579*, 2948-2952.

Yasukawa, T., Suzuki, T., Ueda, T., Ohta, S., and Watanabe, K. (2000). Modification defect at anticodon wobble nucleotide of mitochondrial tRNAs(Leu)(UUR) with pathogenic mutations of mitochondrial myopathy, encephalopathy, lactic acidosis, and stroke-like episodes. The Journal of biological chemistry *275*, 4251-4257.

Yokogawa, T., Kumazawa, Y., Miura, K., and Watanabe, K. (1989). Purification and characterization of two serine isoacceptor tRNAs from bovine mitochondria by using a hybridization assay method. Nucleic acids research *17*, 2623-2638.

Yokogawa, T., Watanabe, Y., Kumazawa, Y., Ueda, T., Hirao, I., Miura, K., and Watanabe, K. (1991). A novel cloverleaf structure found in mammalian mitochondrial tRNA(Ser) (UCN). Nucleic acids research *19*, 6101-6105.

Yu Wai Man, C.Y., Chinnery, P.F., and Griffiths, P.G. (2005). Extraocular muscles have fundamentally distinct properties that make them selectively vulnerable to certain disorders. Neuromuscular disorders : NMD *15*, 17-23.

Yu, X.X., Mao, W., Zhong, A., Schow, P., Brush, J., Sherwood, S.W., Adams, S.H., and Pan, G. (2000). Characterization of novel UCP5/BMCP1 isoforms and differential regulation of UCP4 and UCP5 expression through dietary or temperature manipulation. The FASEB journal : official publication of the Federation of American Societies for Experimental Biology *14*, 1611-1618.

Zeviani, M., and Di Donato, S. (2004). Mitochondrial disorders. Brain : a journal of neurology *127*, 2153-2172.

Zeviani, M., and Klopstock, T. (2001). Mitochondrial disorders. Current opinion in neurology *14*, 553-560.

Zeviani, M., Moraes, C.T., DiMauro, S., Nakase, H., Bonilla, E., Schon, E.A., and Rowland, L.P. (1988). Deletions of mitochondrial DNA in Kearns-Sayre syndrome. Neurology *38*, 1339-1346.

Zhu, H.Y., Wang, S.W., Liu, L., Chen, R., Wang, L., Gong, X.L., and Zhang, M.L. (2009). Genetic variants in mitochondrial tRNA genes are associated with essential hypertension in a Chinese Han population. Clin Chim Acta *410*, 64-69.

Zifa, E., Theotokis, P., Kaminari, A., Maridaki, H., Leze, H., Petsiava, E., Mamuris, Z., and Stathopoulos, C. (2008). A novel G3337A mitochondrial ND1 mutation related to cardiomyopathy co-segregates with tRNALeu(CUN) A12308G and tRNAThr C15946T mutations. Mitochondrion *8*, 229-236.

Danksagung

Auf wissenschaftlicher Ebene möchte ich mich herzlich bei Prof. Walter Rossmanith bedanken, der mir das Thema anvertraut hat und der jederzeit ein offenes Ohr für meine Fragen hatte. Ich habe in der gesamten Zeit sehr viel von ihm gelernt.

Prof. Andrea Barta danke ich für ihre Einwilligung, die Arbeit zu betreuen.

Meiner Arbeitsgruppe danke ich für die schöne Zeit und das Teilen von Freud und Leid. Im Speziellen danke ich Johann für sein positives Gemüt und seine hilfreichen Ratschläge, Christoph für seine humorvolle Art und graphische Unterstützung, Andreas und Christa für die gemeinsame schöne Zeit und das Nahebringen der österreichischen Kultur, Elisa für den wissenschaftlichen und kulturellen Input, Aurelie für ihren netten Beitrag zu französisch-deutschen Beziehungen, Nadia für ihre humorvolle und aufgeschlossene Art und Esther für die akkurate Einarbeitung und ihr Lachen, welches noch heute durch das Labor hallt.

Bei Prof. Robert Lightowlers möchte ich mich für die freundliche und aufgeschlossene Beherbergung in seinem Labor und die hilfreichen Gespräche bedanken. In seinem Team gilt mein Dank vor allem Rica, Sven und Aleksandra, die nicht nur im Labor eine große Unterstützung waren, sondern mir auch außerhalb eine sehr schöne Zeit in Newcastle bereitet haben.

Prof. Adolf Ellinger danke ich für die Anfertigung der elektronenmikroskopischen Bilder und Dipl.-Ing. Karin Moser-Thier für die Hilfestellung bei polarographischen und photometrischen Messungen.

Prof. Michael Pretterklieber möchte ich speziell für die kulinarischen Genüsse danken.

Mircea möchte ich für seine Unterstützung danken und für die Zeit, in welcher er mich während dieser Arbeit begleitet hat. Dirk gilt mein Dank vor allem für sein ausdauerndes Zuhören.

Ich danke meinen Eltern für ihre Liebe und ihr Vertrauen in mich.

Curriculum Vitae

Name	Dipl.-Biol. Andrea Fettermann
Date of birth	1st of May 1980
Nationality	German
Place of Birth	Mainz, Germany

Education

03/2008 – today	PhD Thesis: "Molecular Pathology of Mitochondrial $tRNA^{Ile}$ Mutations" Research Group: Prof. Dr. Mag. Walter Rossmanith **Medizinische Universität, Vienna, Austria**
12/2005 – 09/2006	Diploma Thesis: "Microarray Studies to Identify Novel Biomarkers for the Early Diagnosis of Alzheimer`s Disease" Research Group: Prof. Dr. Thomas Haaf **Universitätsklinikum, Mainz, Germany**
10/2000 – 09/2006	Studies of Biological Sciences, Diploma Focus on Genetics, Microbiology and Zoology **Johannes Gutenberg-Universität, Mainz, Germany**
08/1990 – 06/2000	Secondary School, Abitur **Gymnasium am Römerkastell, Alzey, Germany**

Work experience

01/2008 – today	Research Associate **Medizinische Universität, Vienna, Austria**
10/2007 – 11/2007	Research Associate **Universitätsklinikum, Mainz, Germany**

Research period abroad

03/2010 – 04/2010	Doctoral Research Stay Research Group: Prof. Robert Lightowlers **University of Newcastle upon Tyne, UK**

Publications

03/2011	Wang S., Li R., Fettermann A. et al (2011). Maternally Inherited Essential Hypertension is Associated with the Novel 4263A>G Mutation in the Mitochondrial $tRNA^{Ile}$ Gene in a Large Han Chinese Family. *Circulation Research* 108, 862-870.